e-ISSN 2667-9973
p-ISSN 1512-1127

საქართველოს გეოფიზიკური საზოგადოების ჟურნალი

მყარი დედამიწის, ატმოსფეროს, ოკეანისა და კოსმოსური პლაზმის ფიზიკა

ტომი 26 , № 1

JOURNAL
OF THE GEORGIAN GEOPHYSICAL SOCIETY

Physics of Solid Earth, Atmosphere, Ocean and Space Plasma

Vol. 26 , № 1

Tbilisi
2023

e-ISSN 2667-9973
p-ISSN 1512-1127

საქართველოს გეოფიზიკური საზოგადოების ჟურნალი

მყარი დედამიწის, ატმოსფეროს, ოკეანისა და კოსმოსური პლაზმის ფიზიკა

ტომი 26 , № 1

JOURNAL
OF THE GEORGIAN GEOPHYSICAL SOCIETY

Physics of Solid Earth, Atmosphere, Ocean and Space Plasma

Vol. 26 , № 1

Tbilisi
2023

საქართველოს გეოფიზიკური საზოგადოების ჟურნალი
მყარი დედამიწის, ატმოსფეროს, ოკეანისა და კოსმოსური პლაზმის ფიზიკა
მთავარი რედაქტორი: თ. ჭელიძე

ჟურნალის შინაარსი:

ჟურნალი მოიცავს მყარი დედამიწის, ატმოსფეროს, ოკეანისა და კოსმოსური პლაზმის ფიზიკის ყველა მიმართულებას. ჟურნალში ქვეყნდება: კვლევითი წერილები, მიმოხილვები, მოკლე ინფორმაციები, დისკუსიები, წიგნების მიმოხილვები, განცხადებები, კონფერენციების მოხსენებები.

JOURNAL OF THE GEORGIAN GEOPHYSICAL SOCIETY

Physics of Solid Earth, Atmosphere, Ocean and Space Plasma

Editor-in-chief: T. Chelidze

Scope of the Journal:

The Journal is devoted to all branches of the Physics of Solid Earth, Atmosphere, Ocean and Space Plasma. Types of contributions are: research papers, reviews, short communications, discussions, book reviews, announcements, conference reports.

ЖУРНАЛ ГРУЗИНСКОГО ГЕОФИЗИЧЕСКОГО ОБЩЕСТВА

Физика Твердой Земли, Атмосферы, Океана и Космической Плазмы

Главный редактор: Т. Челидзе

Содержание журнала:

Журнал Грузинского геофизического общества охватывает все направления физики твердой Земли, Атмосферы, Океана и Космической Плазмы. В журнале публикуются научные статьи, обзоры, краткие информации, дискуссии, обозрения книг, объявления, доклады конференций.

მისამართი:

საქართველო, 0160, თბილისი, ალექსიძის ქ. 1, მ. ნოდიას სახ. გეოფიზიკის ინსტიტუტი
ტელ.: 233-28-67; ფაქსი; (995 32 2332867); ელ. ფოეტა: tamaz.chelidze@gmail.com; avtandilamiranashvili@gmail.com;
geophysics.journal@tsu.ge

გამოქვეყნების განრიგი და ხელმოწერა:

გამოიცემა წელიწადში ორჯერ. მყარი ვერსიის წლიური ხელმოწერის ფასია: უცხოელი ხელმომწერისათვის - 30 დოლარი, საქართველოში - 10 ლარი. ხელმოწერის მოთხოვნა უნდა გაიგზავნოს რედაქციის მისამართით. შესაძლებელია უფასო ონლაინ წვდომა:
http://openjournals.gela.org.ge/index.php/GGS

ჟურნალი ინდექსირებულა Google Scholar-ში:
https://scholar.google.com/citations?hl=en&user=pdG-bMAAAAAJ

Address:

M. Nodia Institute of Geophysics, 1 Alexidze Str., 0160 Tbilisi, Georgia
Tel.: 233-28-67; Fax: (99532) 2332867; e-mail: tamaz.chelidze@gmail.com; avtandilamiranashvili@gmail.com;
geophysics.journal@tsu.ge

Publication schedule and subscription information:

The journal is issued twice a year. The subscription price for print version is 30 $ in year.
Subscription orders should be sent to editor's address. Free online access is possible:
http://openjournals.gela.org.ge/index.php/GGS

The journal is indexed in the Google Scholar:
https://scholar.google.com/citations?hl=en&user=pdG-bMAAAAAJ

Адрес:

Грузия, 0160, Тбилиси, ул. Алексидзе, 1. Институт геофизики им. М. З. Нодиа
Тел: 233-28-67; 294-35-91; Fax: (99532)2332867; e-mail: tamaz.chelidze@gmail.com; avtandilamiranashvili@gmail.com;
geophysics.journal@tsu.ge

Порядок издания и условия подписки:

Журнал издается дважды в год. Годовая подписная цена для печатной версии - 30 долларов США. Заявка о подписке высылается в адрес редакции. Имеется бесплатный онлайн доступ
http://openjournals.gela.org.ge/index.php/GGS

Журнал индексирован в Google Scholar:
https://scholar.google.com/citations?hl=en&user=pdG-bMAAAAAJ

This journal uses Open Journal Systems 2.4.8.3, which is open source journal management and publishing software developed, supported, and freely distributed by the Public Knowledge Project under the GNU General Public License.

(http://openjournals.gela.org.ge/index.php?journal=GGS&page=about&op=aboutThisPublishingSystem)

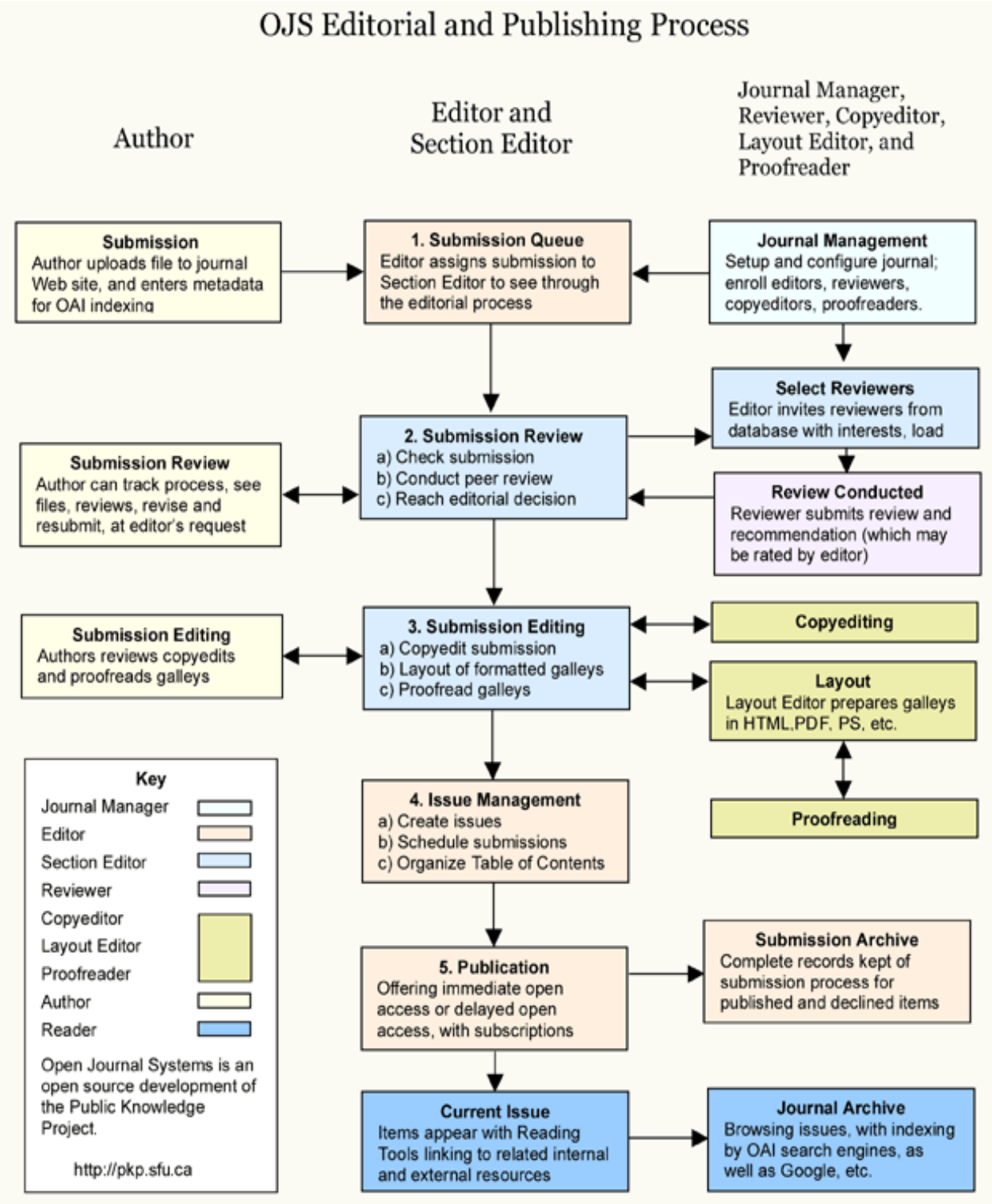

Journal of the Georgian Geophysical Society, ISSN: 1512-1127
Physics of Solid Earth, Atmosphere, Ocean and Space Plasma, v. 26(1), 2023, pp. 5-18

Complex Research of Concrete Structures with Ultrasound and Geolocation Methods

[1]Nodar D. Varamashvili, [2]Bezhan Z. Asanidze, [3]Mamuka N. Jakhutashvili, [4]Vladimir V. Glazunov

[1] Ivane Javakhishvili Tbilisi State University, Mikheil Nodia Institute of Geophysics, [2] British Petroleum Company (BP), [3] Georgian Technical University, [4]Saint-Petersburg Mining University

ABSTRACT

The subject of our research was to study the current state of the Tsageri catchment, using georadiolocation and ultrasound methods. Georadar Zond 12e was used in the research.. Georadar data were collected and processed with Prizm 2.7 regular Software. With the help of georadar, it is possible to highlight voids, cracks and weakened environment. It is also possible to determine the degree of humidity of the environment. Antennas of different frequencies are used to study different environment. By our research was used 1 MHz, 1.5 MHz and other frequencies antennas. Ultrasonic method is also an effective tool for determining the mechanical parameters of the environment and itsl structure. In the presented works, the ultrasonic equipment manufactured by the Swiss company PROCEQ, pulsed echo transmitter - Pundit PL-200PE was used. Processing of the obtained material was performed by means of the Pundit - 200 and Pundit - 20PE working program "PL-Link". Using ultrasonic equipment, it is possible to highlight voids and cracks in the environment and study their geometrical parameters. as well as determining the mechanical characteristics of the environment. When studying the same areas, the results obtained by radar and ultrasonic methods correlate quite well with each other in terms of determining the structure and complement each other in terms of determining the mechanical parameters of the medium and details of the structure.

Key words: *tomography, ultrasonic, georadiolocation, GPR, nondestructive testing*

Introduction

Ultrasound corresponds to a mechanical wave propagating at frequencies above the range of human hearing (conventionally 20 kHz). Ultrasound and sound waves propagate in fluids (gases and liquids) and solids. In particular, the wave propagation depends on the intrinsic elastic properties of the medium as well as on its mass density. In addition to its widespread use in engineering applications (e.g., defect detection / evaluation, material characteristics, etc.), ultrasounds are also used in the medical field. In general, ultrasound testing is based on the recording and quantification of reflected waves (pulse-echo) or transmitting waves [7].

A ultrasonic pulse-echo test concentrates on measuring the transit time of ultrasonic waves traveling through a material and being reflected to the surface of the tested medium. Based on the transit time or velocity, this technique can also be used to indirectly detect the presence of internal flaws, such as cracking, voids, delamination or horizontal cracking, or other damages [7,9].

Each of the two types is used under certain conditions [4,5]. In our scientific research, we use acoustics for geophysical and geotechnical research [1,3,5]. In this paper we present scientific-applied studies in the field of geomechanics using acoustic methods [6].

Equipment and software for ultrasound examination

We used ultrasound equipment produced by the Swiss company (PROCEQ, https://www.proceq.com/) for geophysical work, called Pundit PL-200 and Pundit PL-200PE. Ultrasonic testers (Pundit PL-200 and Pundit PL-200PE) are used to study concrete, wood and stone materials and structures using non-damaging acoustic control methods. Equipment and methods can be used: to study internal defects and cracks, heterogeneities and voids in materials, to calculate material modulus, stiffness and Poisson's ratio.

Pulse Echo Transducer - Pundit PL-200PE

The Pulse Echo transducer is a shear wave transducer designed for single-handed and two-handed operation. It is particularly suited to testing where access is limited to a single side.

The Pundit PL-200 offers three methods of transmission.

Ultrasonic research methods

In our case, we used ultrasonic sounding with piezoelectric 54 kHz sensors. Piezoelectric transverse wave sensors with a frequency of 250 kHz were also used, and piezoelectric sensors with a frequency of 50 kHz were used for ultrasound tomography. With the help of sensors in such frequency ranges, it is possible to study the structure of a solid and concrete at a depth of 50-60 cm, and in some cases even up to 1 m.

Performing ultrasound examinations

Ultrasound examinations were performed on the load-bearing piers and walls of the Tsageri catchment (Fig. 1). Approximately 100 sites were selected in the vertical direction on the walls of the building where the mechanical properties of the concrete were studied.

a.

b.

Fig. 1. a) Tsageri catchment. 1 - East wall, 2 - First (east) pier, 3 - Second (central) pier, 4 - Third (west) pier and 5 - West wall. b) A picture of the ultrasound work on the load-bearing piers and walls of the catchment dam.

About 100 areas were selected in the vertical direction on the walls of the building, where the mechanical characteristics of concrete were studied. In addition, a network of profiles with a step of 0.05 m was carried out on the piers and walls of the reservoir, using the tool. For the further processing of the obtained materials, the values of the velocity parameters of the elastic waves were entered into the existing program, and as a result, the elastic parameters of the reinforced concrete constructions were obtained. Since the velocities of P

and S type elastic waves are theoretically and empirically related to the elastic parameters of the environment, we can judge the presence of weakened, exhausted and relatively damaged zones within the investigated area. Using the sensors designed to generate and receive longitudinal (P) and transversal (S) type of elastic waves of the mentioned device, coverage (sensing) works were performed on the visually preserved and weakened areas of the walls of the building.

With the obtained materials, the propagation velocities of P and S type elastic waves were determined, both in concrete and in the blocks of granite stones near the aqueduct. Based on these velocities, the following physical-mechanical parameters were determined for all tested objects: ρ - density, ν - Poisson's ratio and E - Young's dynamic modulus. Poisson's ratio was used to determine the quality of concrete. Its value is in the range of (0.15-0.20) for normal quality concrete.

Data processing

Ultrasound waveform and tomographic (B-scan) recordings (Fig. 2) were processed using (PL-Link) standard software.

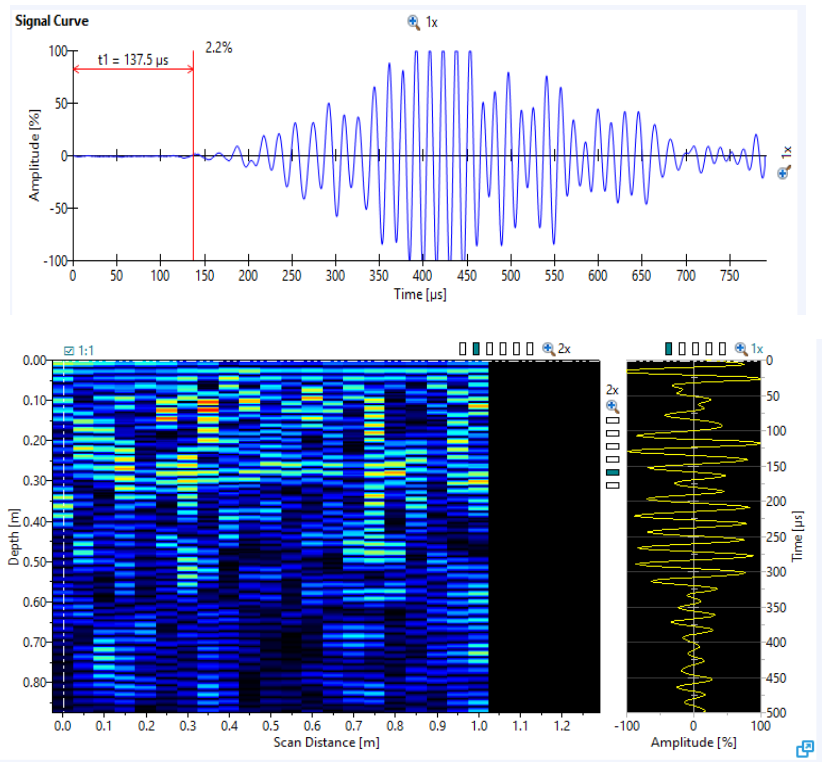

Fig.2. Ultrasound waveform (upper) and tomographic (lower) recordings.

On the records of oscillograms, the separation of longitudinal and transverse waves took place, their velocities were determined and various elastic parameters were calculated on the corresponding profiles. T On the processing and analysis of tomographic recordings (B-scans) took place us to identify possible voids, heterogeneous and weakened areas in the concrete.

Results of ultrasound examinations

About 100 precincts were processed. The image presented for each precinct is indicated by brown lines indicating the relevance of the tomographic images to the profiles. The yellow lines indicate the correspondence of the longitudinal velocities and the Poisson ratio with the profiles. The probable damaged areas localized by the velocity measurement are highlighted in blue, while the probable damage and weakening localized at different depths in the concrete pavement are marked in red by scanning. Here we present two of the location.

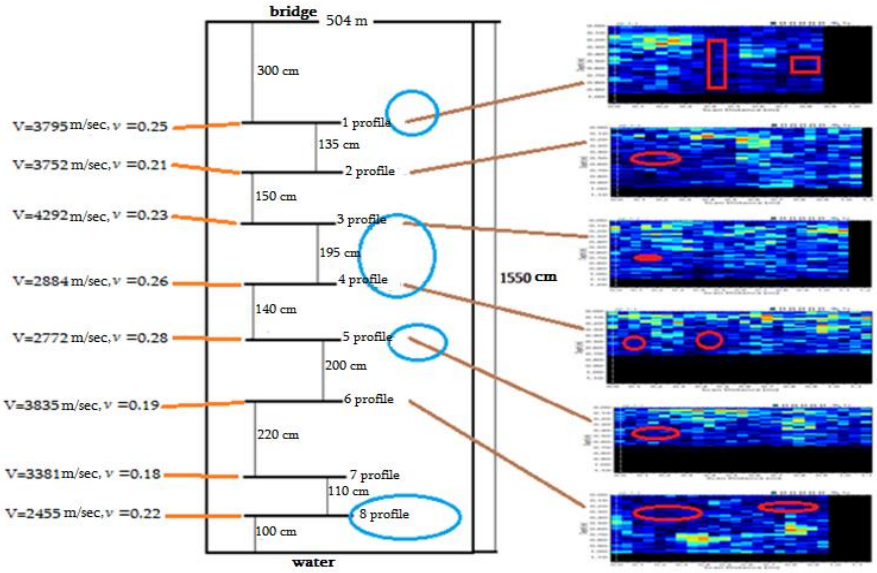

Fig.3. Profiles and tomographic records of one areas of the catchment. (Plot #5. The western wall of the second (central) pier of the reservoir).

Ultrasound testing works were performed on eight profiles at this site. Longitudinal (P) wave velocities in different profile ranges vary from 4292 m / s to 2455 m / s, transverse 2541 m / s to 1483 m / s, Poisson's ratio (ν) from 0,26 to 0 , At 18 intervals, and the Ju ng modulus (E) - (11639-39857) in the MPa interval.

One and more measurements of ultrasonic wave velocities were performed on all profiles in this area. They are made on concrete slab, on "poured concrete" and in the area of transition from concrete to tile. As the transition from the upper profiles of the precinct to the lower profiles, a gradual change in the speed of the ultrasonic wave will be observed. The velocity values are reduced in the vicinity of the third and fourth profiles. The values of the Poisson's ratio change in the range of 0.21-0.28 in the areas of the top five profiles, which probably indicates a weakening of the concrete structure in these areas. The velocity decreases particularly in the vicinity of the eighth (bottom) profile, which probably means damage to the concrete at this site or deterioration of its structure in this part of the pier [8].

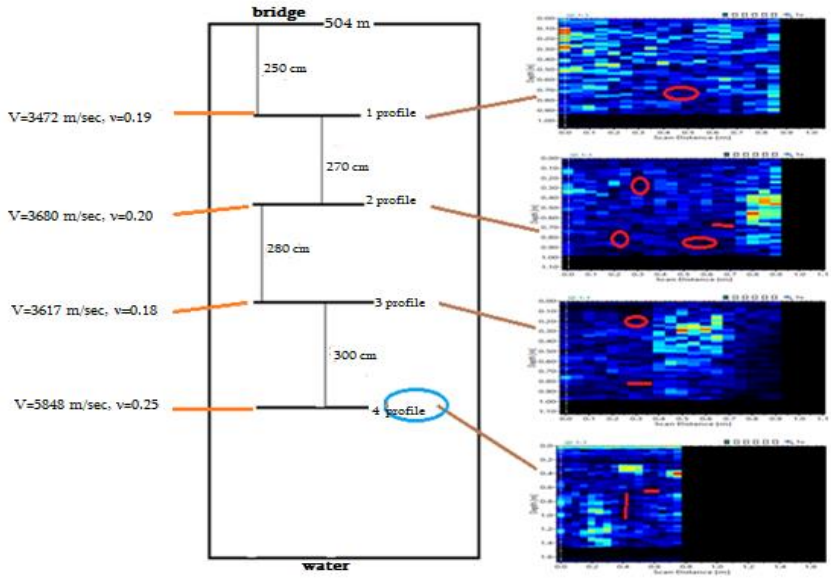

Fig.4. East wall (on the side of the dam) profiles of the first catchment tower and tomographic record of some profiles. (Plot #5. The western wall of the second (central) pier of the reservoir).

At this site (Fig.5) ultrasonic measurements were performed on three profiles along the wall and on the fourth profile on granite stones. Normal values of the Poisson's ratio (0.18-0.20) were be observed on all profiles and almost all measuring points, indicating the stability of the mechanical parameters of the concrete - its good condition. Ultrasound tomography (B-scan) was also performed on this incision. Deep lesions of different nature were observed in the tomographic images of all profiles, at different depths, as indicated in the images. In the tomographic images, in addition to the marked areas, dark colored areas was observed, which should indicate their weakening [8].

Comparison of the data presented in the two precincts (Fig.3, Fig.4) shows that they are relatively different precincts. The mechanical parameters of the bearing concretes in these areas differ from each other and indicate different mechanical states of the different catchment areas.

Conclusion

1.Modern methods of ultrasound examination and tools used have been found to be effective in assessing the condition of concrete structures constructing piers and walls.
2. The measurement results give different values of the elastic parameters. Tomographic scan images have abnormal areas. These anomalous areas must be associated with changes in the structure of the concrete.
3. A sharp change in the values of the Poisson's ratio should also be associated with a change in the rigidity of the material of the studied objects and its structure.
4. In general, it can be said that the results of the examination of the objects under study confirm that the physical and mechanical parameters are more abnormal in the areas adjacent to the lower, blurred-erosive areas than in the areas of concrete slabs above.

The results of checking the concrete mark on the supporting constructions of the research areas.

The purpose of the conducted research was to evaluate grade the used concrete on both the east and west walls, as well as on the piers. The need for this arose after visual inspection of these structures revealed defects. In modern conditions, it is possible to check the density (mark) of concrete products with different types of field tools. One of these types of tools is the Schmidt hammer (photo 5).

Fig. 5. The appearance of the Schmidt hammer.

The advantage of this tool is that in a short time, the strength/grade of the concrete structure can be determined without disturbing the integrity of the product.

The physical basis for the operation of this device is based on the amplitude of its reflection (recoil) when a solid body is struck by a solid surface. Accordingly, the greater the density (strength) of concrete, the greater the amplitude of its reflection and the data on the scale.

During the observation, measurements were made along the surfaces both on the slabs and on the reinforced concrete structures on the south side and lower sections.

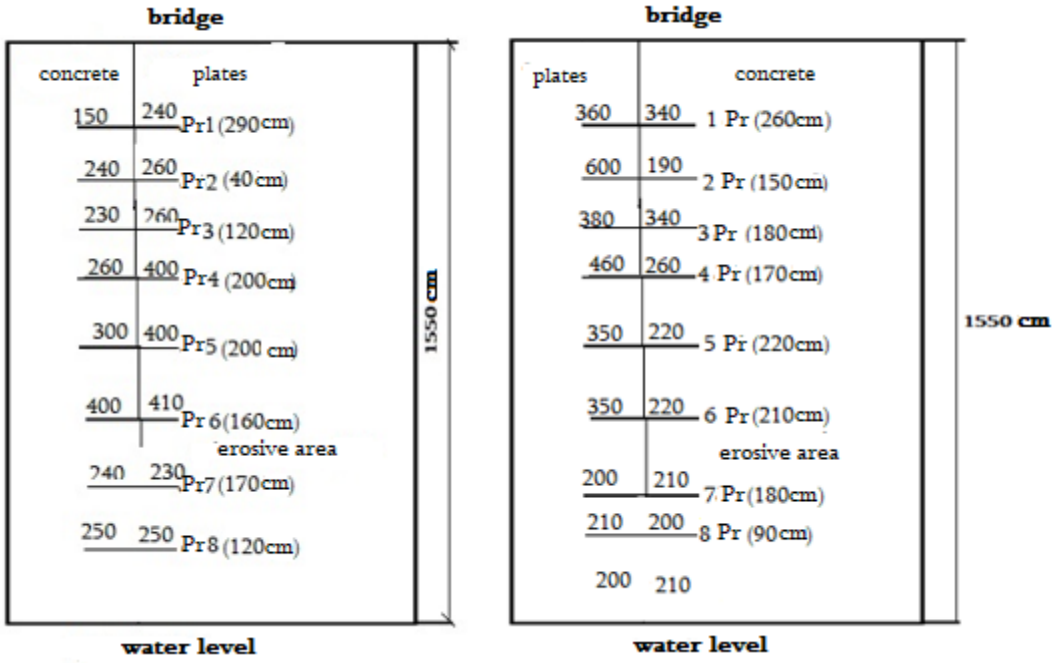

Fig. 6. The results of checking the concrete mark on the east (a) and west (b) side of the first pier (schematic sections).

For the slabs of the first pier, the grade of concrete varies mainly from 240 to 600, and from 210 to 340 on the south side and sides and washed-eroded sections of concrete. Above it, at a depth of 5-5.5 m from the level of the bridge, on the western side, higher values were allocated within the range of 300-340. On the lower, eroded-washed-faulty sections, its value is low here too (within 200-240).

On the basis of the research conducted with the Schmidt hammer on the surfaces of the retaining walls and piers of the dam and the analysis of the obtained results, the following can be concluded:

1. The concrete grade is characterized by higher values for the slabs placed outside the walls and piers than for the rest of the construction surfaces and areas without it.
2. Particularly low values of the concrete grade were revealed for the eroded-washed sections of the eastern and western walls, as well as in the lower sections of the piers.

In our opinion, the change in such a wide range of concrete grades does not correspond to either the old or the new norms of construction. Their causes can be: discrepancy of the cement brand, its insufficient concentration or flaws in the construction technology.

Georadiolocation research

Georadiolocation method has high spatial resolution [10]. There is no limitation on the daily surface and on the surface of different types of artificial cover, as well as in water surface or underwater research.

In our work, georadiolocation research was carried out in the following ways:

1. Hydrogeographic survey from the water surface in the basin.
2. Underwater research from the bottom of the pool to the surface of the water
3. Vertical survey along walls and supporting piers.

Georadiolocation along the terrain on the daily surface.

The selected georadiolocation method and their varietis allowed us to obtain a continuous georadiolocation cut, which reflects the structure of the ground, the structure of the reinforced concrete structure and the study of the underwater space to the maximum possible depth, which is determined by the electrophysical properties of the soil, concrete and water.

The number of profiles, their location, length and orientation for each object under study was carried out independently, taking into account the type of surface and technogenic factors.

Georadiolocation studies were carried out with profile and area planning.

For our article, the part of the profile study that was implemented on the pool walls and supporting piers is interesting.
Georadiolocation method is based on the registration of electromagnetic (EM) nanosecond pulses propagation in the studied environment and further processing taking into account the electromagnetic properties.
Screened antenna blocks with frequencies of 300, 900, 1000 and 1500 MHz were used in georadiolocation studies.

Georadiolocation equipment and software.

A certified "ZOND-12e Advance" (Ltd. "RadarSystemInc", Riga, Latvia) with screened antennas was used for geophysical research. Management of geo-radar, data processing, visualization of georadarograms is performed with the help of certified computer program «PRISM v.2.60» (Ltd. «Radar System Inc»). This type of georadar is certified in the European Union. It has antennas of different frequencies to penetrate to different depths and to conduct different types of research. In this article, we are interested in comparing the results obtained with ultrasound and georadiolocation equipment, so we will consider only the vertical planning along the walls and supporting piers conducted with 1 and 1.5 gigahertz antennas.

Fig. 7. 1 GHz antenna and 1.5 GHz antenna with its own odometer wheel.

Surface georadar surveys of walls and piers are carried out with the help of a 1000 MHz antenna. A 1500 MHz antenna has also been used for testing on the second pier. During research with this method, the antenna was removed from the surface of the wall by a minimum distance and moved along it.

Fig. 8. a) Georadar research process along the second pier (using 1000 MHz antenna), b) low-threshold dam condition investigation process using 1000 MHz antenna.

During the georadio-radar profiling of the low-threshold dams located at the base of the first and second barrier shields, the geophysical team, with the help of a crane, descended to the level of the dam and moved the 1000 MHz antenna along the inclined surface from the ground up, along its entire length, by means of a designated cable-rope with markings of meters (Fig. 8).

Results of georadiolocation investigation

The results of the main georadiolocation survey are presented in the form of georadiolocation section profiles. The types of wave EM fields correspond to different types of concrete, as well as reflect their uniformity and moisture content. Along the supporting piers and walls, the location of the iron reinforcement grids and metal elements supporting the walls is characterized. Below, the results of the georadiolocation survey are described according to the respective areas.

Georadiolocation investigation results of the walls and piers of the dam

The results of the georadiolocation survey of these objects are presented in the form of cuts on Figures 9-15. Diffraction effects of waves characteristic of armature rods are clearly visible on them (diffraction hyperbolas, Fig. 9). With this method and with the help of the antenna, the location of the reinforcement rods arranged in the profile was well defined.

According to the type of arrangement of reinforcement rods, two types of reinforcement were identified: walls (a) and piers (b) Fig.9). The first type of reinforcement is characterized by the arrangement of small-diameter iron reinforcement rods close to the surface in the form of a grid (type 1). This type is typical for the concrete slabs on the walls and the sections towards the bottom of the pier.

The second (type 2) is characterized by an irregular and deep placement of the reinforcement rods. The amplitude of the change of the EM wave field on this type of constructions is characterized by low intensity, technological boundaries, flaws and layering will be observed in the concrete structure.

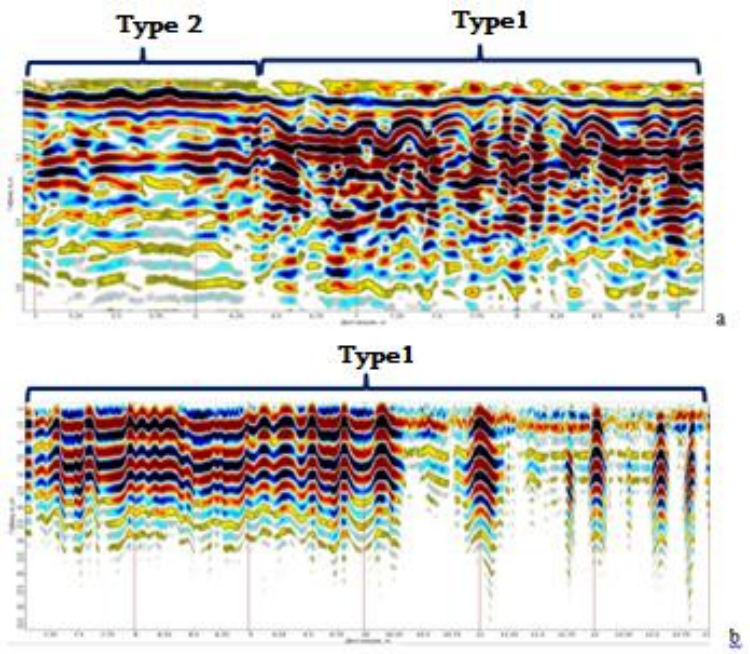

Fig. 9. Fragments of geolocation slices obtained with the help of 1000 and 1500 MHz antennas. The drawing shows two types of reinforcement of concrete structures: eastern wall (a) and piers (b).

Type 1 and 2 intervals are separated by vertical arrows on georadiolocation cuts Pr1 and Pr2 of the eastern wall. The numbers next to the arrows show the appearance of reinforcements.

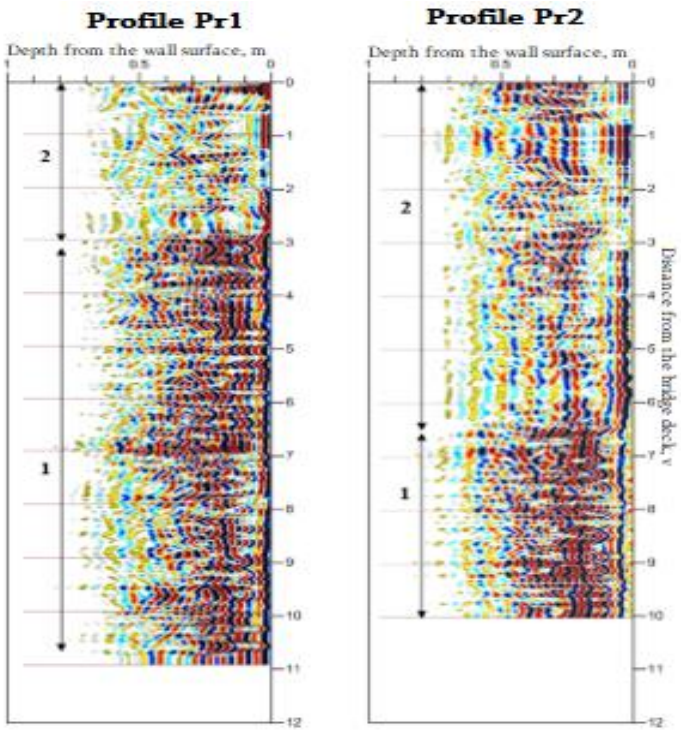

Fig. 10. Georadiolocation slices Pr1 and Pr2 taken along the eastern wall.

Corresponding reinforcement types (1 and 2) were not identified on the profiles (Pr3 and Pr4) obtained for the above-water sections of the first pier. Depending on the nature of the wave field, the second type of reinforcement can be seen here.

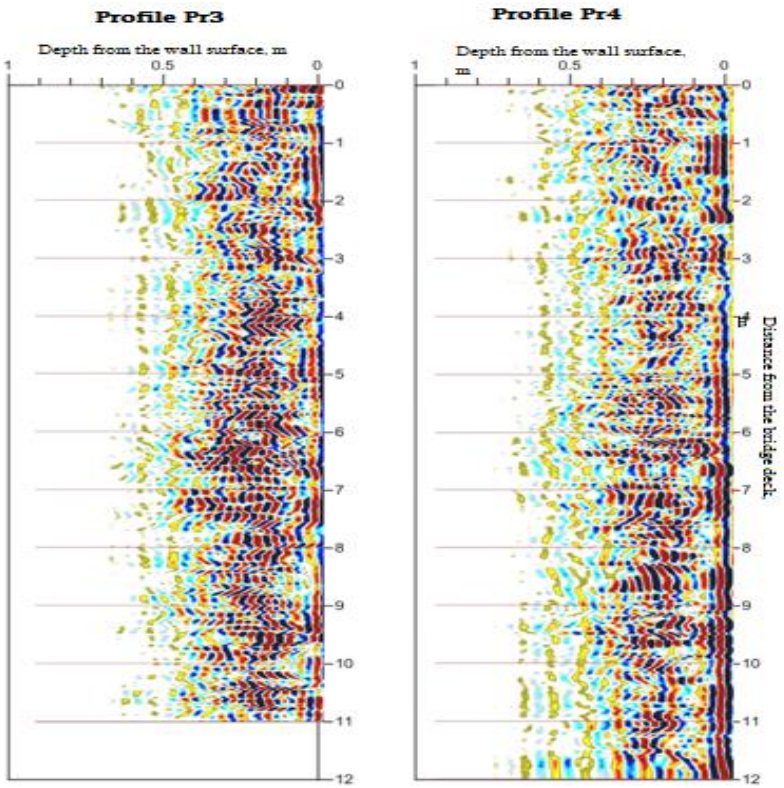

Fig. 11. Georadiolocation slices Pr3 and Pr4 obtained along the first pier.

Sections of type 1 and 2 reinforcements are separated along the georadiolocation cuts Pr5 and Pr6 obtained along the surfaces of the above-water parts of the second pier. The arrows on these slices are conventionally marked as dots, because the effect of individual reinforcement was not sufficiently reflected on them. In order to clarify their boundaries, additional georadiolocation surveys were conducted along these profiles using a 1500 MHz antenna (Figure 12).

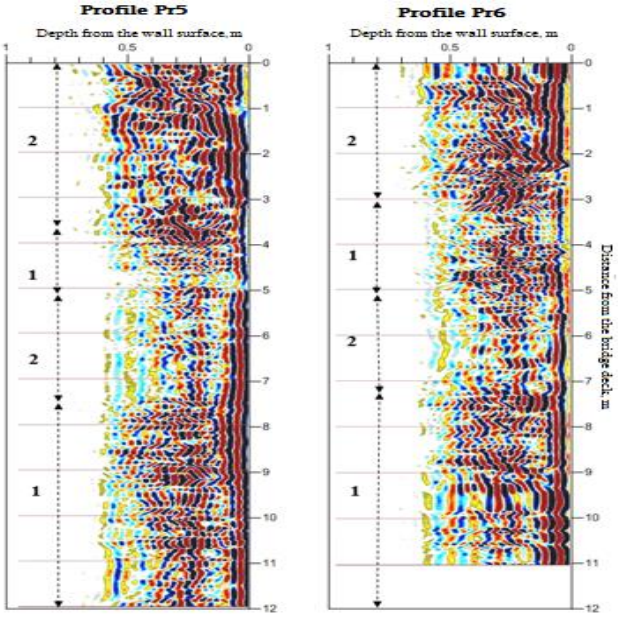

Fig. 12. Georadiolocation slices taken along the second pier (Pr5 and Pr6).

Sections of type 1 and 2 reinforcements are separated by vertical arrows Pr7 and Pr8 along the georadiolocation slices taken along the surface of the third pier's above-water part. The types and intervals of these reinforcements are almost similar to the results of the survey of the second pier (Fig. 13).

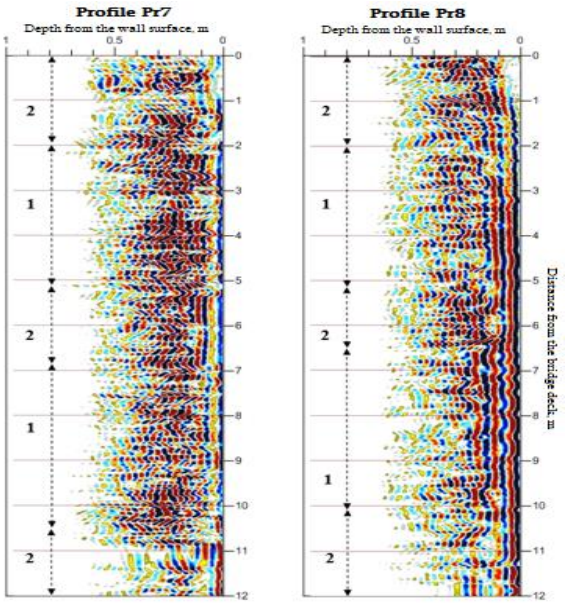

Fig. 13. Georadiolocation slices taken along the third pier (Pr7 and Pr8).

On georadiolocation slices (Pr9 and Pr10) obtained during the survey of the above-water part of the western wall, the reinforcement intervals of type 1 and 2 were well distinguished. They are separated by vertical arrows (Fig. 14).

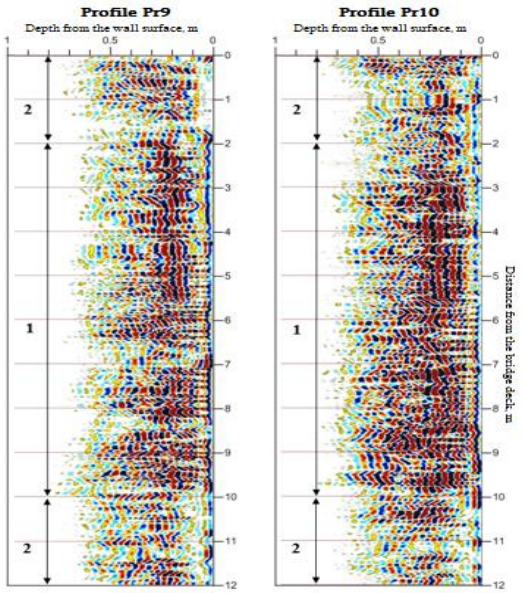

fig. 14. Types of reinforcement found along the western wall along Pr9 and Pr10.

Along the second pier, in its above-water part, we additionally conducted geolocation studies with the help of a 1500 MHz antenna. On the georadiolocation profile (Pr5) obtained by this method, the diffraction hyperbolas caused by the presence of reinforcement rods clearly appeared (Fig. 15). These georadarograms also showed intense, disturbing reverberation waves, which must be due to insufficient (not tight) contact between the antenna and the surface of the pier during investigation.

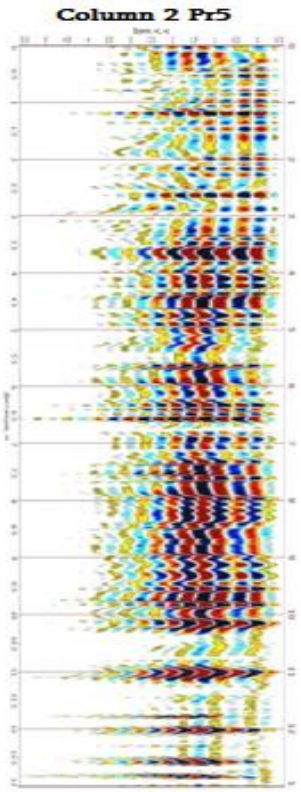

Fig. 15. Georadiolocation profile (Pr5) obtained by means of 1500 MHz antenna along the above-water part of the second pier.

Based on the georadiolocation studies, we can conclude the following:

1. Georadiolocation research method and selected equipment proved to be effective for researching the condition of Lajanur Dam structures located in Tsageri district. In particular:
2. We investigated the condition of the underwater and above-water parts of the supporting piers and the eastern and western walls, their washing depth, the arrangement and frequency of the horizontal bars of the reinforcing mesh of reinforced concrete structures. This part of the research is directly related to the topic of our paper.
3. We were given the opportunity to study the condition of the downstream located in front of the shutter shields, the configuration, depth and width of its damaged bottom.
4. Condition of low-threshold dams 1 and 2 under shutter shields.
5. Ground structure of the three areas surrounding the derivation channel and the filtration areas under the ground.

Conclusion

1. As a result of the ultrasound work, different types of damaged strength and weakened areas of the structure were identified on the piers and supporting walls. Damaged areas were mainly detected near the water surface, in the lower (489-492m) sections of the piers and walls, in the vicinity of washed-eroded areas and also at different heights. The entire vertical section of the eastern and western wall structures is characterized by a weakened structure. Here, the value of Poisson's ratio is significantly increased on the profiles sampled in the interval from 504m to 489m.
2. A relatively better quality concrete structure was found on the north side of the first pier, in the vicinity of the shutter shield along the vertical cut of the entire wall. This is confirmed by the results of both the Schmidt hammer test and the ultrasound survey.
3. The slabs placed outside the walls and piers are characterized by high concrete grade values. Their change is within 260-600. Particularly low concrete grade values were found for the eroded-washed areas of the eastern and western walls, as well as in the lower sections of the piers. In these sections, the grade of concrete varies between 150-220. The causes of these anomalies can probably be: incompatibility of the cement brand, its insufficient quantity or technological violations made during the construction.
4. With the georadiolocation method, the solution of a wide range of engineering and technical tasks can be successfully implemented at various sites and facilities. It can be used in other regions as well, for the purpose of research and diagnosis of the state of hydrotechnical structures of this type.
5. The results of the radiolocation and ultrasound research of the above-water part of the supporting piers and walls are quite well correlated. In addition, these two methods complement each other. Ultrasonic and Schmidt hammer research provides additional information on the mechanical parameters of reinforced concrete for piers and walls. And georadar allows to quickly determine inhomogeneities and defects in reinforced concrete supporting piers and walls.

References

[1] Varamashvili N., Chelidze T., Devidze M., Chikhladze V. Laboratory and mathematical modeling of landslides triggered by external factors. Field research. Transactions of Mikheil Nodia Institute of Geophysics of Ivane Javakhishvili Tbilisi State University, vol. LXVIII, Monography, Tbilisi, 2017, (in Georgian).
[2] Chelidze T., Varamashvili N., Chelidze Z., Kiria T., Ghlonti N., Kiria J., Tsamalashvili T. Costeffective telemetric monitoring and early warning systems for signaling landslide initiation. Mikheil Nodia Institute of Geophysics of Ivane Javakhishvili Tbilisi State University. Monography. Tbilisi, 2018 (in Georgian).
[3] Varamashvili N., Chelidze T., Chelidze Z., Chikhladze V., Tefnadze D. Acoustic pulses detecting methods in granular media. Journal of Georgian Geophysical Society, 2013, v. 16.

[4] Varamashvili N., Chelidze T., Chelidze Z., Gigiberia M., Ghlonti N. Acoustical methods in geodynamical and geomechanical problems. International Scientific Conference „Modern Problems of Ecology“, Kutaisi, Georgia, 21-22 September, 2018, (in Georgian)
[5] Varamashvili N., Chelidze T., Chelidze Z., Gigiberia M., Ghlonti N. Acoustics in Geophysics and Geomechanics. Journal of Georgian Geophysical Society, v. 21, 2019
[6] Heutschi K. Lecture Notes on Acoustics I. Swiss Federal Institute of Technology, ETH Zurich, 201
[7] Tomographic reconstruction for concrete using attenuation of ultrasound H.K. Chai, S. Momoki, Y.Kobayashi, D.G.Aggelis, T.Shiotani. NDT&E International 44, 2011
[8] Varamashvili N., Asanidze B., Jakhutashvili M. Ultrasonic methods for assessing the state of hydrotechnic concrete structures. International scientific conference, Natural Disasters in Georgia: Monitoring, Prevention, Mitigation. Proceedings, 2019, (in Georgian)
[9] Gucunski N., Imani A., Romero F., Nazarian S., Yuan D., Kutrubes D. Nondestructive Testing to Identify Concrete Bridge Deck Deterioration. Strategic Highway Research Program. Transportation research bord, WASHINGTON, D.C. 2013
[10] Bigman D. P. GPR Basics: A Handbook for Ground Penetrating Radar Users. Bigman Geophysical, LLC. Suwanee, GA, 2018

ბეტონის სტრუქტურების კომპლექსური კვლევა ულტრაბგერითი და გეორადიოლოკაციური მეთოდებით

ნ. ვარამაშვილი, ბ. ასანიძე, მ. ჯახუტაშვილი, ვ. გლაზუნოვი

რეზიუმე

ჩვენი კვლევის საგანი იყო, გეორადიოლოკაციური და ულტრაბგერითი მეთოდებით, ცაგერის წყალშემკრების თანამედროვე მდგომარეობის შესწავლა. გამოყენებულ იქნა გეორადარი Zond 12e. გეორადარული მონაცემები შეკრებილ და დამუშავებულ იქნა საშტატო კომპიუტერული პროგრამული უზრუნველყოფით Prizm 2.7. გეორადარის საშუალებით შესაძლებელია სხვადასხვა გარემოში არსებული სიცარიელეების, ბზარების, შესუსტებული გარემოს გამოყოფა. შესაძლებელია ასევე გარემოს დატენიანების ხარისხის განსაზღვრა. გეორადილოკაციის მეთოდით სხვადასხვა გარემოს შესასწავლად გამოიყენება სხვადასხვა სიხშირის ანტენები. ჩვენი კვლევისას გამოყენებული იქნა 1 მგჰც, ა.5 მგჰც და სხვა სიხშირის ანტენები. გარემოს მექანიკური პარამეტრების განსაზღვრისათვის და მისი სტრუქტურის დადგენისთვის ასევე ეფექტური საშუალებაა ულტრაბგერითი მეთოდი. წარმოდგენილ სამუშაოებში გამოყენებული იქნა შვეიცარული კომპანიის PROCEQ-ის მიერ წარმოებული ულტრაბგერითი აპარატურა, იმპულსური ექო გადამწოდი - Pundit PL-200PE. მიღებული მასალის დამუშავება შესრულდა Pundit - 200 და Pundit – 20PE-ს სამუშაო პროგრამის “PL-Link” საშუალებით. ულტრაბგერითი აპარატურით შესაძლებელია გარემოში არსებული სიცარიელეების, ბზარების გამოყოფა და მათი გეომეტრიული პარამეტრების შესწავლა. ასევე გარემოს მექანიკური მახასიათებლების დადგენა. ერთი და იგივე უბნების კვლევისას რადიოლოკაციით და ულტრაბგერითი მეთოდებით მიღებული შედეგები ერთმანეთთან საკმაოდ კარგ კორელაციაშია სტრუქტურის დადგენის თვალსაზრისით და ერთმანეთს ავსებენ გარემოს მექანიკური პარამეტრების და სტრუქტურის დეტალების განსაზღვრის კუთხით.

საკვანძო სიტყვები: ტომოგრაფია, ულტრაბგერითი, გეორადიოლოკაცია, GPR, არადესტრუქციული ტესტირება

Комплексное исследование бетонных конструкций ультразвуковыми и геолокационными методами

Н.Д. Варамашвили, Б.З. Асанидзе, М.Н. Джахуташвили, В.В. Глазунов

Резюме

Предметом нашего исследования было изучение современного состояния водосбора Цагери методами георадиолокации и ультразвука. В исследованиях использовался георадар Zond 12e. Данные георадара собирались и обрабатывались с помощью штатной программы Prizm 2.7. С помощью георадара можно выделить пустоты, трещины и ослабленную среду. Также возможно определение степени влажности окружающей среды. Антенны разных частот используются для исследования разных сред. При нашем исследований были использованы антенны 1 МгГц, 1.5 МгГц и других частот. Ультразвуковой метод также является эффективным средством определения механических параметров окружающей среды и ее строения. В представленных работах использовалось ультразвуковое оборудование производства швейцарской фирмы PROCEQ, импульсный эхопередатчик - Pundit PL-200PE. Обработку полученного материала проводили с помощью рабочих программ Pundit-200 и Pundit-20PE «PL-Link». С помощью ультразвукового оборудования можно выделить пустоты и трещины в окружающей среде и изучить их геометрические параметры, а также определить механические характеристики окружающей среды. При исследовании одних и тех же участков результаты, полученные радиолокационным и ультразвуковым методами, достаточно хорошо коррелируют между собой в части определения структуры и дополняют друг друга в части определения механических параметров среды и деталей строения.

Ключевые слова: томография, ультразвук, георадиолокация, георадар, неразрушающий контроль.

Journal of the Georgian Geophysical Society, e-ISSN: 2667-9973, p-ISSN: 1512-1127
Physics of Solid Earth, Atmosphere, Ocean and Space Plasma, v. 26(1), 2023, pp. 19-29

Study of the Relationship Between the Mean Annual Sum of Atmospheric Precipitation and Re-Activated and New Mudflow Cases in Georgia

[1]Avtandil G. Amiranashvili, [1]Tamaz L. Chelidze,
[1]David T. Svanadze, [2]Tamar N. Tsamalashvili, [3]Genadi A. Tvauri

[1]M. Nodia Institute of Geophysics of I. Javakhishvili Tbilisi State University, Tbilisi, Georgia
avtandilamiranashvili@gmail.com; https://orcid.org/0000-0001-6152-2214
[2]A. Janelidze Geological Institute of I. Javakhishvili Tbilisi State University, Tbilisi, Georgia
[3]E. Andronikashvili Institute of Physics of I. Javakhishvili Tbilisi State University, Tbilisi, Georgia

ABSTRACT

Taking into account the earlier statistical analysis of long-term variations in the of annual sum of precipitation for 21 Georgian meteorological stations (P) located in mudflow areas, the relationship between the average annual precipitation for these stations (P_a) and the number of re-activated and new cases of mudflows (MF) was studied. Using previously obtained forecast data for P_a, the MF values were calculated up to 2045. The data of the Georgian Environment Agency on MF for the period 1996-2018 were used.
In particular, the following results are obtained.
Cross-correlation analysis of the time series of P_a and MF values showed that the best correlation between the indicated parameters is observed with a five-year advance of precipitation data. With this in mind, a linear regression equation between the five-year moving average P_a and the five-year moving average MF is derived. Using this equation and P_a forecast data, five-year moving averages of re-activated and new mudflow events up to 2045 were estimated.

Key words: *atmospheric precipitation, mudflows, climate change.*

Introduction

Mudflows (MF), like landslides (LS), are one of the types of natural disasters. Mudflow processes are widespread almost everywhere and are dangerous with destruction, often accompanied by human casualties [1-5]. This problem is also very relevant for Georgia, where the number of reactivated and new cases of mudflows only in 1996-2020 exceeded 3200 [6,7]. In this regard, special attention has always been paid to the study of mudflow processes in this area [5–9].

The urgency of this problem increased significantly after the tragedy that happened on August 3, 2023 in the western Georgia in the Shovi resort (Oni municipality of Racha-Lechkhumi and Kvemo Svaneti region), when, as a result of an intense landslide-mudflow process, the central part of the resort was filled with mud flows (Fig. 1,2), which led to the death of more than thirty people [https://civil.ge/archives/554327].

According to preliminary report by the National Environmental Agency the landslide-mudflow was caused by intense melting of glaciers, collapse of rock formations in their headwaters, heavy rains, erosive processes and a glacier runoff.

The Agency said a collapse of a rocky mass on the western side of the Buba glacier had led to its collision with the glacier after coming into motion and caused a collapse of a part of the glacier. The body said the development may have caused an overflow of subglacial waters, with the resulting flow directed through the valley bed at a high speed in the locality [https://agenda.ge/en/news/2023/2999].

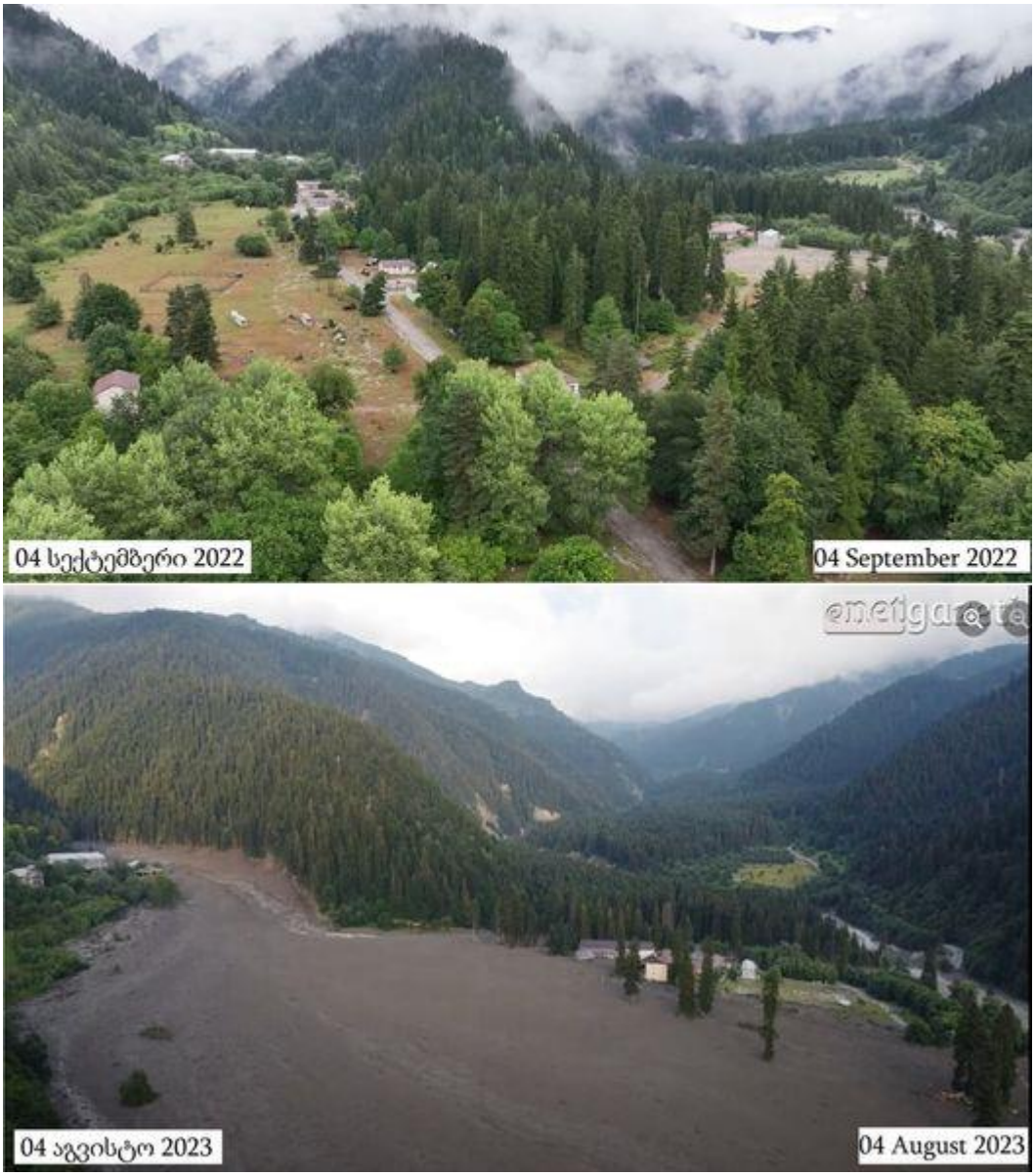

Fig. 1. View of the Shovi resort 11 months before mudflow and on the second day after the mudflow [https://www.facebook.com/photo/?fbid=6326794327369246&set=a.412771738771564]

Mudflows, as well as landslides, depend on many individual and complex processes, in particular, on precipitation. At the same time, the time scale of the influence of atmospheric precipitation on the provocation of mudflows has a wide range - from several tens of minutes to several days, months and years (climatic time scale) [9-12]. For exampe, according to [9] activation of landslide processes in accordance with atmospheric precipitation regime clearly indicates the correlation regularities: the intervals between atmospheric precipitations able to provoke landslide processes, fluctuate within 2,5-5 years, while the sequence line between the increase and deficit of precipitations, which represents one cycle of development of the landslide processes, ranges within 3-8 years.

In recent years, we have carried out a number of additional studies of the relationship between atmospheric precipitation and landslide processes. In this case, data from ground-based and satellite

measurements of precipitation were used [13,14]. Thus, using the example of the study of landslides, it was found in [15] that in Georgia, with an increase in the annual amount of atmospheric precipitation, there is a tendency to increase their landslides in accordance with the second degree of the polynomial. In another work [16], in particular, it was found that with an increase in the monthly amount of precipitation, a linear trend of an increase in the number of landslides is observed.

The paper [17] is aimed to assess the rainfall conditions, which can lead to initiation of mass-movement using limited terrestrial and satellite-based data on the summary rainfall and landslide occurrence. In particular, for administrative regions of Georgia precipitation effects on landslides activity for 1, 3, 5, 7, 10, 20 and 30 days before their onset is studied.

This approach can be useful for a lot of regions in the world, where LS and meteorological data are not detailed enough to calculate the standard rainfall intensity/duration threshold graph for landslide occurrence.

Some results of statistical analysis of long-term variations of annual amount of atmospheric precipitation for 21 meteorological stations of Georgia (P) located in areas with landslides, average annual amount of precipitation for these stations (P_a), relationship between the P_a and number of re-activated and new cases of landslides (LS), and the estimated values of LS up to 2045 using predictive data on P_a are presented in [18]. Data from the Environmental Agency of Georgia on the P in period 1936 - 2020 and data on LS in period 1996 – 2018 are used.

In particular, the following results are obtained.

The correlations between the annual amounts of P at each of the meteorological stations with averaged data for all 21 stations P_a are established.

In 1981-2020, compared with 1936-1975, no significant variability of the mean P values is observed at 11 stations, an increase - at 6 stations, and a decrease - at 4 stations. The P_a value do not change during the indicated time periods.

The forecast of the P_a value up to 2040 were estimated taking into account the periodicity of precipitation variability, which is 11 years.

A cross-correlation analysis of the time series of the P_a and LS values showed that the best correlation between the indicated parameters is observed with a five-year advance of precipitation data. With this in mind, a linear regression equation was obtained between the five-year moving average of the P_a and the five-year moving average of the LS values.

Using this equation and predictive P_a data, five-year moving averages of re-activated and new landslides cases up to 2045 were estimated.

This work is a continuation of previous studies [18]. Below are the results of a study of the relationship between the average annual precipitation (Pa) for 21 meteorological stations and the number of re-activated and new mudflows (MF) in Georgia, and an assessment of the MF values until 2045 using predictive data on Pa.

Study Area, Materials and Methods

Study Area – Georgia. Data from the Environmental Agency of Georgia on the annual amount of atmospheric precipitation for 21 meteorological stations of Georgia located in areas with landslides (fig. 1) and data on re-activated and new mudflows cases (fig. 2) are used. Period of observation: for atmospheric precipitation from 1936 to 2020, for re-activated and new landslides cases from 1996 to 2018.

Fig 1. Location of 21 meteorological stations on the mudflow risk zones map of Georgia by probability and damage.

In the proposed work the analysis of data is carried out with the use of the standard statistical analysis methods [19].

The following designations will be used below: Mean – average values; Max - maximal values; Min – minimal values; Range – Max-Min; St Dev - standard deviation; St Err - standard error; Cv – coefficient of variation = 100·St Dev/Mean, %; Conf. Lev. - confidence level of the mean; Low and Upp – lower and upper levels of the confidence interval of the mean; R – coefficient of linear correlation; CR - coefficient of cross correlation; α - the level of significance; P - annual sum of atmospheric precipitation for separated meteorological station; Pa - mean annual sum of atmospheric precipitation for 21 meteorological stations; MF - re-activated and new lmudflows cases. The forecast of P_a using the AAA version of the Exponential Smoothing (ETS) algorithm was carried out [20]. Programs Excel 16 and Mesosaur for calculation were used.

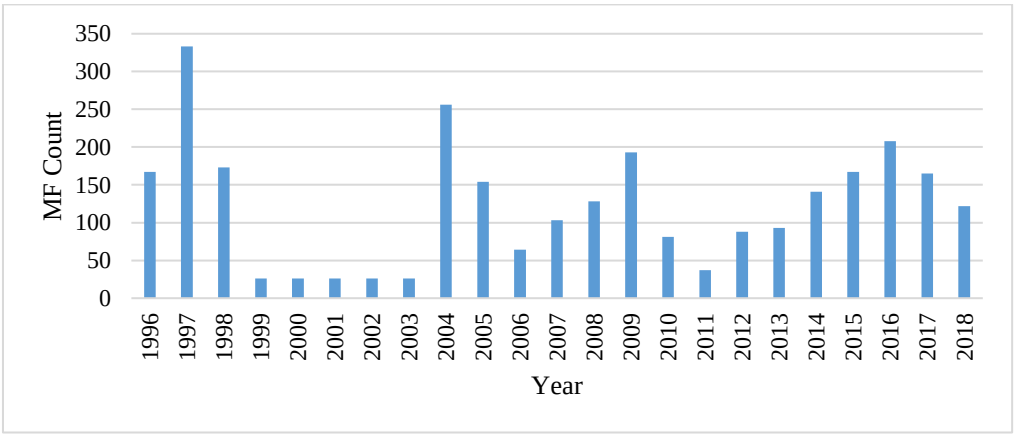

Fig 2. Changeability of re-activated and new mudflows cases in Georgia from 1996 to 2018.

Results and Discussions

Results of statistical analysis of relationship between the P_a and number of re-activated and new cases of mudflows, and the estimated values of MF up to 2045 using predictive data on P_a [18] are presented below in Table 1,2 and Fig. 3-7.

Table 1. Statistical characteristics of MF cases in Georgia in 1996-2018.

Parameter	Mean	Max	Min	Range	St Err	St Dev	Cv, %	Conf. Lev. , 95.0%
MF	122	333	26	307	17	81	66.7	35

Table 1 presents the statistical characteristics of MF cases in Georgia in 1996-2018. On average, 122 cases of MF were recorded per year with a range of changes from 26 to 333 cases. Significant variations in the amount of MF were observed in the specified time period (Cv = 66.7%, Conf. Lev. = 35).

Let us consider the nature of the relationship between the annual number of re-activated and new landslides and the annual sum of precipitations. Fig. 3 shows the cross-correlation between values of P_a and the MF cases.

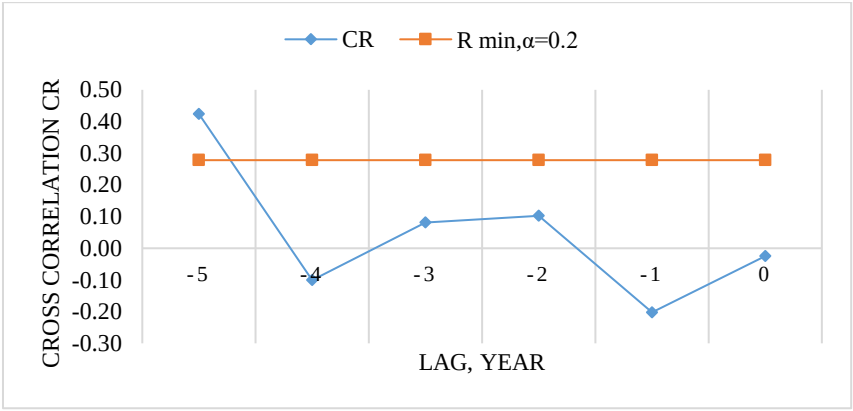

Fig 3. Cross-correlation between the P_a and MF values.

As follows from this figure, a significant correlation between the studied parameters is observed in the fifth lag before the landslide phenomena.

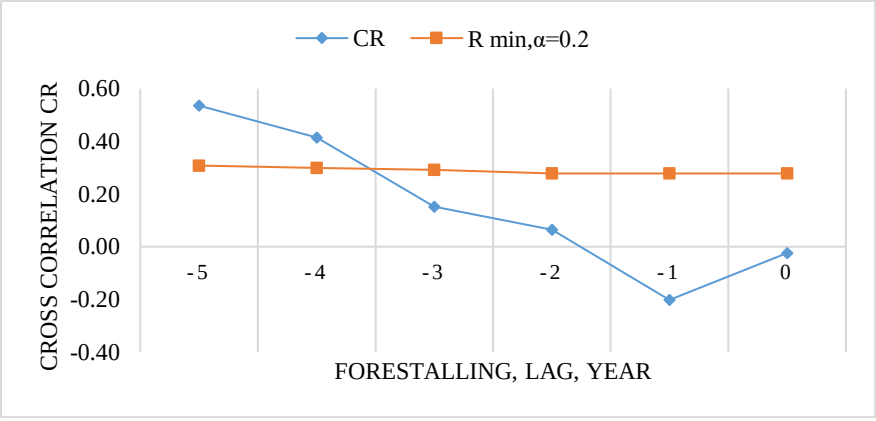

Fig 4. Cross-correlation between the five-year moving average of the P_a and five-year moving average of the MF values.

Another Fig. 4 shows the cross-correlation between the moving average of the P_a values and the moving average of the LS cases. As follows from Fig. 4, a significant relationship between the studied parameters is observed in the fourth and fifth lags before the landslides. Comparison fig. 3 and 4 shows that in the second case the relationship between P_a values and MF number is more representative than in the first case. Taking into account that in the fifth lag before the onset of mudflows, the correlation

coefficient is higher than in the fourth lag, a linear regression was built between the five-year moving averages of P_a values and the five-year moving averages of MF number (Fig. 5).

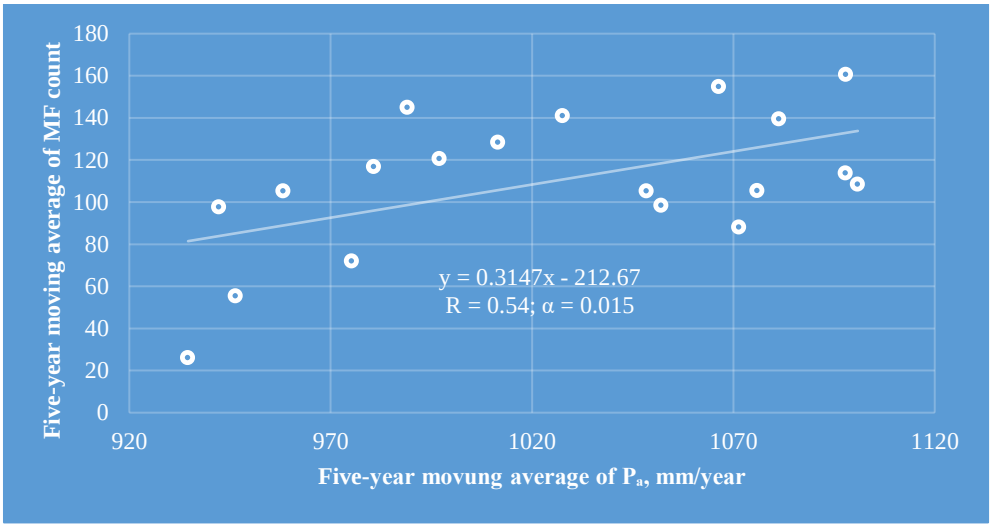

Fig 5. Linear correlation and regression between the five-year moving average of the P_a (1991-1995, 1992-1996, …, 2009-2013) and the five-year moving average of the MF (1996-2000, 2001-2005 ,…, 2014-2018) values.

As follows from Fig. 5, there is a significant direct linear relationship between the values of these parameters, which can be used to predict five-year moving averages of MF cases from the forecast values of the average annual sum precipitation per one meteorological station.

Fig. 6 shows data on the expected five-year moving average of re-activated and new mudflows cases up to 2041-2045, calculated according to the formula presented in Fig. 5 with using the data of predicted five-year moving average of P_a values [18].

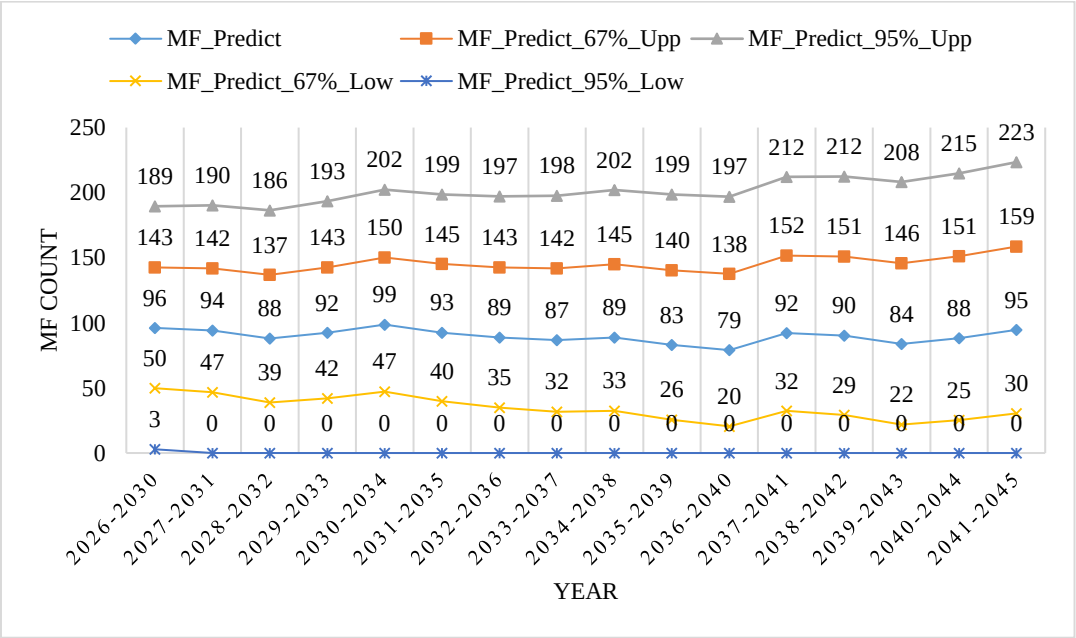

Fig 6. Interval prediction of five-year moving averages of re-activated and new mudflows cases from 2026 up to 2045.

Graphs in Fig. 6 represent the center points of the forecast of the number of mudflows (MF_Predict), as well as the lower and upper confidence levels of this forecast (MF_Predict_67%_Low, MF_Predict_67%_Upp, etc.). Note that all values of MF_Predict_95%_Low = 0.

Table 2 shows the comparative statistical characteristics of predicted (2026-2045) and real (1996-2018) five-year moving averages of re-activated and new mudflows cases.

Table 2. Statistical characteristics of predicted (2026-2045) and real (1996-2018) five-year moving averages re-activated and new mudflows cases in Georgia.

Period	2026-2045				1996-2018
Parameter	MF_Predict_ 67%_Low	MF_Predict	MF_Predict_ 67%_Upp	MF_Predict_ 95%_Upp	MF_Real
Mean	34	90	145	201	110
Max	50	99	159	223	161
Min	20	79	137	186	26
Range	29	20	22	37	135
St Err	2.3	1.3	1.5	2.6	7.9
St Dev	9.0	5.1	5.8	10.3	33.7
Cv, %	26.4	5.7	4.0	5.1	30.8
Conf. Lev., 95.0%	4.6	2.6	2.9	5.2	15.6

As follows from this Table, the average MF_Real values fall within the range of values between MF_Predict and MF_Predict_67%_Upp (90<110<145). The maximum values of MF_Real fall within the range of values between MF_Predict_67%_Upp and MF_Predict_95%_Upp (159<161<223). The minimum values of MF_Real fall within the range of values between MF_Predict and MF _Predict_67%_ Low (20<26<79). Thus, in general, in the next two decades, one should not expect a significant intensification of mudflow processes in Georgia due to the expected variability of the annual sum of atmospheric precipitation. However, in certain regions of Georgia, where a significant increase in precipitation is observed a significant activation of mudflow phenomena (as well as landslides [18]) quite possible.

Finally, in Fig. 7 and 8 linear correlation and regression between LS and MF cases and between five-year moving averages LS and MF cases in Georgia in 1996-2018 are presented.

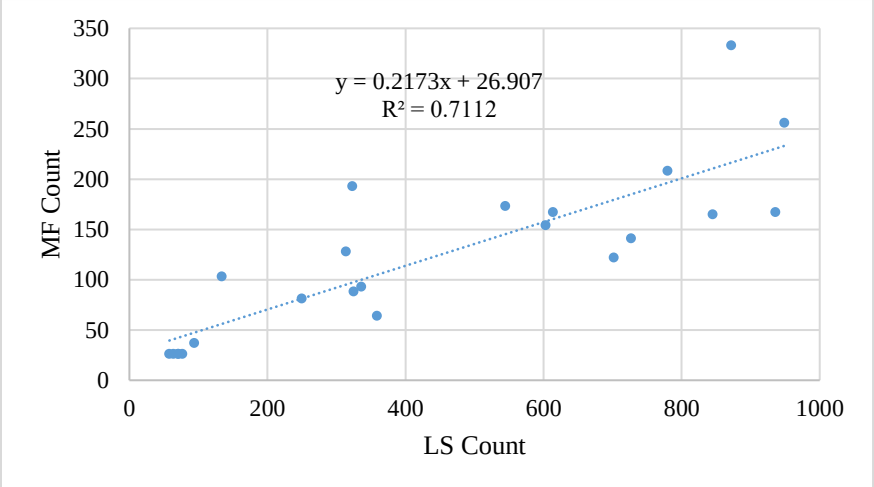

Fig.7. Linear correlation and regression between LS and MF cases in Georgia in 1996-2018.

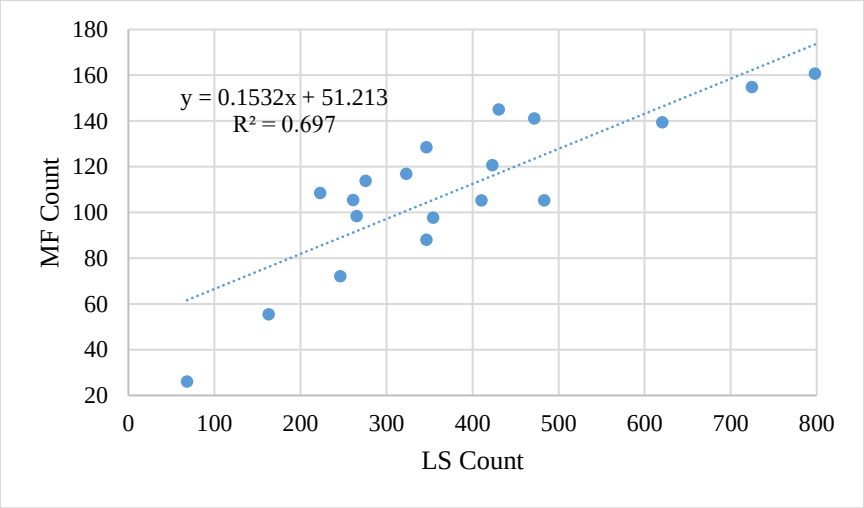

Fig.8. Linear correlation and regression between five-year moving averages LS and MF cases in Georgia in 1996-2018.

The linear correlation coefficient between LS and MF is 0.84 and 0.83, respectively (Fig. 7 and 8, high correlation [19]).

Conclusion

In the future, using the data of the new catalog of natural hazards being prepared in Georgia [21,22], we plan to continue more detailed studies of landslides and mudflows both for the territory of Georgia as a whole and for its individual regions, taking into account climate change [4].

It is also planned to carry out work on the implementation of the existing early warning system for the activation of landslide / mudflow events [23]. In addition, it is planned to develop research on long-term and short-term forecasting of landslide and mudflow processes using ground-based, radar and satellite information on the parameters associated with these processes [13,14,17,24-27].

Acknowledgement

This work was supported by Shota Rustaveli National Science Foundation of Georgia (SRNSFG), Grant number FR-19-8190, "Assessment of landslide and mudflow hazards for Georgia using stationary and satellite rainfall data".

References

[1] Landslides and Mudflows. Volume 1-2, Center for International Projects UNESCO-UNEP, 1984.

[2] Sheko A., Krupaderov V., Malneva M., Dykonova V., Balandin G. Factors of Formation Factor of Landslides and Mudflows. Monography – Landslide and Mudflow, Center for International Projects UNESCO-UNEP, 1984, pp. 16-51.

[3] Amiranashvili A.G. Increasing Public Awareness of Different Types of Geophysical Catastrophes, Possibilities of Their Initiation as a Result of Terrorist Activity, Methods of Protection and Fight with Their Negative Consequences. Engaging the Public to Fight Consequences of Terrorism and Disasters. NATO Science for Peace and Security Series E: Human and Societal Dynamics, vol. 120. IOS Press, Amsterdam•Berlin•Tokyo•Washington, DC, ISSN 1874-6276, 2015, pp.155-164. http://www.nato.int/science; http://www.iospress.nl http://www.springer.com

[4] Kartvelishvili L., Tatishvili M., Amiranashvili A.,Megrelidze L., Kutaladze N. Weather, Climate and their Change Regularities for the Conditions of Georgia. Monograph, Publishing House "UNIVERSAL", Tbilisi 2023, 406 p., https://doi.org/10.52340/mng.9789941334658

[5] Varazanashvili O., Tsereteli N., Amiranashvili A., Tsereteli E., Elizbarashvili E., Dolidze J., Qaldani L., Saluqvadze M., Adamia Sh., Arevadze N., Gventcadze A. Vulnerability, Hazards and Multiple Risk Assessment for Georgia. Natural Hazards, Vol. 64, Number 3, 2012, pp. 2021-2056. DOI: 10.1007/s11069-012-0374-3, http://www.springerlink.com/content/9311p18582143662/fulltext.pdf.
[6] Fourth National Communication of Georgia Under the United Nations Framework Convention on Climate Change. Chapter 4.9 Geological Hazards in Georgia, Tbilisi, 2021, pp. 278-286.
[7] Tsereteli E., Bolashvili N., Gaprindashvili G., Gaprindashvili M., Machavariani N. Risk of Natural Hazards in Georgia. Journal of the Georgian Geophysical Society, e-ISSN: 2667-9973, p-ISSN: 1512-1127, Physics of Solid Earth, Atmosphere, Ocean and Space Plasma, v. 24(2), 2021, pp. 22 – 29. DOI: https://doi.org/10.48614/ggs2420213316
[8] Gaprindashvili M., Tsereteli E., Gaprindashvili G., Kurtsikidze O. Landslide and Mudflow Hazard Assessment in Georgia. In: Bonali, F.L., Pasquaré Mariotto, F., Tsereteli, N. (eds) Building Knowledge for Geohazard Assessment and Management in the Caucasus and other Orogenic Regions. NATO Science for Peace and Security Series C: Environmental Security. Springer, Dordrecht, 2021, https://doi.org/10.1007/978-94-024-2046-3_14
[9] Tsereteli E., Gaprindashvili G., Gaprindashvili M. Natural Disasters (Mudflow, Landslide, Etc.). In: Bolashvili, N., Neidze, V. (eds) The Physical Geography of Georgia. Geography of the Physical Environment. Springer, Cham., 2022 https://doi.org/10.1007/978-3-030-90753-2_7
[10] Segoni S., Piciullo L., Gariano S.L. A review of the recent literature on rainfall thresholds for landslide occurrence. Landslides, 15, 2018, pp. 1483–1501, DOI 10.1007/s10346-018-0966-4.
[11] Kirschbaum D., Stanley T. Satellite-Based Assessment of Rainfall-Triggered Landslide Hazard for Situational Awareness. Earth's Future, 6, 2018, pp.505-523, https:// doi.org/10.1002/, 2017EF000715
[12] Chelidze, T., Tsamalashvili, T., Fandoeva, M. Mass-movement stationary hazard maps of Georgia including precipitation triggering effect: fuzzy logic approach. Bull. Georg. Nat. Acad. Sci., vol. 16, no. 2, 56-63, 2022, http://science.org.ge/bnas/t16-n2/07_Chelidze_Geophysics.pdf
[13] Amiranashvili A., Chelidze T., Svanadze D., Tsamalashvili T., Tvauri G. On the Representativeness of Data from Meteorological Stations in Georgia for Annual and Semi-Annual Sum of Atmospheric Precipitation Around of These Stations. International Scientific Conference „Natural Disasters in the 21st Century: Monitoring, Prevention, Mitigation". Proceedings, ISBN 978-9941-491-52-8, Tbilisi, Georgia, December 20-22, 2021. Publish House of Iv. Javakhishvili Tbilisi State University, Tbilisi, 2021, pp. 79 - 83. http://openlibrary.ge/bitstream/123456789/9566/1/20_Conf_ND_2021.pdf
[14] Amiranashvili A., Chelidze T., Svanadze D., Tsamalashvili T., Tvauri G. Comparison of Data from Ground-Based and Satellite Measurements of the Monthly Sum of Atmospheric Precipitation on the Example of Tbilisi City in 2001-2020. Int. Conf. of Young Scientists "Modern Problems of Earth Sciences". Proceedings, ISBN 978-9941-36-044-2, Publish House of Iv. Javakhishvili Tbilisi State University, Tbilisi, November 21-22, 2022, pp. 154-158. http://openlibrary.ge/bitstream/123456789/10251/1/37_YSC_2022.pdf
[15] Amiranashvili A., Chelidze T., Dalakishvili L., Svanadze D., Tsamalashvili T., Tvauri G. Preliminary Results of a Study of the Relationship Between the Variability of the Mean Annual Sum of Atmospheric Precipitation and Landslide Processes in Georgia. Int. Sc. Conf. „Modern Problems of Ecology", Proc., ISSN 1512-1976, v. 7, Tbilisi-Telavi, Georgia, 26-28 September, 2020, pp. 202-206. http://www.dspace.gela.org.ge/bitstream/123456789/8809/1/Eco_2020_3.33.pdf
[16] Amiranashvili A., Chelidze T., Dalakishvili L., Svanadze D., Tsamalashvili T., Tvauri G. Preliminary Results of a Study of the Relationship Between the Monthly Mean Sum of Atmospheric Precipitation and Landslide Cases in Georgia. Journal of the Georgian Geophysical Society, ISSN: 1512-1127, Physics of Solid Earth, Atmosphere, Ocean and Space Plasma, v. 23(2), 2020, pp. 37 – 41. DOI: https://doi.org/10.48614/ggs2320202726
[17] Chelidze T., Amiranashvili A., Svanadze D., Tsamalashvili T., Tvauri G. Terrestrial and Satellite-Based Assessment of Rainfall Triggered Landslides Activity in Georgia, Caucasus. Bull. Georg. Nat. Acad. Sci., vol. 17, no. 2, 71-77, 2023, http://science.org.ge/bnas/vol-17-2.html
[18] Amiranashvili A., Chelidze T., Svanadze D., Tsamalashvili T., Tvauri G. Some Results of a Study of the Relationship Between the Mean Annual Sum of Atmospheric Precipitation and Re-Activated and New Landslide Cases in Georgia Taking into Account of Climate Change. Journal of the Georgian Geophysical Society, e-ISSN: 2667-9973, p-ISSN: 1512-1127, Physics of Solid Earth, Atmosphere,

Ocean and Space Plasma, v. 25(2), 2022, pp. 38–48. https://openjournals.ge/index.php/GGS/article/view/5959,
DOI: https://doi.org/10.48614/ggs2520225959
[19] Hinkle D. E., Wiersma W., Jurs S. G. Applied Statistics for the Behavioral Sciences. Boston, MA, Houghton Mifflin Company, ISBN: 0618124055; 9780618124053, 2003, 756 p.
[20] Box G.E.P, Jenkins G.M., Reinsel G.C. Time Series Analysis: Forecasting & Control (3rd Edition). ISBN10: 0130607746, ISBN13: 9780130607744. Prentice Hall, 1994, 592 p.
[21] Varazanashvili O.Sh., Gaprindashvili G.M., Elizbarashvili E.Sh., Basilashvili Ts.Z., Amiranashvili A.G. Principles of Natural Hazards Catalogs Compiling and Magnitude Classification. Journal of the Georgian Geophysical Society, e-ISSN: 2667-9973, p-ISSN: 1512-1127, Physics of Solid Earth, Atmosphere, Ocean and Space Plasma, v. 25(1), 2022, pp. 5-11. DOI: https://doi.org/10.48614/ggs2520224794
[22] Gaprindashvili G., Varazanashvili O., Elizbarashvili E., Basilashvili Ts., Amiranashvili A., Fuchs S. GeNHs: the First Natural Hazard Event Database for the Republic of Georgia. EGU General Assembly 2023, EGU23-1614.
[23] Chelidze T., Varamashvili N., Chelidze Z., Kiria T., Ghlonti N., Kiria J., Tsamalashvili T. Cost-Effective Telemetric Monitoring and Early Warning Systems for Signaling Landslide Initiation. Monograph, M. Nodia Institute of Geophysics, TSU, Tbilisi, 2018,127 p., (in Georgian).
[24] Amiranashvili A., Chikhladze V., Dzodzuashvili U., Ghlonti N., Sauri I., Telia Sh., Tsintsadze T. Weather Modification in Georgia: Past, Present, Prospects for Development. Int. Sc. Conf. „Natural Disasters in Georgia: Monitoring, Prevention, Mitigation“. Proc., Tbilisi, Georgia, December 12-14, 2019, pp. 213-219.
[25] Gvasalia G., Loladze D. Modern Meteorological Radar “WRM200” In Kutaisi (Georgia). International Scientific Conference „Natural Disasters in the 21st Century: Monitoring, Prevention, Mitigation“. Proceedings, ISBN 978-9941-491-52-8, Tbilisi, Georgia, December 20-22, 2021. Publish House of Iv. Javakhishvili Tbilisi State University, Tbilisi, 2021, pp. 147 - 150. http://www.dspace.gela.org.ge/bitstream/123456789/9548/1/38_Conf_ND_2021.pdf
[26] Amiranashvili A., Chelidze T., Svanadze D., Tsamalashvili T., Tvauri G. Abnormal Precipitation Before the Landslide in Akhaldaba (A Suburb of Tbilisi, Georgia) on June 13, 2015 According to Radar Measurements. Journal of the Georgian Geophysical Society, e-ISSN: 2667-9973, p-ISSN: 1512-1127, Physics of Solid Earth, Atmosphere, Ocean and Space Plasma, v. 26(1), 2023, pp. 30–41.
[27] Stankevich S.A., Titarenko O.V, Svideniuk M.O. Landslide Susceptibility Mapping using GIS-based Weight-of-Evidence Modelling in Central Georgian Regions. International Scientific Conference „Natural Disasters in Georgia: Monitoring, Prevention, Mitigation“, Proceedings, Tbilisi, Georgia, December 12-14, 2019, pp. 187-190. http://openlibrary.ge/bitstream/123456789/8668/1/44_Conf_NDG_2019.pdf

საქართველოში ატმოსფერული ნალექების ჯამური საშუალო წლიური და რე-აქტივიზებული და ახალი ღვარცოფების შემთხვევებს შორის კავშირის კვლევა

ა. ამირანაშვილი, თ. ჭელიძე, დ. სვანაძე, თ. წამალაშვილი, გ. თვაური

რეზიუმე

წლიური ნალექების რაოდენობის გრძელვადიანი ცვალებადობის ადრინდელი სტატისტიკური ანალიზის გათვალისწინებით ღვარცოფულ რაიონებში მდებარე 21

საქართველოს მეტეოროლოგიური სადგურისთვის (P), შესწავლილია კავშირი ამ სადგურების საშუალო წლიურ ნალექს (P_a) და რეაქტივირებულთა და ღვარცოფის (MF) ახალი შემთხვევების რაოდენობას შორის. P_a-ისთვის ადრე მიღებული საპროგნოზო მონაცემების გამოყენებით, გამოითვალა MF მნიშვნელობები 2045 წლამდე. გამოყენებული იქნა საქართველოს გარემოს დაცვის სააგენტოს მონაცემები MF-ის შესახებ 1996-2018 წლებში.
კერძოდ, მიღებულია შემდეგი შედეგები.
P_a და MF მნიშვნელობების დროის სერიების კროს-კორელაციურმა ანალიზმა აჩვენა, რომ საუკეთესო კორელაცია მითითებულ პარამეტრებს შორის შეინიშნება ნალექების მონაცემების მცოცავი ხუთწლიანი ინტერვალისათვის. ამის გათვალისწინებით, მიღებულია წრფივი რეგრესიის განტოლება ხუთწლიან მოძრავ საშუალო P_a-სა და ხუთწლიან მოძრავ საშუალო MF-ს შორის.
ამ განტოლებისა და P_a პროგნოზის მონაცემების გამოყენებით, შეფასდა 2045 წლამდე ხელახლა გააქტიურებული და ახალი ღვარცოფული მოვლენების ხუთწლიანი მოძრავი საშუალო მაჩვენებლები.

საკვანძო სიტყვები: ნალექი, ღვარცოფი, კლიმატის ცვლილება.

Изучение связи между среднегодовой суммой атмосферных осадков и количеством ре-активированных и новых случаев селей в Грузии

А.Г. Амиранашвили, Т.Л. Челидзе, Д.Т. Сванадзе, Т.Н. Цамалашвили, Г.А. Тваури

Резюме

С учетом проведенного ранее статистического анализа многолетних вариаций суммы годовых осадков для 21 метеостанции Грузии (P), расположенных в селевых районах, изучена связь между среднегодовым количеством осадков для этих станций (P_a) и количеством ре-активированных и новых случаев селей (MF). С использованием ранее полученных прогнозных данных для P_a проведены расчеты значений MF до 2045 г. Использовались данные Агентства окружающей среды Грузии по MF за период 1996-2018 гг.
В частности, получены следующие результаты.
Кросс-корреляционный анализ временных рядов значений P_a и MF показал, что наилучшая корреляция между указанными параметрами наблюдается при пятилетнем упреждении данных об осадках. С учетом этого получено уравнение линейной регрессии между пятилетним скользящим средним значением P_a и пятилетним скользящим средним значением MF.
Используя это уравнение и прогностические данные о P_a, были оценены пятилетние скользящие средние ре-активированных и новых случаев селей до 2045 года.

Ключевые слова: атмосферные осадки, сели, изменение климата.

Journal of the Georgian Geophysical Society, e-ISSN: 2667-9973, p-ISSN: 1512-1127
Physics of Solid Earth, Atmosphere, Ocean and Space Plasma, v. 26(1), 2023, pp. 30-41

Abnormal Precipitation Before the Landslide in Akhaldaba (A Suburb of Tbilisi, Georgia) on June 13, 2015 According to Radar Measurements

[1]Avtandil G. Amiranashvili, [1]Tamaz L. Chelidze, [1]David T. Svanadze, [2]Tamar N. Tsamalashvili, [3]Genadi A. Tvauri

[1]M. Nodia Institute of Geophysics of I. Javakhishvili Tbilisi State University, Tbilisi, Georgia
avtandilamiranashvili@gmail.com; https://orcid.org/0000-0001-6152-2214
[2]A. Janelidze Geological Institute of I. Javakhishvili Tbilisi State University, Tbilisi, Georgia
[3]E. Andronikashvili Institute of Physics of I. Javakhishvili Tbilisi State University, Tbilisi, Georgia

ABSTRACT

Results of the analysis of radar measurements of precipitation intensity (P) preceding the landslide in the vicinity of Akhaldaba (a suburb of Tbilisi, Georgia) on June 13, 2015 from 21.00 to 23.97 h are presented. In particular, the following results are obtained. Time-series of precipitation intensity under zone with the maximum radar reflectivity of the cloud has the form of a fifth power of polynomial. Time series of areas of precipitation of different intensity under the cloud were obtained and their statistical characteristics were studied. Dependence of the average intensity of precipitation under the cloud on the effective radius from the zone with the maximum radar reflectivity is obtained.
Statistical characteristics of precipitation intensity over the center of the landslide top is presented. Sum of precipitation under zone with the maximum radar reflectivity of the cloud and over the center of the landslide top on 13 June 2015 from 21.00 to 23.97 h and before landslide from 21.00 to 22.45 h is assessed.

Key words: *atmospheric precipitation, radar observations, landslides.*

Introduction

Almost all types of natural disasters are observed in Georgia (earthquakes, floods, hurricanes, thunderstorms, hail, droughts, landslides, mudflows, avalanches, tornadoes, forest fires, etc.), often causing heavy economic damage and human casualties [1-18]. The last such example is the landslide-mudflow process that occurred on August 3, 2023 in the Oni municipality of Racha-Lechkhumi and Kvemo Svaneti region of Georgia, which led to a many-meter filling of the central part of the Shovi resort with mudflows and more than thirty human victims [https://civil .ge/archives/554327]. The last case, in terms of the scale of human losses, exceeded the consequences of the flood in Tbilisi on June 13-14, 2015, when 20 people were confirmed dead [14,15; https://en.wikipedia.org/wiki/2015_Tbilisi_flood].

At the same time, many of these processes are associated with climate change in Georgia [10, 18-22], which affects regime of temperature, atmospheric precipitation, melting glaciers and other parameters that provoke an increase in the number of natural disasters (droughts, floods, landslides, mudflows, forest fires, etc.).

As regards the study of landslide-mudflow processes, the activation of which is often associated with the regime of atmospheric precipitation of various time scales (from minutes to several years) [23], we have created and are improving a modern database of these processes [12, 13], as well as precipitation based on ground, satellite and radar observations [14,15,24-28].

Using this database, in recent years, we have studied the relationship of landslides and mudflows with atmospheric precipitation of various time scales (from hours to climatic scales) and territories (landslide site, regions of Georgia, the territory of Georgia [14,15,29-34].

In particular, in the works [14,15] data on the radar characteristics of a rain cloud that caused a landslide in Akhaldaba and a catastrophic flood in Tbilisi on June 13-14, 2015 are presented. The temporal variability of the maximum radar reflectivity of the cloud, precipitation intensity, etc. was studied. It is noteworthy that the cloud did not move much and was over the zone where the landslide descended for more than 5 hours. The consequences of this landslide are well known - the closure of the Vere River, the accumulation of water, the breaking of an artificial dam and the catastrophic flood in Tbilisi.

This work is a continuation of previous studies [14,15]. The results of a more detailed analysis of the temporal variability of precipitation over the landslide zone in Akhaldaba on June 13, 2015 are presented below.

Study Area, Materials and Methods

Study Area – landslide zone in Akhaldaba (a suburb of Tbilisi, Georgia, Fig. 1).

Fig.1. Landslide in Akhaldaba on June 13, 2015 [https://reliefweb.int/map/georgia/landslide-affected-areas-west-tbilisi-georgia-16-jul-2015].

Fig.1 illustrates satellite-detected areas of landslide damage in Akhaldaba. Following flash floods in the region on 14 June 2014, a landslide on the Vere River near the village of Akhaldaba damaged several road sections in the area. Using a satellite image acquired 24 June 2015 by the GeoEye-1 satellite, UNOSAT delineated the primary landslide areas stretching southeast of the Vere River,

between Akhaldaba and Tskneti. The area directly affected by the landslide measures about 537065 square meters, while 1110 meters of roadway were buried or damaged by the landslide.

Coordinates of the center of the landslide top: 41.68 N°, 44.68 E°,1289 m a.s.l. [14].

Precipitation intensity was measured using meteorological radar "METEOR 735 CDP 10 - Doppler Weather Radar". Radar is established in the village Chotori of the Signagi municipality of Kakheti region of Georgia [35,36]. In this work radar product MPPI (dBz) is used [37-39]. Example of this radar product on Fig. 2 is presented. Time designation (Fig. 2), for example, t = 14 hour 33 min – 14:33 h. In Fig. 3-5 minutes are given in fractions of an hour, for example, t = 21 hour 55 min – 21.92 h, etc. The data of the Georgian Environment Agency on atmospheric precipitation were also used in the work.

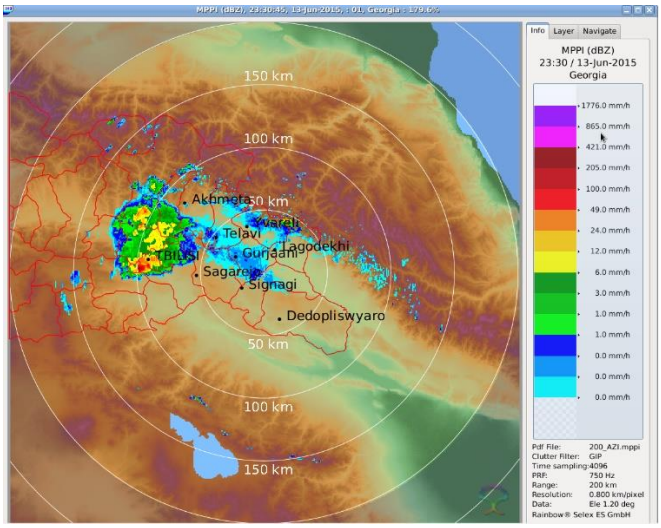

Fig. 2. Example of radar data of the precipitation intensity in Tbilisi on 13 June 2015 in 23:30 h.

In the proposed work the analysis of data is carried out with the use of the standard statistical analysis methods [20].

The following designations will be used below: Max - maximal values; Min – minimal values; Range – Max-Min; St Dev - standard deviation; St Err - standard error; C_V – coefficient of variation = 100·St Dev/Mean, %; R^2 - coefficient of determination; R - coefficient of linear correlation; K_{DW} - Durbin-Watson statistic; P - precipitation intensity, mm/h; P_s – sum of precipitation, mm; P_a - average intensity of precipitation under the cloud, mm/h; S - areas of precipitation of different intensity, km² - S(P≥3 mm/h) … S(P≥100 mm/h); r - the effective radius from the zone with the maximum radar reflectivity to average intensity of precipitation under different cloud zones, km.

Results and Discussions

Results in Table 1-5 and Fig. 3-7 are presented.

In Fig. 3 real and calculated time-series of precipitation intensity P under zone with the maximum radar reflectivity of the cloud on 13 June 2015 from 21.00 to 23.97 h are presented. Statistical characteristics of the time-series of P and the values of the coefficients of the corresponding regression equation in Table 1 are presented. As follows from Fig. 3 and Table 1 the average value of P for the entire observation period was 134.7 mm/h, the range of variability was 23.5÷371.4 mm/h. The time series of P values is satisfactorily described by a fifth power polynomial (corresponding values of the parameters R^2 and K_{DW}).

In Fig. 4 time-series of areas of precipitation of different intensity S under the cloud from 21.00 to 23.97 h are presented. Corresponding statistical characteristics of S values in Table 2 are presented.

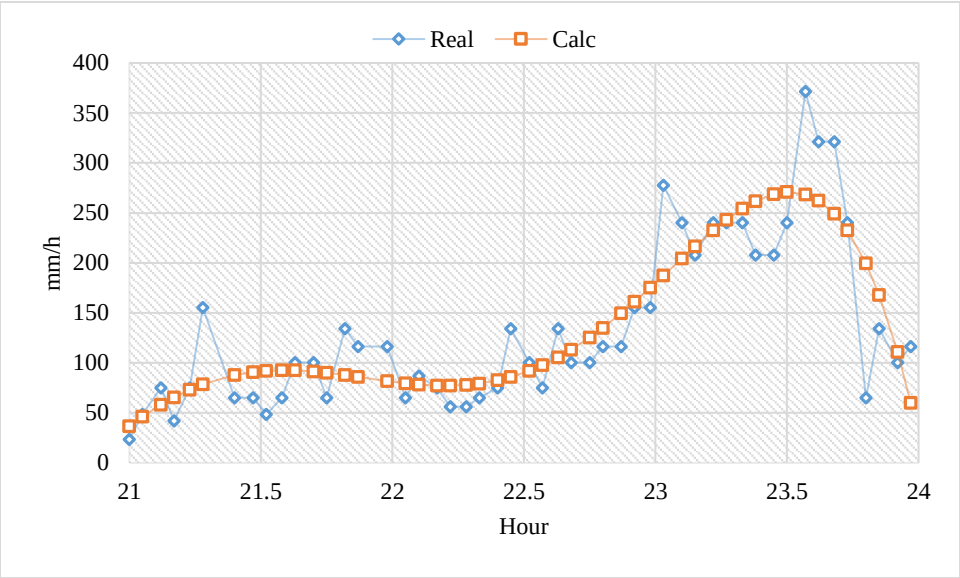

Fig.3. Time-series of precipitation intensity under zone with the maximum radar reflectivity of the cloud on 13 June 2015 from 21.00 to 23.97 h.

Table 1. Statistical characteristics of the precipitation intensity of cloud in the region of Akhaldaba on 13 June 2015 with 21.00 to 23.97 h. under the zone with the maximum radar reflectivity (mm/h).

Max	Min	Average	St Dev	R^2	K_{DW}
371.4	23.5	134.7	83.4	0.76	1.46
$P = a \cdot t^5 + b \cdot t^4 + c \cdot t^3 + d \cdot t^2 + e \cdot t + f$					
a	b	c	d	e	f
-31.243	3420.807	-149678	3271531	-3.6E+07	1.56E+08

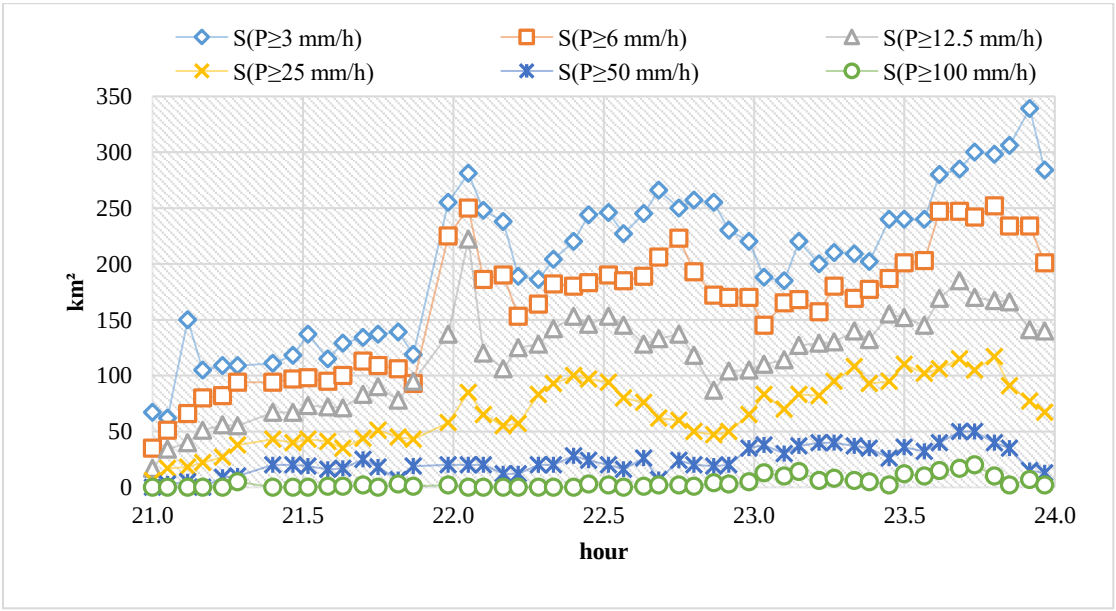

Fig.4. Time-series of areas of precipitation of different intensity under the cloud from 21.00 to 23.97 h.

As follows from Fig. 4 and Table 2 average values of S change from 3.9 km² (P≥100 mm/h) to 204.6 km² (P≥3 mm/h). The range of variability – from 0 (P≥100 mm/h) to 339 km² (P≥3 mm/h).

Coefficient of linear correlation between S values change from 0.42 (pair S(P≥3 mm/h)÷ S(P≥100 mm/h), low correlation) to 0.96 (pair S(P≥3 mm/h)÷ S(P≥6 mm/h), very high correlation).

Table 2. Statistical characteristics of areas of precipitation of different intensity under the cloud from 21.00 to 23.97 h (km²).

Variable	S(P≥3 mm/h)	S(P≥6 mm/h)	S(P≥12.5 mm/h)	S(P≥25 mm/h)	S(P≥50 mm/h)	S(P≥100 mm/h)
Max	339	252	222	117	50	20
Min	62	35	17	6	0	0
Range	277	217	205	111	50	20
Average	204.6	162.7	116.2	67.8	22.9	3.9
St Dev	67.8	56.9	42.6	28.7	12.3	5.1
Cv,%	33.1	35.0	36.7	42.3	53.6	130.1
St Err	9.68	8.13	6.09	4.10	1.75	0.73
Correlation Matrix						
S(P≥3 mm/h)	1	0.96	0.86	0.73	0.52	0.42
S(P≥6 mm/h)	0.96	1	0.93	0.81	0.60	0.47
S(P≥12.5 mm/h)	0.86	0.93	1	0.89	0.65	0.43
S(P≥25 mm/h)	0.73	0.81	0.89	1	0.80	0.60
S(P≥50 mm/h)	0.52	0.60	0.65	0.80	1	0.77
S(P≥100 mm/h)	0.42	0.47	0.43	0.60	0.77	1

The minimum value of R between adjacent values of S is 0.77 (pair S(P≥50 mm/h) - S(P≥100 mm/h), high correlation)

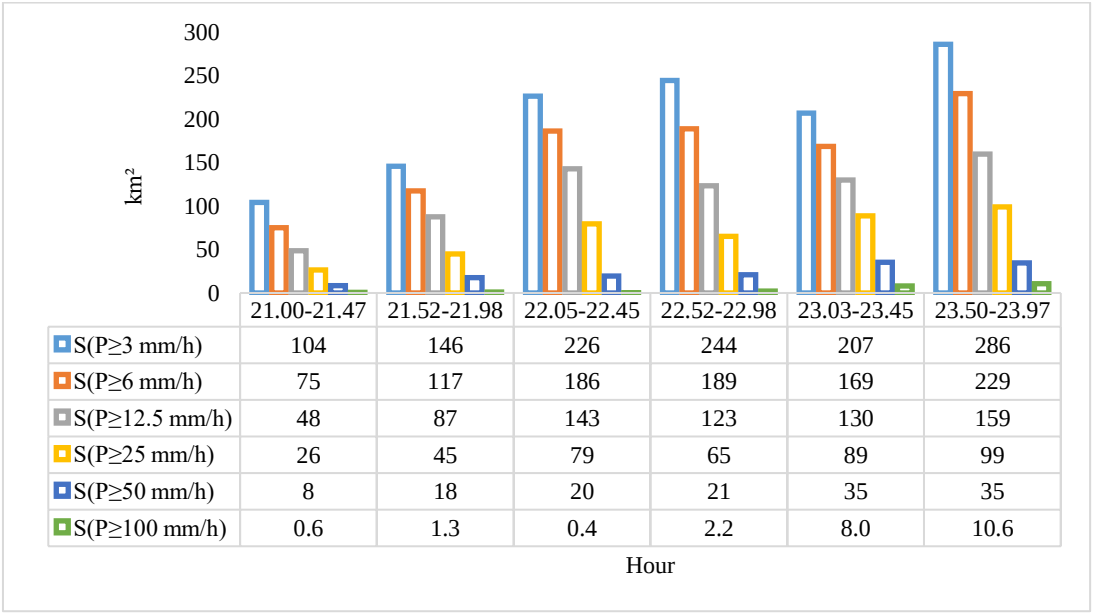

Fig.5. Areas of precipitation of different intensity under the cloud at different time intervals.

In Fig. 5 areas of precipitation of different intensity under the cloud at different time intervals are presented. For example, this area in time interval 21.00-21.47 h change from 0.6 km² (P≥100 mm/h) to 104 km² (P≥3 mm/h). In time interval 23.50-23.97 h value of S change from 10.6 km² (P≥100 mm/h) to 286 km² (P≥3 mm/h). About half an hour before the landslide (22.05-22.45 h) value of S change from 0.4 km² (P≥100 mm/h) to 226 km² (P≥3 mm/h).

In Fig. 6 graph of dependence of the average intensity of precipitation under different cloud zones (with P≥3 mm/h … P≥100 mm/h) on the effective radius from the zone with the maximum radar reflectivity (r).

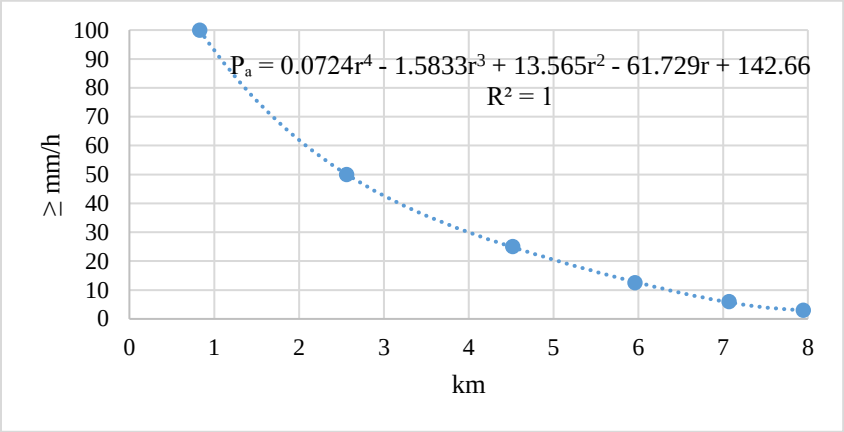

Fig.6. Dependence of the average intensity of precipitation under different cloud zones (P_a) on the effective radius from the zone with the maximum radar reflectivity (r).

This dependence has the form of a fourth power polynomial (Fig. 6). This regularity was used to estimate the intensity of precipitation over the center of the landslide top (Table 3).

Table 3. Statistical characteristics of precipitation intensity over the center of the landslide top on June 13, 2015 from 21.00 to 23.97 (≥mm/h)

Max	Min	Average	St Dev
65.1	1.0	43.6	28.8

As follows from Table 3 average value of precipitation intensity over the center of the landslide top on June 13, 2015 from 21.00 to 23.97 was ≥43.6 mm/h, min - ≥1.0 mm/h and max - ≥65.1 mm/h.

Sum of precipitation (P_s) under zone with the maximum radar reflectivity of the cloud and over the center of the landslide top on 13 June 2015 from 21.00 to 23.97 h and before landslide from 21.00 to 22.45 h are also evaluated (Table 4).

Table 4. Sum of precipitation under zone with the maximum radar reflectivity of the cloud and over the center of the landslide top on 13 June 2015 from 21.00 to 23.97 h and before landslide from 21.00 to 22.45 h.

Location	Time	Sum of precipitation, mm
Under zone with the maximum radar reflectivity of the cloud	21-23.97	402
	21-22.45	120
Center of the landslide top	21-23.97	≥134
	21-22.55	≥53

As follows from this Table P_s value under zone with the maximum radar reflectivity of the cloud was 402 mm in 21-23.97 h and 120 mm in 21-22.45 h (before landslide). P_s value over center of the landslide top was ≥134 mm in 21-23.97 h and ≥53 mm in 21-22.45 h (before landslide).

For comparison in the Table 5 data of the mean accumulated sum of precipitation in Tbilisi in days with landslides and 3, 5, 7, 10, 20 and 30 days before landslides' onset and on 15.05-13.06.2015, and in Fig. 7 daily sum of precipitation in Tbilisi from 1901 to 2020 are presented.

Table 5. Data of the mean accumulated sum of precipitation in Tbilisi in days with landslides and 3, 5, 7, 10, 20 and 30 days before landslides' onset [34] and on 15.05-13.06.2015, (mm).

Days	1 day	3 days	5 days	7 days	10 days	20 days	30 days
Average for 21 landslide	14.5	21.2	27.4	37.0	40.5	62.5	74.8
15.05-13.06.2015	49.3	49.3	51.0	51.7	58.9	143.8	146.6

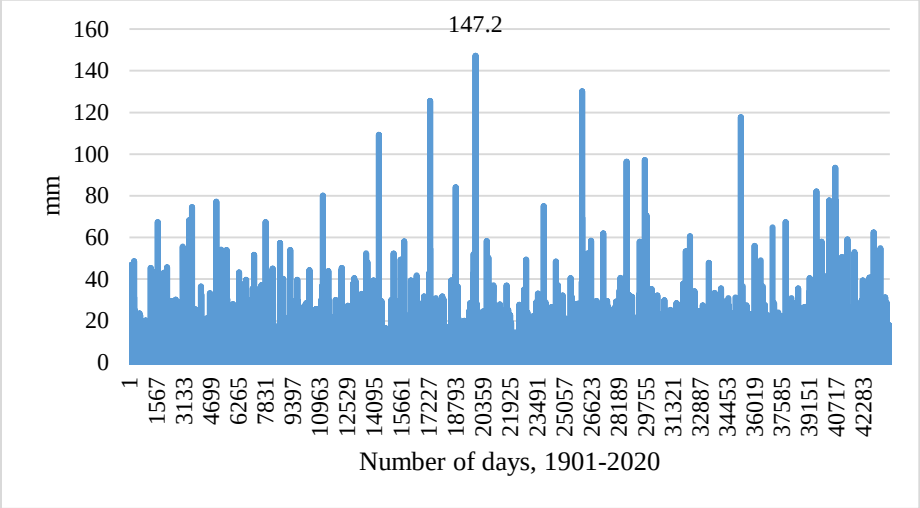

Fig.7. Daily sum of precipitation in Tbilisi from 1901 to 2020 (max sum of precipitation = 147.2 mm on August 16, 1955)

Over a 120-year period max sum of daily precipitation was 147.2 mm and on August 16, 1955 was observed. Note that the sum of precipitation under zone with the maximum radar reflectivity of the cloud in 21-23.97 h (Table 4) 2.73 times higher than max daily P_s value in Tbilisi in 1901-2020 (Fig. 7) and 2.74 times higher than 30 days sum of precipitation before landslide on 15.05-13.06.2015 (Table 5).

Value of P_s over the center of the landslide top before landslide activation (≥53 mm) at least 3.66 times higher landslide daily thresholds level for Tbilisi (14.5 mm, Table 5).

It should be noted that at the meteorological station in Tbilisi, a daily amount of precipitation equal to 49.3 mm was recorded, which is also higher landslide daily thresholds level for Tbilisi.

Thus, all conditions were created for the activation of the landslide process, followed by a catastrophic flood in Tbilisi.

Conclusion

As this study showed, radar measurements of precipitation intensity can be an effective tool for monitoring and short-term forecasting of the activation of landslide processes. This is especially true for locations where ground-based precipitation measurements are not available. In the future, we plan to deepen research in this direction.

Acknowledgement

This work was supported by Shota Rustaveli National Science Foundation of Georgia (SRNSFG), Grant number FR-19-8190, "Assessment of landslide and mudflow hazards for Georgia using stationary and satellite rainfall data".

References

[1] Varazanashvili O., Tsereteli N., Amiranashvili A., Tsereteli E., Elizbarashvili E., Dolidze J., Qaldani L., Saluqvadze M., Adamia Sh., Arevadze N., Gventcadze A. Vulnerability, Hazards and Multiple Risk Assessment for Georgia. Natural Hazards, Vol. 64, Number 3, 2021-2056, 2012, DOI: 10.1007/s11069-012-0374-3 , http://www.springerlink.com/content/9311p18582143662/fulltext.pdf.

[2] Amiranashvili A., Dolidze J., Tsereteli N., Varazanashvili O. Statistical Characteristics of Flash Flood in Georgia. Papers of Int. Simp. On Floods and Modern Methods of Control Measures, ISSN 1512-2344, 23-28 September 2009, Tbilisi, pp. 28-36.

[3] Amiranashvili A.G. Increasing Public Awareness of Different Types of Geophysical Catastrophes, Possibilities of Their Initiation as a Result of Terrorist Activity, Methods of Protection and Fight with Their Negative Consequences. Engaging the Public to Fight Consequences of Terrorism and Disasters. NATO Science for Peace and Security Series E: Human and Societal Dynamics, vol. 120. IOS Press, Amsterdam•Berlin•Tokyo•Washington, DC, ISSN 1874-6276, 2015, pp.155-164. http://www.nato.int/science; http://www.iospress.nl http://www.springer.com

[4] Gaprindashvili M., Tsereteli E., Gaprindashvili G., Kurtsikidze O. Landslide and Mudflow Hazard Assessment in Georgia. In: Bonali, F.L., Pasquaré Mariotto, F., Tsereteli, N. (eds) Building Knowledge for Geohazard Assessment and Management in the Caucasus and other Orogenic Regions. NATO Science for Peace and Security Series C: Environmental Security. Springer, Dordrecht, 2021, https://doi.org/10.1007/978-94-024-2046-3_14

[5] Fourth National Communication of Georgia Under the United Nations Framework Convention on Climate Change. Chapter 4.9 Geological Hazards in Georgia, Tbilisi, 2021, pp. 278-286.

[6] Gaprindashvili G., Van Westen C. J. Generation of a National Landslide Hazard and Risk Map for the Country of Georgia. Natural Hazards, vol. 80, no 1, pp. 69-101, 2016.

[7] Stankevich S.A., Titarenko O.V., Svideniuk M.O. Landslide Susceptibility Mapping Using GIS-Based Weight-of-Evidence Modelling in Central Georgian Regions. Int. Sc. Conf. „Natural Disasters in Georgia: Monitoring, Prevention, Mitigation“, Proc., ISBN 978-9941-13-899-7, pp. 187-190, Tbilisi, Georgia, December 12-14, 2019.

[8] Tsereteli E., Bolashvili N., Gaprindashvili G., Gaprindashvili M., Machavariani N. Risk of Natural Hazards in Georgia. Journal of the Georgian Geophysical Society, e-ISSN: 2667-9973, p-ISSN: 1512-1127, Physics of Solid Earth, Atmosphere, Ocean and Space Plasma, v. 24(2), 2021, pp. 22 – 29. DOI: https://doi.org/10.48614/ggs2420213316

[9] Tsereteli E., Gaprindashvili G., Gaprindashvili M. Natural Disasters (Mudflow, Landslide, Etc.). In: Bolashvili, N., Neidze, V. (eds) The Physical Geography of Georgia. Geography of the Physical Environment. Springer, Cham., 2022 https://doi.org/10.1007/978-3-030-90753-2_7

[10] Kartvelishvili L., Tatishvili M., Amiranashvili A.,Megrelidze L., Kutaladze N. Weather, Climate and their Change Regularities for the Conditions of Georgia. Monograph, Publishing House “UNIVERSAL”, Tbilisi 2023, 406 p., https://doi.org/10.52340/mng.9789941334658

[11] Amiranashvili A., Basilashvili Ts., Elizbarashvili E., Varazanashvili O. Catastrophic Floods in the Vicinity of Tbilisi. Transactions IHM, GTU, vol.133, 2023, pp. 56-61, (in Georgian), doi.org/10.36073/1512-0902-2023-133-56-61;
http://openlibrary.ge/bitstream/123456789/10337/1/133-11.pdf

[12] Varazanashvili O.Sh., Gaprindashvili G.M., Elizbarashvili E.Sh., Basilashvili Ts.Z., Amiranashvili A.G. Principles of Natural Hazards Catalogs Compiling and Magnitude Classification. Journal of the Georgian Geophysical Society, e-ISSN: 2667-9973, p-ISSN: 1512-1127, Physics of Solid Earth, Atmosphere, Ocean and Space Plasma, v. 25(1), 2022, pp. 5-11. DOI: https://doi.org/10.48614/ggs2520224794

[13] Gaprindashvili G., Varazanashvili O., Elizbarashvili E., Basilashvili Ts., Amiranashvili A., Fuchs S. GeNHs: the First Natural Hazard Event Database for the Republic of Georgia. EGU General Assembly 2023, EGU23-1614.
[14] Amiranashvili A., Kereselidze Z., Mitin M., Khvedelidze I., Chikhladze V. Alarming factors of the Microclimate of the Vere River Valley and their Influence on the Floods Intensity. Trans. of Mikheil Nodia Institute of Geophysics, ISSN 1512-1135, v. 69, Tbilisi, 2018, pp. 204-218, (in Georgian).
[15] Mitin M., Khvedelidze I. Radar Characteristics of Rain Cloud wich Caused Landslide into Akhaldaba and Catastrophic Flood in Tbilisi on June 13-14, 2015. Int. Sc. Conf. „Natural Disasters in Georgia: Monitoring, Prevention, Mitigation“, Proc., ISBN 978-9941-13-899-7, pp. 167-171, Tbilisi, Georgia, December 12-14, 2019.
[16] Chikhladze V., Amiranashvili A., Gelovani G., Tavidashvili Kh., Laghidze L., Jamrishvili N. Assessment of the Destructive Power of a Tornado on the Territory of the Poti Terminal on September 25, 2021. II International Scientific Conference "Landscape Dimensions of Sustainable Development Science – Carto/GIS – Planning – Governance", Dedicated to the 75th Anniversary of Professor Nikoloz (Niko) Beruchashvili, Proceedings, 12-16 September 2022, Tbilisi, Georgia, Ivane Javakhishvili Tbilisi State University Press, 2022, ISBN 978-9941-36-030-5, pp. 275-281. http://www.dspace.gela.org.ge/handle/123456789/10120
[17] Bliadze T., Amiranashvili A., Chkhitunidze M., Laghidze L. Statistical Analysis of Angstrom Fire Index for Kutaisi, Georgia. II International Scientific Conference "Landscape Dimensions of Sustainable Development Science – Carto/GIS – Planning – Governance", Dedicated to the 75th Anniversary of Professor Nikoloz (Niko) Beruchashvili, Proceedings, 12-16 September 2022, Tbilisi, Georgia, Ivane Javakhishvili Tbilisi State University Press, 2022, ISBN 978-9941-36-030-5, pp. 270-274. http://www.dspace.gela.org.ge/handle/123456789/10119
[18] Amiranashvili A., Bliadze T., Davitashvili M., Khakhiashvili M. Variability of the Angstrom Fire Index in Kakheti Due to Climate Change. Trans. of Mikheil Nodia Institute of Geophysics, ISSN 1512-1135, v. 75, Tbilisi, 2022, pp. 117-136, (in Georgian). http://dspace.gela.org.ge/bitstream/123456789/10298/1/12_Tr_IG_75_2022.pdf
[19] Amiranashvili A.G., Kartvelishvili L.G., Megrelidze L.D. Changeability of the Meteorological Parameters Associated with Some Simple Thermal Indices and Tourism Climate Index in Adjara and Kakheti (Georgia). Journal of the Georgian Geophysical Society, ISSN: 1512-1127, Physics of Solid Earth, Atmosphere, Ocean and Space Plasma, v. 21(2), Tbilisi, 2018, pp. 77-94. http://www.adry.tsu.ge/index.php/GGS/article/view/2529
[20] Amiranashvili A., Bliadze T., Kartvelishvili L. Statistical Characteristics of Monthly Sums of Atmospheric Precipitations in Tianeti (Georgia) in 1956-2015. Trans. of Mikheil Nodia institute of Geophysics, ISSN 1512-1135, vol. 70, Tb., 2019, pp. 112-118, (in Russian), http://dspace.gela.org.ge/handle/123456789/254;
[21] Amiranashvili A. Changeability of Air Temperature and Atmospheric Precipitations in Tbilisi for 175 Years. International Scientific Conference "Natural Disasters in Georgia: Monitoring, Prevention, Mitigation". Proceedings, ISBN 978-9941-13-899-7, Publish House of Iv. Javakhishvili Tbilisi State University, December 12-14, Tbilisi, 2019, pp. 86-90, http://dspace.gela.org.ge/handle/123456789/8613
[22] Amiranashvili A.G., Kartvelishvili L.G., Kutaladze N.B., Megrelidze L.D., Tatishvili M.R. Changeability of the Meteorological Parameters Associated with Holiday Climate Index in Different Mountainous Regions of Georgia in 1956-2015. Journal of the Georgian Geophysical Society, e-ISSN: 2667-9973, p-ISSN: 1512-1127, Physics of Solid Earth, Atmosphere, Ocean and Space Plasma, v. 24(2), 2021, pp. 78-91. DOI: https://doi.org/10.48614/ggs2420213326
[23] Segoni S., Piciullo L., Gariano S.L. A Review of the Recent Literature on Rainfall Thresholds for Landslide Occurrence. Landslides, vol. 15, pp. 1483–1501, 2018. DOI 10.1007/s10346-018-0966-4.
[24] Khvedelidze Z., Amiranashvili A., Dolidze J., Chitaladze D., Pavlenishvili N. Statistical Structure of Diurnal Precipitation Distribution on the Territory of Eastern Georgia. Proc. of I. Javakhishvili Tbilisi State University, Physics, N 357, ISSN 1512-1461, Tbilisi University Press, Tbilisi, 2004, pp. 79-87.

[25] Amiranashvili A.G. Special Features of Changeability of Daily Sum of Precipitation in Tbilisi in 1957-2006. Journal of the Georgian Geophysical Society, Issue B. Physics of Atmosphere, Ocean and Space Plasma, v.18B, Tbilisi, 2015, pp.81-91.
[26] Amiranashvili A., Chelidze T., Svanadze D., Tsamalashvili T., Tvauri G. On the Representativeness of Data from Meteorological Stations in Georgia for Annual and Semi-Annual Sum of Atmospheric Precipitation Around of These Stations. International Scientific Conference „Natural Disasters in the 21st Century: Monitoring, Prevention, Mitigation". Proceedings, ISBN 978-9941-491-52-8, Tbilisi, Georgia, December 20-22, 2021. Publish House of Iv. Javakhishvili Tbilisi State University, Tbilisi, 2021, pp. 79 - 83. http://openlibrary.ge/bitstream/123456789/9566/1/20_Conf_ND_2021.pdf
[27] Amiranashvili A., Chelidze T., Svanadze D., Tsamalashvili T., Tvauri G. Comparison of Data from Ground-Based and Satellite Measurements of the Monthly Sum of Atmospheric Precipitation on the Example of Tbilisi City in 2001-2020. Int. Conf. of Young Scientists "Modern Problems of Earth Sciences". Proceedings, ISBN 978-9941-36-044-2, Publish House of Iv. Javakhishvili Tbilisi State University, Tbilisi, November 21-22, 2022, pp. 154-158. http://openlibrary.ge/bitstream/123456789/10251/1/37_YSC_2022.pdf
[28] Banetashvili V., Gelovani G., Grebentsova A., Javakhishvili N., Iobadze K., Mitin M., Saginashvili N., Samkharadze I., Khurtsidze G., Tsereteli A., Tskhvediashvili G., Chkhaidze B. Some Examples of Strong Precipitation in Eastern Georgia According to the Data of Radar Surveillance of 2015. Trans.of Mikheil Nodia Institute of Geophysics, ISSN 1512-1135, v. 66, Tbilisi, 2016, pp. 75-83, (in Russian).
[29] Amiranashvili A., Chelidze T., Dalakishvili L., Svanadze D., Tsamalashvili T., Tvauri G. Preliminary Results of a Study of the Relationship Between the Variability of the Mean Annual Sum of Atmospheric Precipitation and Landslide Processes in Georgia. Int. Sc. Conf. „Modern Problems of Ecology", Proc., ISSN 1512-1976, v. 7, Tbilisi-Telavi, Georgia, 26-28 September, 2020, pp. 202-206. http://www.dspace.gela.org.ge/bitstream/123456789/8809/1/Eco_2020_3.33.pdf
[30] Amiranashvili A., Chelidze T., Dalakishvili L., Svanadze D., Tsamalashvili T., Tvauri G. Preliminary Results of a Study of the Relationship Between the Monthly Mean Sum of Atmospheric Precipitation and Landslide Cases in Georgia. Journal of the Georgian Geophysical Society, ISSN: 1512-1127, Physics of Solid Earth, Atmosphere, Ocean and Space Plasma, v. 23(2), 2020, pp. 37 – 41. DOI: https://doi.org/10.48614/ggs2320202726
[31] Amiranashvili A., Chelidze T., Svanadze D., Tsamalashvili T., Tvauri G. Some Results of a Study of the Relationship Between the Mean Annual Sum of Atmospheric Precipitation and Re-Activated and New Landslide Cases in Georgia Taking into Account of Climate Change. Journal of the Georgian Geophysical Society, e-ISSN: 2667-9973, p-ISSN: 1512-1127, Physics of Solid Earth, Atmosphere, Ocean and Space Plasma, v. 25(2), 2022, pp. 38–48. https://openjournals.ge/index.php/GGS/article/view/5959,
DOI: https://doi.org/10.48614/ggs2520225959
[32] Chelidze, T., Tsamalashvili, T., Fandoeva, M. Mass-movement stationary hazard maps of Georgia including precipitation triggering effect: fuzzy logic approach. Bull. Georg. Nat. Acad. Sci., vol. 16, no. 2, 56-63, 2022, http://science.org.ge/bnas/t16-n2/07_Chelidze_Geophysics.pdf
[33] Chelidze T., Amiranashvili A., Svanadze D., Tsamalashvili T., Tvauri G. Terrestrial and Satellite-Based Assessment of Rainfall Triggered Landslides Activity in Georgia, Caucasus. Bull. Georg. Nat. Acad. Sci., vol. 17, no. 2, 71-77, 2023, http://science.org.ge/bnas/vol-17-2.html
[34] Amiranashvili A., Chelidze T., Svanadze D., Tsamalashvili T., Tvauri G. Study of the Relationship Between the Mean Annual Sum of Atmospheric Precipitation and Re-Activated and New Mudflow Cases in Georgia. Journal of the Georgian Geophysical Society, e-ISSN: 2667-9973, p-ISSN: 1512-1127, Physics of Solid Earth, Atmosphere, Ocean and Space Plasma, v. 26(1), 2023, pp. 19–29.
[35] Amiranashvili A.G., Chikhladze V.A., Dzodzuashvili U.V., Ghlonti N.Ya., Sauri I.P. Reconstruction of Anti-Hail System in Kakheti (Georgia). Journal of the Georgian Geophysical Society, Issue B. Physics of Atmosphere, Ocean and Space Plasma, vol.18B, 2015, pp. 92-106.

[36] Amiranashvili A., Chikhladze V., Dzodzuashvili U., Ghlonti N., Sauri I., Telia Sh., Tsintsadze T. Weather Modification in Georgia: Past, Present, Prospects for Development. International Scientific Conference "Natural Disasters in Georgia: Monitoring, Prevention, Mitigation". Proceedings, ISBN 978-9941-13-899-7, Publish House of Iv. Javakhishvili Tbilisi State University, December 12-14, Tbilisi, 2019, pp. 216-222, http://dspace.gela.org.ge/handle/123456789/8613
[37] Selex ES GmbH · Gematronik Weather Radar Systems. Rainbow®5 User Guide, 464 p., www. gematronik.com
[38] Abaiadze O., Avlokhashvili Kh., Amiranashvili A., Dzodzuashvili U., Kiria J., Lomtadze J., Osepashvili A., Sauri I., Telia Sh., Khetashvili A., Tskhvediashvili G., Chikhladze V. Radar Providing of Anti-Hail Service in Kakheti. Trans. of Mikheil Nodia Institute of Geophysics, ISSN 1512-1135, Tbilisi, 2016, vol. 66, pp. 28-38, (in Russian).
[39] Avlokhashvili Kh., Banetashvili V., Gelovani G., Javakhishvili N., Kaishauri M., Mitin M., Samkharadze I., Tskhvediashvili G., Chargazia Kh., Khurtsidze G. Products of Meteorological Radar «METEOR 735CDP10». Trans. of Mikheil Nodia Institute of Geophysics, ISSN 1512-1135, Tb., 2016, vol. 66, pp. 60-65, (in Russian).
[40] Hinkle D. E., Wiersma W., Jurs S. G. Applied Statistics for the Behavioral Sciences. Boston, MA, Houghton Mifflin Company, ISBN: 0618124055; 9780618124053, 2003, 756 p.

ანომალური ნალექი 2015 წლის 13 ივნისს ახალდაბაში (თბილისის შემოგარენი, საქართველო) მეწყერამდე რადარის გაზომვების მიხედვით

ა. ამირანაშვილი, თ. ჭელიძე, დ. სვანაძე, თ. წამალაშვილი, გ. თვაური

რეზიუმე

წარმოდგენილია 2015 წლის 13 ივნისს 21:00-დან 23:97 საათამდე ახალდაბის რაიონში (თბილისის გარეუბანში) მეწყერის წინ ნალექის ინტენსივობის (P) რადარული გაზომვების ანალიზის შედეგები. კერძოდ, მიღებულია შემდეგი შედეგები. ღრუბლის მაქსიმალური რადარის არეკვლის ზონაში ნალექების ინტენსივობის დროის სერიას აქვს მეხუთე ხარისხის პოლინომის ფორმა. მიღებულ იქნა ღრუბლის ქვეშ სხვადასხვა ინტენსივობის ნალექის არეების დროის სერია და შესწავლილი იქნა მათი სტატისტიკური მახასიათებლები. მიღებულია ღრუბლის ქვეშ ნალექების საშუალო ინტენსივობის დამოკიდებულება მაქსიმალური რადიოამრეკვლადობის ზონის ეფექტურ რადიუსზე.
მოცემულია ნალექის ინტენსივობის სტატისტიკური მახასიათებლები მეწყრული მწვერვალის ცენტრში. შეფასებულია ნალექების რაოდენობა ღრუბლის რადარის მაქსიმალური არეკვლის ზონაში და მეწყრის მწვერვალის ცენტრის ზემოთ 2015 წლის 13 ივნისს 21:00 საათიდან 23:97 საათამდე და მეწყერამდე 21:00 საათიდან 22:45 საათამდე.

საკვანძო სიტყვები: ატმოსფერული ნალექები, რადიოლოკაციური დაკვირვებები, მეწყერები.

Аномальные осадки перед оползнем в Ахалдаба (пригород Тбилиси, Грузия) 13 июня 2015 г. по данным радиолокационных измерений

А.Г. Амиранашвили, Т.Л. Челидзе, Д.Т. Сванадзе, Т.Н. Цамалашвили, Г.А. Тваури

Резюме

Представлены результаты анализа радиолокационных измерений интенсивности осадков (P), предшествующих оползню в районе Ахалдаба (пригород Тбилиси, Грузия) 13 июня 2015 г. с 21.00 до 23.97 ч. В частности, получены следующие результаты. Временной ряд интенсивности осадков в зоне максимальной радиолокационной отражаемости облака имеет вид полинома пятой степени. Были получены временные ряды областей выпадения осадков разной интенсивности под облаком и изучены их статистические характеристики. Получена зависимость средней интенсивности осадков под облаком от эффективного радиуса от зоны с максимальной радиоотражательной способностью.

Приведены статистические характеристики интенсивности осадков над центром вершины оползня. Оценивается сумма осадков под зоной максимальной радиолокационной отражаемости облака и над центром вершины оползня 13 июня 2015 г. с 21.00 до 23.97 ч. и перед оползнем с 21.00 до 22.45 ч.

Ключевые слова: атмосферные осадки, радиолокационные наблюдения, оползни.

Journal of the Georgian Geophysical Society, e-ISSN: 2667-9973, p-ISSN: 1512-1127
Physics of Solid Earth, Atmosphere, Ocean and Space Plasma, v. 26(1), 2023, pp. 42-48

Numerical Study of Variability of Hydrological Regime for the Southeastern Part of the Black Sea (2010-2021)

[1,2]Demuri I. Demetrashvili, [1]Vepkhia G. Kukhalashvili, [1]Diana U. Kvaratskhelia

[1]M. Nodia Institute of Geophysics of I. Javakhishvili Tbilisi State University, Tbilisi, Georgia
demetr_48@yahoo.com,
[2]Institute of Hydrometeorology of Georgian Technical University, Tbilisi, Georgia

ABSTRACT

The study and forecast of mesoscale dynamic processes in the coastal/shelf zones of seas and oceans is one of the main issues of physical oceanography, because these zones experience the most significant anthropogenic load. Circulation processes, which are closely related to temperature and salinity fields, make a significant contribution to the distribution of various impurities of anthropogenic and natural origin in the marine environment. In the present paper, a high-resolution numerical regional model of the Black Sea dynamics of M. Nodia Institute of Geophysics of Ivane Javakhishvili Tbilisi State University (RM-IG) is used to simulate and study some peculiarities of regional hydrophysical processes occurring in 2010-2021 in the southeastern part of the Black Sea covering Georgian sector of the Black Sea and surrounding water area. The RM-IG is based on a primitive system of ocean hydro and thermodynamics equations in hydrostatic approximation written in the Cartesian coordinate system and is implemented with a spatial resolution of 1 km under real atmospheric forcing.

Key words: *circulation, pollution, modeling system, system of equations, boundary conditions.*

1. Introduction

The study of formation and variability of main hydrological characteristics - currents, temperature, salinity of the seas and oceans is of particular scientific and practical interest for coastal and shelf zones, which experience the most significant anthropogenic load. Modeling and forecasting of coastal circulation and thermohaline fields plays an important role in solving problems related to navigation and construction of coastal structures, in the spatial-temporal distribution different impurities of anthropogenic and natural origin, in assessing the state of the marine ecosystem. Many marine organisms are known to be very sensitive to thermohaline conditions [1, 2]. Sea water temperature and water salinity play an important role in forming of normal environment for marine living organisms and have a significant affect on species biodiversity. Additionally, the important role of dynamic processes in the upper layer of the sea in the interaction between the sea and the atmosphere should be noted.

In recent decades, the progress of computer technology has largely contributed to the widespread use of numerical modeling methods in oceanology and, in particular, in the study of the Black Sea dynamics (e. g., [3-12]). At present, numerical models of the Black Sea hydrodynamics are mainly based on a full system of ocean hydro thermodynamics equations using different coordinate systems, methods of parameterization of some physical factors and numerical algorithms.

In our previous works [13-15], some features of regional circulation processes in 2010-2013 and 2017-2019 were numerically studied for the Georgian sector of the Black Sea.

In the present paper a numerical regional model of Black Sea dynamics of M. Nodia Institute of Geophysics of Ivane Javakhishvili Tbilisi State University (RM-IG) is used to simulate and study some peculiarities of regional hydrophysical processes developed in 2010-2021 in the southeastern part of the Black Sea covering Georgian Sector of the Black Sea and surrounding water area. Our Participation in EU scientific and technical projects ARENA (2003-2006) and ECOOP (2007-2010) provided us to calculate

hydrophysical fields using real input data. We were able to receive all input data, corresponding to the above time period, via Internet regularly. All these data provided the setting of the necessary initial and boundary conditions on the sea surface and on the liquid boundary of the calculation area.

2. Description of the RM-IG

A high-resolution RM-IG is developed on the basis of the basin-scale model of the Black Sea dynamics [16, 17], adapted to the southeastern part of the Black Sea, and is based on a full system of ocean hydrothermodynamics equations written in Cartesian coordinate system for deviations of temperature, salinity, pressure and density from corresponding standard vertical distributions. The RM-IG takes into account: 1. The sea bottom relief and shoreline configuration; 2. Atmospheric forcing; 3. The absorption of total solar radiation by the sea upper layer; 4. the spatial-temporal variability of factors of horizontal and vertical turbulent viscosity and diffusion; 5. discharge of some rivers entering the eastern coast of the Black Sea. Atmospheric forcing is taken into account by given at the sea surface wind stress, heat fluxes, atmospheric precipitation and evaporation. Corresponding meteorological fields at the sea surface were provided from models of atmospheric dynamics ALADIN or SKIRON.

As envisaged by the EU projects ARENA and ECOOP the RM-IG was nested in the basin-scale model of Marine Hydrophysical Institute (Sevastopol) and is a core of the regional marine forecasting system for the southeastern part of the Black Sea, which covers Georgian coastal zone and surrounding water area [18, 19].

To solve the model equation system the two-cycle splitting method is used with respect to physical processes, coordinate plains and lines [20, 21].

3. Results and discussion

At present, as a result of numerous experimental and theoretical studies, the basin-scale circulation pattern of the Black Sea is well known. In general, the Black Sea circulation is cyclonic and consists: of the Rim Current, which, in the form of a cyclonic jet stream, passes along the periphery of the sea basin; internal cyclonic eddies; coastal anticyclonic eddies formed in the area between the Rim Current and shoreline. Numerous comprehensive studies show that against the background of this general circulation picture, the coastal and shelf zones of the Black Sea are characterized by a large variability of dynamic processes [22, 23]. Numerical experiments on modeling regional dynamic processes in the southeastern part of the Black Sea, carried out by us using RM-IG, confirm these conclusions. Circulation processes in the Georgian water area of the Black Sea are characterized by great diversity and variability with permanent generation and dissipation of mesoscale and submesoscale eddies, which significantly affects the distribution of various impurities, temperature and salinity fields. The main factor providing seasonal and interannual variability of hydrophysical processes is atmospheric forcing. Atmospheric processes over the Black Sea are characterized by high variability, which significantly affects the circulation of the Black Sea and the distribution of thermohaline fields in the upper layer [24].

With the purpose of model computer realization, the solution domain, which is limited by Caucasus and Turkish shorelines and by western liquid boundary passing along the meridian 39.08E, was covered with a grid 215x347 having horizontal resolution 1 km. On a vertical the non-uniform grid with 30 calculated levels on depths: 2, 4, 6, 8, 12, 16, 26, 36, 56, 86, 136, 206, 306,…, 2006 m was considered. The time step was equal to 0.5 h.

The model results were compared with available observational data – satellite SST (sea surface temperature) derived from NOAA satellites (http://dvs.net.ru/mp/data/201806bs_sst.shtml) and the Geostrophyc currents reconstructed on the basis of satellite altimeter data [19, 25, 26]. These comparisons have shown the ability of the RM-IG to reliably predict hydrophysical fields in the southeastern coastal zone of the Black Sea.

The structure of the surface regional circulation is characterized by significant seasonal changes and often differs in the warm (April-October) and cold (November-March) periods of the year. In the warm season, the main element of regional circulation is often the Batumi anticyclonic eddy, although it can also form in the cold period. In October-November, the Batumi eddy often gradually weakens and it gradually transforms into smaller eddy formations.

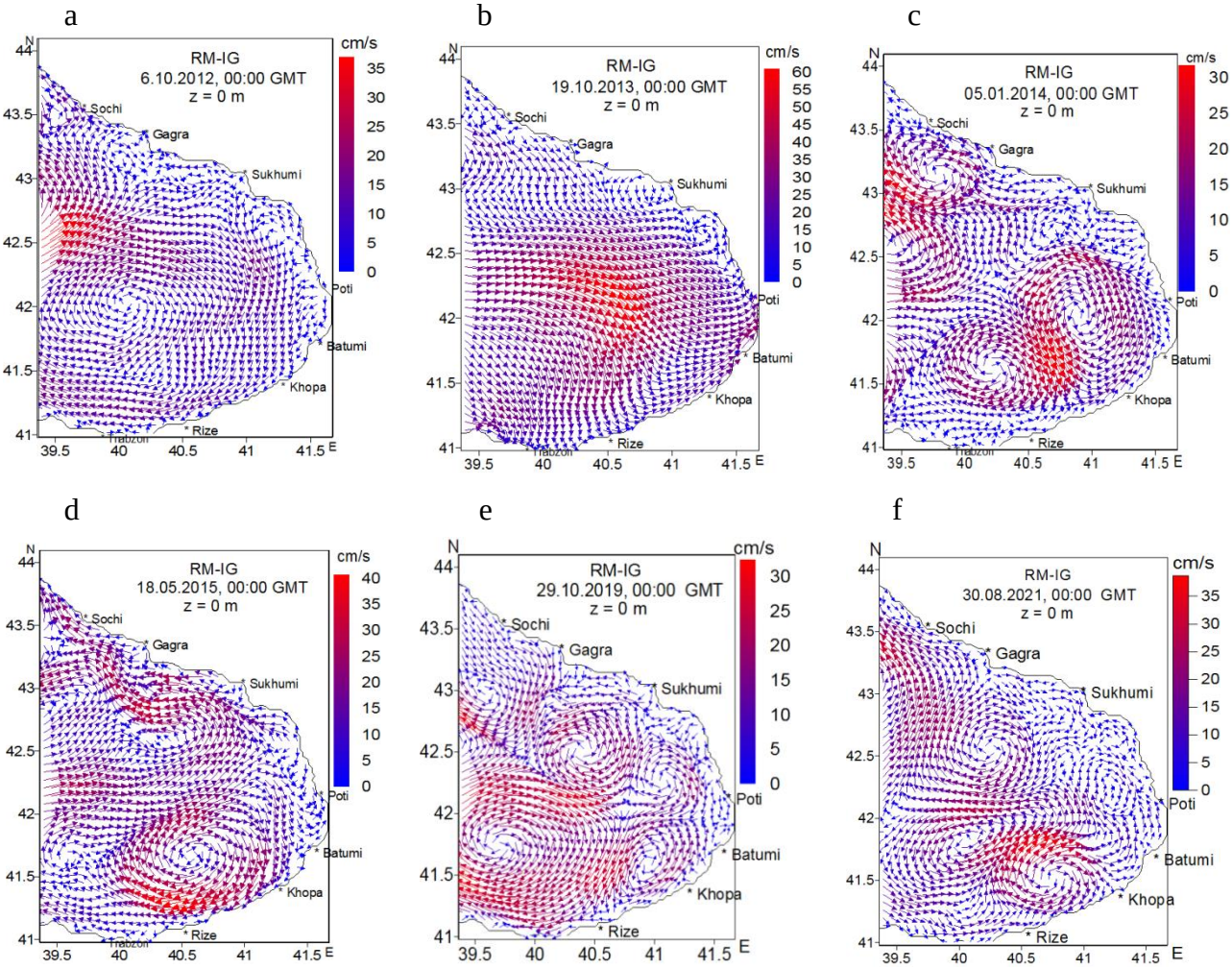

Fig. 1. Simulated sea surface circulation for different moments of time: (a) – 6 October 2012, (b) – 19 October 2013, (c) – 5 January 2014, (d) – 18 May 2015, (e) – 29 October 2019, (f) – 30 August 2021.

Often the winter circulation is dominated by cyclonic motion; in some cases the winter circulation is characterized by the formation of relatively small cyclonic and anticyclonic eddy formations with a diameter of about 40-60 km.

Fig.1 shows the simulated sea surface flow corresponding to different years and seasons. The Figure well illustrates the significant diversity of the circulation mode in the southeastern part of the Black Sea. From Fig.1a is well visible, that on October 6, 2012, the sea circulation was characterized by the formation of a stable Batumi anticyclonic eddy with a diameter of about 200 km. This circulation mode was maintained almost throughout October. It should be noted that the Batumi eddy appears with different intensity in different years. Our calculations showed that the Batumi eddy was the most stable formation in the summer and first half of the autumn of 2010 and 2011during 2010-2021. It covered the largest area of the considered modelling area and its structure remained practically unchanged vertically for several hundred meters**.** Calculations show that in some warm seasons the Batumi eddy may be practically absent. For example, the Batumi eddy was practically not observed during the summer 2018 and circulation was characterized with formation of different eddies with relatively small sizes. In our opinion, the question of the Batumi eddy

generation mechanism has not yet been finally established. There is a hypothesis of the direct impact of the wind associated with negative wind vorticity over the southeastern region, but there are also other hypotheses [23]. Numerical study carried out in [27] using the basin-scale model of Black Sea dynamics [16, 17] with different climate data shows that thermohaline conditions are a very important factor in the generation of the Batumi eddy.

An analysis of computational experiments shows that strong winds acting over the Black Sea basin prevent the development of eddy-forming processes and have a smoothing effect on the surface current. At this time, the flow velocities increase significantly and can exceed 100 cm/s. The circulation presented in Fig. 1b corresponds to October 19, 2013, when strong winds prevailed over the eastern part of the Black Sea. It can be seen from this Figure that the wind had a smoothing effect on the circulation, and the flow was practically irrotational. The maximum current velocity in this case reached 60 cm/s, and in a large part of the water area the current was directed from the west towards the coast of Georgia.

In Fig.1 is well visible, that in many cases the regional circulation in the southeastern part of the Black Sea is characterized by intense mesoscale cyclonic and anticyclonic vortex formations during all seasons in a wide range of scale sizes. In a narrow zone along the Georgian coastline, the formation of small unstable submesoscale eddies is observed (Fig.1e,1f), which is typical for the Caucasian coast [22].

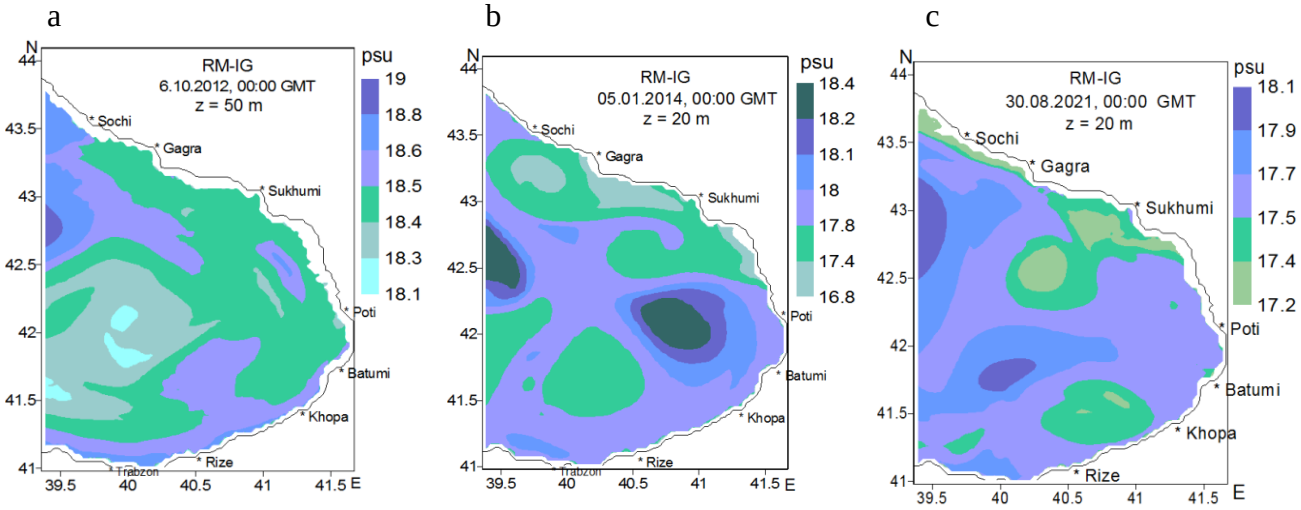

Fig.2. simulated salinity fields at following time moments: (a) – 6 October 2012, z = 50 m; (b) – 5 January 2014, z = 20 m; (c) – 30 August, 2021, z= 20 m.

Eddy formations make significant contribution to the formation of salinity and temperature fields having feedback with the flow field. The influence of mesoscale eddies on the distribution of various pollutants is also of great importance.

Data analysis 2010-2021 shows that the distribution of the salinity field in the considered regional area has undergone certain changes and correlates well with the current field. To illustrate this fact, Fig.2 shows the calculated salinity fields at the depths of 20 and 50 m in different years and seasons. Comparison of salinity fields illustrated in Fig.2 with corresponding circulation fields (Fig. 1a, 1c, 1f) shows that anticyclonic eddies contribute to the formation of low salinity waters in its central part, while in the central part of cyclonic eddies waters with high salinity are observed. The ascending current in the center of the cyclone contribute to the transfer of more saline waters from the deep layers to the upper ones, but the downward current in the central part of the anticyclonic eddy carries less saline water from the surface layers to the lower ones.

In Fig. 3 simulated sea surface temperature (SST) fields are shown at the same time moments as in Fig.2. SST is one of the main factors contributing to sea-atmosphere interaction. The sea surface temperature field is formed by the influence of several factors - the thermal interaction between the sea and the atmosphere, the absorption of solar radiation, advection-diffusion factors. It is a regularity that waters at

the Georgian nearshore are characterized by a relatively high temperature, which is apparently due to meteorological conditions.

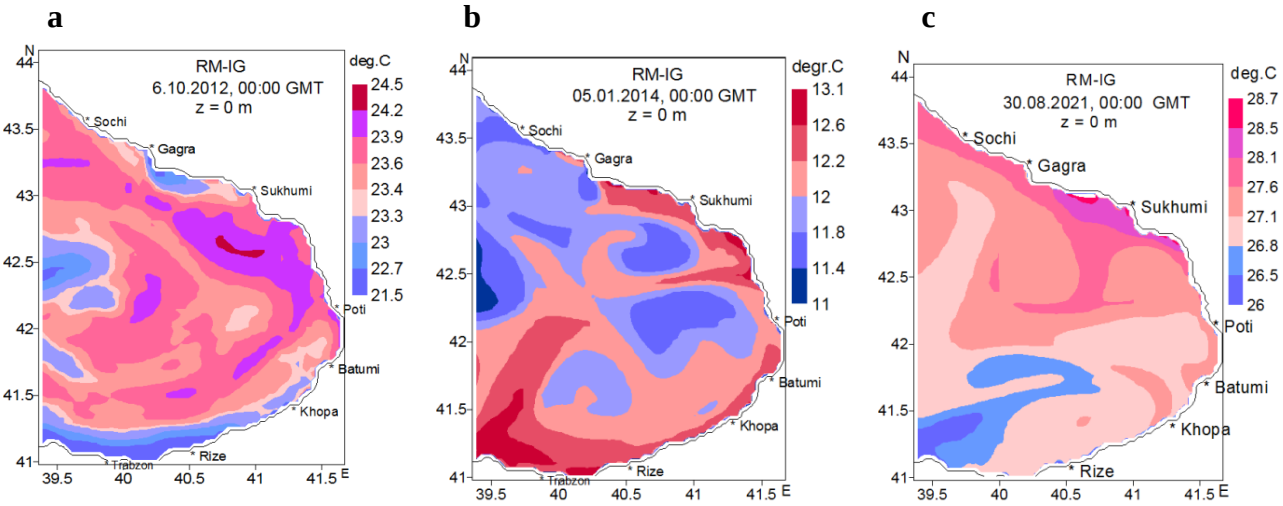

Fig.3. simulated sea surface temperature at the same time moments as in Fig.2.

Conclusion

The regional hydrophysical processes occurring in 2010-2021 in the southeastern part of the Black Sea, which covers the Georgian sector of the Black Sea and surrounding water area, are numerically investigated. The basis for these studies was the numerical baroclinic regional model of the Black Sea dynamics, developed at M. Nodia Institute of Geophysics of Ivane Javakhishvili Tbilisi State University (RM-IG). The RM-IG is based on a full system of ocean hydrothermodynamics equations and provides to calculate main hydrophysical fields – the current, temperature and salinity with 1 km spacing. All real input data required for initial and boundary conditions of model equation system were providing via Internet. Calculations showed some specific features of the regional circulation for the southeastern part of the sea basin, which is characterized by generation and transformation of different mesoscale eddies. Such eddies make a certain contribution to formation of thermohaline fields. Anticyclonic eddies promote formation of waters with low salinity in the central part of the eddy, but cyclonic eddies - formation waters with relatively high salinity in the central part. For the distribution of the SST field, it is characteristic that the waters close to the coastline of Georgia are often characterized by relatively high temperatures.

Acknowledgment. This work was supported by Shota Rustaveli National Science Foundation of Georgia (SRNSFG) [grant number FR-22-365].

References

[1] Sezgin M., Bat L., Katagan T., Ates A. S. Likely effects of global climate change on the Black Sea benthic ecosystem. J. Environ. Prot. Ecol., 11(1), 2010, pp. 238-246.
[2] Krivoguz D., Semenova A., Mal'ko S. Spatial analysis of seasonal patterns in sea surface temperature and salinity distribution in the Black Sea (1992-2017). IOP Conf. Series: Earth and Environmental Science 937 032013, 2021, pp.1-6. DOI: 10.1088/1755-1315/937/3/032013.
[3] Oguz T., Malalnote-Rizzoli P., Aubrey D. Wind and thermohaline circulation of the Black Sea by yearly mean climatological forcing. J. Geophys Rsearch 100, C4, 1995, pp. 6845-6863. https://doi.org/10.1029/95JC00022 .
[4] Oguz T., Malalnote-Rizzoli P. Seasonal variability of wind and thermohaline –driven circulation in the Black Sea: Modeling studies. J Geophys. Research. 101(C7), 1996, pp. 16551-16569. DOI:10.1029/96JC01093
[5] Staneva J. V., Dietrich D. E., Stanev E. V., Bouman M. J. Mesoscale circulation in the Black Sea: New results from DiaCast model simulation. J. Mar. Sys, 31, 2001, pp. 137-157.
[6] Kara A. B., Wallcraft A. J., Hurlburt H. E. Sea surface temperature sensitivity to water turbidity from simulations of the turbid Black Sea using HYCOM. J. Physic. Oceanography 35(1), 2005,pp. 33-54. .https://doi.org/10.1175/JPO-2656.1 .

[7] Kara A. B, Wallcraft A.J., Hurlburt H. E. A new solar radiation penetration scheme for use in ocean mixed layer studies: An application to the Black Sea a fine resolution Hybrid Coordinate Ocean Model (HYCOM). J. Phys. Oceanography 35(1), 2005, pp.13-22. https://doi.org/10.1175/JPO2677.1
[8] Stanev E. V. Understanding Black Sea dynamics: overview of recent numerical modeling. Oceanography, 18 (2), 2005, pp. 56-75. https://doi.org/10.5670/oceanog.2005.42
[9] Zalesny V. B., Gusev A. V., Moshonkin S. N. Numerical model of the hydrodynamics of the Black Sea and the sea of Azov with variational initialization of temperature and salinity. Izvestia, Atmospheric and Oceanic Physics, 49 (6), 2013, pp. 642-658.
[10] Zalesny V. B., Gusev A. V., Agoshkova V. I. Modeling Black Sea circulation with high resolution in the coastal zone. Izvestia AN, Fizika Atmosfery i Okeana, *52* (3), 2016, pp. 316-333. DOI:10.7868/S0002351516030147 (in Russian).
[11] Demyshev S. G., Dymova O. A. Analyzing interannual variations in the energy characteristics of circulation in the Black Sea. Izvestia, Atmospheric and Oceanic Physics, *52* (4), 2016, pp. 386-393.
[12] Dymova O. (2017) High-resolving simulation of the Black Sea circulation. In: Ozhan E(ed) Proceedings of the 13th International MEDCOAST Congress on Coastal and Marine Sciences, Engineering, Management and Conservation, 31 Oct-04 Nov 2017, Melliecha, Malta. vol.2,2017, pp. 1203-1213. https://www.medcoast.net/modul/index/menu/Proceedings/36
[13] Kordzadze A. A., Demetrashvili D. I., Surmava A. A. Dynamical processes developed in the easternmost part of the Black Sea in warm period for 2010-2013. J. Georgian Geophys. Soc., 16b, 2013, pp. 3-12.
[14] Kordzadze A. A., Demetrashvili D. I. Short-range forecast of hydrophysical fields in the eastern part of the Black Sea. Izvestya RAN, Fizika Atmosfery i Okeana, 49 (6), 2013, pp. 733-745 (in Russian).
[15] Demetrashvili D., Kukhalashvili V., Surmava A., Kvaratskhelia D. Modeling of variability of the regional dynamic processes developed during 2017-2019 in the easternmost part of the Black Sea. Proceedings of the International Conference GEOLINKS 2020. Book 2, Vol. 2. 2020, pp. 111-120.
[16] Demetrashvili D. I., Kvaratskhelia D. U., Gvelesiani A. On the vortical motions in the Black Sea by the 3D hydrothermodynamical numerical model. Advances in Geosciences, 2008, 14, pp. 295-299. www.adv-geosci.net/14/295/2008/.
[17] Kordzadze D. I., Demetrashvili D. I., Surmava A. A. Numerical modeling of hydrophysical fields of the Black Sea under the conditions of alternation of atmospheric circulation processes. Izvestya AN, Fizika Atmosfery i Okeana 44 (2), 2008, pp. 227-238 (in Russian).
[18] Kordzadze A., Demetrashvili D. Development of the Black Sea regional forecasting system for its easternmost part with inclusion of oil spill transport forecast. Bulletin of the Georgian National Academy of Sciences 8(3), 2014, pp. 40-47.
[19] Kordzadze A. A., Demetrashvili D. I. Operational forecast of hydrophysical fields in the Georgian Black Sea coastal zone within the ECOOP. Ocean Science 7, 2011, pp.793-803, www.ocean-sci.net/7/793/2011/ .
[20] Marchuk G. I. Numerical solution of problems of atmospheric and oceanic dynamics. Gidrometeoizdat, Leningrad, 1974, 303 p. (in Russian).
[21] Kordzadze A. A. Mathematical modeling of the sea current dynamics (the theory, the algorithms, the numerical experiments), Moscow, 1989, 218 p (in Russian).
[22] Zatsepin A. G., Baranov V. I., Kondrashov A. A., Korzh A. O., Kremenetskiy V. V., Ostrovskii A. G., Soloviev D. M. Submesoscale eddies at the Caucasus Black Sea shelf and the mechanisms of their generation. Oceanology, 51(4), 2011, pp. 554-567.
[23] Ivanov V. A., Belokopytov V. N. Oceanography of the Black Sea. Sevastopol, 2011, 209 p (in Russian).
[24] Efimov V. V., Anisimov A. E. Climatic parameters of wind-field variability in the Black Sea region: numerical reanalysis of regional atmospheric circulation. Izvestya AN, Fizika Atmosfery i Okeana, 47 (3), 2011, pp. 380-392 (in Russian).
[25] Kordzadze A. A., Demetrashvili D. I. Operational forecasting for the eastern Black Sea. Proceed.of the 13thInternational MEDCOAST Congress on Coastal and Marine Sciences, Engineering, Management and Conservation MEDCOAST 2017, 30 October – 4 November, 2017, Melieha, Malta, t.2, pp.1215-1224.
[26] Demetrashvili D., Kukhalashvili V. High-resolving modeling and forecast of regional dynamic and transport processes in the easternmost Black Sea basin. Proceed. of the International Conference on Geosciences (GEOLINKS 2019), 26-29 March 2019, Athens, Greece, Book 3, vol.1, pp.99-107.
[27] Demetrashvili D. Modeling of hydrophysical fields in the Black Sea. J. Georgian Geophys Soc., 8b, 2003. pp. 19-27.

შავი ზღვის სამხრეთ-აღმოსავლეთ ნაწილის ჰიდროლოგიური რეჟიმის ცვალებადობის რიცხვითი გამოკვლევა (2010-2021)

დ. დემეტრაშვილი, ვ. კუხალაშვილი, დ. კვარაცხელია

რეზიუმე

მეზომასშტაბური დინამიკური პროცესების შესწავლა და პროგნოზირება ზღვების და ოკეანეების სანაპირო/შელფურ ზონებში ფიზიკური ოკეანოგრაფიის ერთ-ერთი მთავარი საკითხია, რადგან ეს ზონები განიცდიან ყველაზე მნიშვნელოვან ანთროპოგენურ დატვირთვას. ცირკულაციურ პროცესებს, რომლებიც მჭიდრო კავშირშია ტემპერატურისა და მარილიანობის ველებთან, მნიშვნელოვანი წვლილი შეაქვს ზღვის გარემოში ანთროპოგენური და ბუნებრივი წარმოშობის სხვადასხვა მინარევების გავრცელებაში. წინამდებარე ნაშრომში, ივანე ჯავახიშვილის სახ. თბილისის სახელმწიფო უნივერსიტეტის მ. ნოდიას სახ. გეოფიზიკის ინსტიტუტის შავი ზღვის დინამიკის მაღალი გარჩევისუნარიანი რეგიონული რიცხვითი მოდელის (RM-IG) გამოყენებით მოდელირებულია და გამოკვლეულია 2010-2021 წწ.-ში მიმდინარე რეგიონული ჰიდროფიზიკური პროცესების ზოგიერთი თავისებურები შავი ზღვის სამხრეთ-აღმოსავლეთ ნაწილში, რომელიც მოიცავს შავი ზღვის საქართველოს სექტორსა და მიმდებარე აკვატორიას. RM-IG ეფუძნება ოკეანის ჰიდროთერმოდინამიკის განტოლებათა სრულ სისტემას ჰიდროსტატიკურ მიახლოებაში, ჩაწერილს დეკარტის კოორდინატთა სისტემაში და რეალიზებულია 1 კმ სივრცითი გარჩევისუნარიანობით რეალური ატმოსფერული ზემოქმედების პირობებში.

საკვანძო სიტყვები: მიმოქცევა, დაბინძურება, მოდელირების სისტემა, განტოლების სისტემა, სასაზღვრო პირობები.

Численное исследование изменчивости гидрологического режима юго-восточной части Черного моря (2010-2021 гг.)

Д. И. Деметрашвили, В. Г. Кухалашвили, Д.У. Кварацхелиа

Резюме

Изучение и прогноз мезомасштабных динамических процессов в прибрежно-шельфовых зонах морей и океанов является одним из основных вопросов физической океанографии, так как эти зоны испытывают наиболее значительную антропогенную нагрузку. Циркуляционные процессы, которые тесно связанны с полями температуры и солености, вносят значительный вклад в распространение различных примесей антропогенного и природного происхождения в морской среде. В настоящей работе, с использованием высокоразрешающей региональной, численной модели динамики Черного моря института геофизики им. М. Нодиа (RM-IG) Тбилисского государственного университета им. Ив. Джавахишвили моделируются и исследуются некоторые особенности региональных гидрофизических процессов, происходящих в 2010-2021 гг. в юго-восточной части Черного моря, которая включает в себя грузинский сектор Черного моря и прилегающую акваторию. RM-IG основана на примитивной системе уравнений гидротермодинамики океана в гидростатическом приближении, записанной в декартовой системе координат, и реализована с пространственным разрешением 1 км при реальном атмосферном воздействии.

Ключевые слова: циркуляция, загрязнение, система моделирования, система уравнений, граничные условия.

Journal of the Georgian Geophysical Society, e-ISSN: 2667-9973, p-ISSN: 1512-1127
Physics of Solid Earth, Atmosphere, Ocean and Space Plasma, v. 26(1), 2023, pp. 49-62

Atmospheric Periodic Oscillations

Marika R. Tatishvili, Ana M. Palavandishvili

Institute of Hydrometeorology of Georgian Technical University, Tbilisi, Georgia
m.tatishvili@gtu.ge; https://orcid.org/0000-0003-3327-2208
an.palavandishvili@gmail.com; https://orcid.org/0000-0002-7254-685X

ABSTRACT

The North Atlantic Oscillation, Quasi Biennial Oscillation, their negative and positive phases are discussed in presented article An El Niño event is a prolonged period of abnormally high sea-surface temperatures (SST) in the tropical Pacific Ocean. It goes hand in hand with changes in atmospheric conditions and can have strong repercussions on global weather patterns. El Niño can also significantly affect the global average temperature The ECMWF seasonal forecast system has been operational for more than five years and will soon be replaced by an upgraded system SEAS5.

Key Words: *North Atlantic Oscillation (NAO), sea level pressure, Quasi Biennial Oscillation (QBO), sea surface temperature, El NINO.*

Introduction

The North Atlantic Oscillation (NAO) is a prominent "seesaw" of atmospheric surface pressure fluctuation between the Azores and Iceland that has been meteorologically well defined since at least the late 19th century [1]. It is defined using the NAO index, which is typically a normalized mean sea-level pressure (SLP) index between a southern station located in the Azores or continental Iberia and a northern station in western Iceland [2-5]. The NAO has historically been recognized since at least the time of the Vikings; pioneering work based on early instrumental meteorological records was undertaken by Hildebrandsson (1897), who using surface air pressure data discovered the inverse relation between Iceland and Azores pressure, and by Sir Gilbert Walker who in works published in 1924 and 1932 (the latter with Bliss) undertook correlation analysis and constructed a robust multivariate NAO index based on surface air pressure and surface air temperature data from several European stations [6].

The strength of the pressure difference between the high- and low-SLP centers of action exerts a strong control over the strength and direction of the mid-latitude westerly storm tracks. As such, the NAO has been linked to a variety of climatological, biological, hydrological, and ecological variables across several locations [7,8], but is most frequently recognized as directly affecting the west of Europe (from Iberia to Scandinavia) and North America. A greater than normal pressure difference between the Azores and Iceland is a positive NAO, and a weaker than normal pressure difference is a negative NAO. During the winter months, a positive NAO is associated with warmer and wetter conditions across northwest Europe and cooler and drier conditions across southern Europe as the stronger pressure gradient between the Azores and Iceland drives the storm tracks poleward. The opposite is generally true for negative NAO conditions as the weaker pressure gradient generally results in southward-shifted storm tracks, and a SLP reversal will typically result in more easterly conditions. As such, the NAO index is strongly related to favored positions of the North Atlantic atmospheric polar jet stream.

The principal component (PC)–based NAO index [9], uses the first empirical orthogonal function (EOF) of atmospheric pressure variability across the North Atlantic region and is strongly correlated with the station-based index. NAO indices are closely related to the Arctic Oscillation (AO) index—the latter being the first EOF of variability of atmospheric surface pressure across the whole Northern Hemisphere north of 20°N [10], but there are subtle and notable differences in NAO and AO variations [11], and the NAO can perhaps best be seen as the regional Atlantic-wide manifestation of the AO.

The Quasi-Biennial Oscillation (QBO) is an oscillation of equatorial stratospheric zonal winds with a downward propagating phase taking approximately 1 year from the stratopause to the tropopause. It is

relevant for interannual variability of stratospheric dynamics and composition, both in the tropics and the Polar Regions. It has also been demonstrated that the QBO affects tropospheric weather, either through its effect on the stratospheric polar or perhaps directly through interaction with tropical convection. Tropospheric imprints were found in the Eurasian region, including the North Atlantic or Arctic Oscillation and Eurasian snow cover. The QBO has also been claimed to affect the Indian monsoon system, Atlantic hurricane frequency.

Direct observations of equatorial stratospheric winds by means of balloons go back to 1908, when Berson, in an expedition to East Africa, reported unexpected westerly winds in the lower. These westerlies were confirmed by van Bemmelen and Braak (1910), who performed observations of upper-level winds in Batavia from 1909 to 1918. Lower stratospheric westerlies were also confirmed by the observations of another volcanic eruption plume (Semeru, 15 November 1911), as reported by Hann and Süring (Hamilton, 2012). Reconciling Berson's westerlies with the expected easterly winds remained a challenge until the discovery of the QBO in the 1960s [12]. Stratospheric wind observations were very sparse prior to the 1950s. The early results were summarized by Schove ([13] and Hamilton [14]. After the 1950s, when a global radiosonde network was built up, stratospheric winds were operationally observed in the equatorial region.

It is known that the QBO affects the atmospheric circulation in the temperate latitudes and its influence propagates to the Earth surface. Regular measurements of the mean zonal wind components are carried by the radiosonde stations of the equatorial belt since 1953.The period of the oscillation is about 28 months. The winds in the eastward phase of the QBO are approximately twice as strong as those in the westward phase. The signal of the QBO cycle was detected not only in the variability of the stratospheric zonal and meridional wind, temperature, and geopotential height [15,16], but also in its influence on the surface meteorological parameters as well, for example, air temperature [17,18], precipitation [19-22], and snow cover [23,24]. In previous studies, the significant QBO signal was detected in September and October precipitation in the period from1953 to the 1980s in the region of the British Isles, in the Central European region and in Belarus. Regions of the eastern Ukraine and adjoined regions of Russia had the significant QBO signal in precipitation in May.

The quasi-biennial oscillation (QBO) is the dominant variability in the equatorial stratosphere characterized by alternating downward easterly and westerly winds every ~28 months on average driven by propagating waves. Though originating in the equatorial region, the QBO is known to influence the Arctic stratosphere, most prominently during boreal winters via the Holton–Tan (H-T) mechanism : During the descending easterly QBO (eQBO) phase, the westerly part of the waveguide for the planetary stationary waves is narrowed and squeezed more poleward, causing greater perturbation of the polar vortex and sometimes resulting in more sudden stratospheric warming events (SSWs conversely, during the descending westerly QBO (wQBO) phase, the waves are less restricted latitudinally and the polar vortex is more stable, resulting in an anomalously cold Arctic stratosphere.

Discussion

One current hypothesis to explain possible solar-climate connections is based on the fact that solar ultraviolet (UV) variability in the Schumann-Runge bands (175–200 nm) alters the radiative heating of the equatorial upper stratosphere through changes in ozone photochemistry. Subsequent changes in stratospheric temperatures and winds resulting from this initial heating perturbation could then propagate downward, affecting the tropospheric circulation and climate through a feedback mechanism involving wave-mean flow interactions.

There is observational evidence that the duration of the westerly QBO phase is 3 to 6 months shorter during periods of solar maximum than during solar minimum, and this modulation requires a temperature change of 1–2 K near the equator for the inferred changes in vertical wind shear to balance a solar-induced anomaly in the meridional temperature gradient via the thermal wind relationship [21,22].

The first significant observed deviation from the normal QBO since its discovery in early 1950s was noted beginning in February 2016 when the transition to easterly winds was disrupted by a new band of westerly winds that formed unexpectedly. The lack of a reliable QBO cycle deprives forecasters of a valuable tool. Since the QBO has a strong influence on the North Atlantic Oscillation and thereby north European weather, the coming winter could be warmer and stormier in that region. NASA scientists have been researching to test if the extremely strong El Niño event of 2015/16, climate change, or some other

factor might be involved. They are trying to determine if this is more of a once in a generation event, or if this is a sign of the changing climate

The Quasi-Biennial Oscillation can affect the Atlantic jet stream. The speed of the winds in the jet stream weakens and strengthens with the direction of the QBO. The jet stream is an important atmospheric feature that brings us our weather here in the UK, and the risk of winter conditions in Northern Europe can differ depending on the phase of the QBO:

- When the QBO is easterly, the chance of a weak jet stream, sudden stratospheric warming events and colder winters in Northern Europe is increased.
- A sudden stratospheric warming (SSW) is an event in which the polar stratospheric temperature rises by several tens of Kelvin (up to increases of about 50 °C (122 °F)) over the course of a few days. The change is preceded by a situation in which the Polar jet stream of westerly winds in the winter hemisphere is disturbed by natural weather patterns or disturbances in the lower atmosphere.
- When the QBO is westerly, the chance of a strong jet, a mild winter, winter storms and heavy rainfall increases.

QBO and solar variability modulate stratospheric winds in the winter hemisphere, which modifies the propagation conditions for planetary waves and feeds back on winds and temperature. It has been suggested by Holton and Tan [25,26] that, during the westerly QBO phase, the polar vortex is stronger and colder than during the easterly phase. Since then, several authors have shown that this effect holds mainly for early winter months and also depends on the solar cycle phase being significant only during solar minimum

The North Atlantic Oscillation (NAO) is measured as the difference in pressure between the Icelandic Low and the Bermuda-Azores high. Positive NAO occurs with a large pressure difference and a strong storm track, which brings wet and stormy weather to North West Europe; Negative NAO has a small pressure difference and is associated with dry weather in North West Europe. The NAO is associated with the Arctic Oscillation (AO), which is defined as the leading Empirical Orthogonal Function of the NAO and extends up into the stratosphere. Many researches consider the NAO as a \bell", because it is an amplified response to small forthings and is amplified beyond what one might expect compared to the stratospheric / upper tropospheric signal.

Two factors, which force the NAO, are the solar cycle and to a lesser extent the Quasi-Biennial Oscillation QBO); the oscillation between easterly and westerly winds in the equatorial stratosphere. Solar activity is found to influence the NAO such that strongly negative winter NAO values (which cause cold and dry conditions in North West Europe) rarely occur during periods of high solar activity [18,19].

The North Atlantic Oscillation (NAO) is one of the major modes of variability of the Northern Hemisphere atmosphere. It is a large scale see-saw in atmospheric mass between the subtropical high and the polar low exerting a strong control on winter climate in Europe, North America, and Northern Asia. The NAO index is defined as the normalized pressure difference between stations on the Azores and Iceland.

A positive NAO index indicates a stronger than usual subtropical high pressure center and a deeper than normal Icelandic low. The increased pressure difference results in more and stronger winter storms, crossing the Atlantic Ocean on a more northerly track. This results in warm and wet winters in Europe and cold and dry winters in Greenland and Northern Canada, while the eastern United States experiences mild and wet winter conditions. A negative NAO index points to a weak subtropical high and a weak Icelandic low. The reduced pressure gradient results in fewer and weaker winter storms crossing mostly on west-east paths bringing moist air into the Mediterranean and cold air to Northern Europe. The east cost of the United States gets more cold air and snow while Greenland enjoys mild winters

After ENSO, the NAO is one of the most dominant modes of global climate variability. Like El Niño, La Niña, and the Southern Oscillation, it is considered a free internal oscillation of the climate system not subjected to external forcing. It is shown, however, that it is closely linked to energetic solar eruptions. Surprisingly, it turns out that features of solar activity that have been shown to be related to El Niños and La Niñas, also have an impact on the NAO.

Westerly winds blowing across the Atlantic bring moist air into Europe. In years when westerly are strong, summers are cool, winters are mild and rain is frequent. If westerlies are suppressed, the temperature is more extreme in summer and winter leading to heat waves, deep freezes and reduced rainfall.

A permanent low-pressure system over Iceland (the Icelandic Low) and a permanent high-pressure system over the Azores (the Azores High) control the direction and strength of westerly winds into Europe. The relative strengths and positions of these systems vary from year to year and this variation is known as the NAO. A large difference in the pressure at the two stations (a high index year, denoted NAO+) leads to increased westerlies and, consequently, cool summers and mild and wet winters in Central Europe and its Atlantic facade. In contrast, if the index is low (NAO-), westerlies are suppressed, northern European areas suffer cold dry winters and storms track southwards toward the Mediterranean Sea. This brings increased storm activity and rainfall to southern Europe and North Africa.

Especially during the months of November to April, the NAO is responsible for much of the variability of weather in the North Atlantic region, affecting wind speed and wind direction changes, changes in temperature and moisture distribution and the intensity, number and track of storms. Research now suggests that the NAO may be more predictable than previously assumed and skillful winter forecasts may be possible for the NAO.

The North Atlantic Oscillation is usually described as a movement of atmospheric mass between the Arctic and the subtropical Atlantic [27]. There is no unique way to define the NAO. However, there are two pressure areas often used when describ-ing the phenomenon, the Icelandic low- and the Azores high-pressure systems. The variations in sea level pressure between these two areas generate a pres-sure gradient. Because of this pressure gradient, west-erly winds over the North Atlantic are generated [27]. The westerly winds, also known as “jets”, reach their maximum speed of 40 m/s at about 12 km up in the troposphere [1].

The NAO exhibits considerable inter-seasonal and inter-annual variability, and prolonged periods (several months) of both positive and negative phases of the pattern are common. The wintertime NAO also exhibits significant multi-decade variability [2, 28]. For example, the negative phase of the NAO dominated the circulation from the mid-1950's through the 1978/79 winter. During this approximately 24-year interval, there were four prominent periods of at least three years each in which the negative phase was dominant and the positive phase was notably absent. In fact, during the entire period the positive phase was observed in the seasonal mean only three times, and it never appeared in two consecutive years.

An abrupt transition to recurring positive phases of the NAO then occurred during the 1979/80 winter, with the atmosphere remaining locked into this mode through the 1994/95 winter season. During this 15-year interval, a substantial negative phase of the pattern appeared only twice, in the winters of 1984/85 and 1985/86. However, November 1995 - February 1996 (NDJF 95/96) was characterized by a return to the strong negative phase of the NAO.

When measuring the NAO different statistical methods can be used, either station-based or pattern-based [27]. A station-based index is measured as the normalized sea level pressure differences between two monitoring stations in the vicinity of the Icelandic low and Azores high. Alternatively, a spatial-based index, or a principal component based index, can be calculated from performing principle component analysis on the mean sea level pressure anomalies over the North Atlantic sector (usually between 20-80ºN and 90ºW-40ºE) [27]. The NAO is described as being in an either positive or negative phase (see Fig. 1). These phases are describing the strength of the circulation pattern. In a positive (NAO+) state the Icelandic low and the Azores high are well developed, resulting in a greater pressure gradient between these two areas. A greater pressure gradient causes stronger and more northern westerly winds. In a negative (NAO-) phase the pressure anomalies at the nodes of the NAO are less developed than normal and as a result the westerly winds get weaker and are positioned further south. However it is important to point out is that there is not only a confined positive and negative phase of the NAO, but also everything in between [27]. The NAO affects the climate mainly during wintertime when the NAO accounts for more than one-third of the total sea level pressure variance over the North Atlantic Ocean [1]. During summertime the spatial extent of the NAO and the sea level pressure variance are smaller than during winter. Atmospheric variations are lager during wintertime which makes the effect of the NAO on surface climate bigger than during summertime. Because of this, most research on the NAO is restricted to wintertime, however the NAO is still noticeable all year around [1]. There have been periods when the NAO persisted in an either positive or negative phase. During the beginning of the last century until approximately 1930 the NAO winters were characterized by a positive phase. During the 1960s the NAO winters instead showed persistent negative NAO anomalies [1]. Although decadal NAO trends is shown, it is observed that variations in the NAO can occur on very different timescales, making it hard to assess any preferred timescale of the NAO variability. The positive and negative NAO phases are also connected to different

patterns of precipitation as a result of variations in the strength and paths of storms generated over the Atlantic. During a positive NAO the North Atlantic storm track is usually directed more north-eastward over northern Europe than during negative NAO winters [1]. This makes positive NAO phases associated to precipitation anomalies above normal in northern Europe and Scandinavia, while the precipitation levels over southern and central Europe are below average. The opposite precipitation pattern is notable during negative NAO phases.

The Southern Oscillation and the North Atlantic Oscillation are comparable climate phenomena though located in different world regions. So I adopted the working hypothesis that the NAO, if subjected to solar forcing, would be related to the same phases of eruptional activity within the 11-year sunspot cycle as ENSO events. To test this hypothesis, I investigated yearly means of the NAO index covering 1825 to 2000. Jones et al. **(1997)** used early instrumental data to extend the index back to 1825. These data are available at the Climate Research Unit of the University of East Anglia **(2001)**. When I subjected the time series to 5-year moving window Gaussian kernel smoothing **(Lorczak)**, the smoothed curve displayed 36 extrema (maxima and minima). I related the dates of these NAO extrema to the respective sunspot cycles normalized to 11 years [14,15,16]. An analysis of the normalized positions of the extrema within the 11-year cycle showed that just the points **a**, **d**, **a/d**, and **d/a**, which play a major role in the relationship with ENSO events, show a close connection with NAO extrema when the data are shifted to offset a 1.5-year lag of the NAO maxima and minima. As to ENSO events in the Pacific, such lags reach at most a few months. A wider lag in the North Atlantic is acceptable as its location is far north of the equator where El Niño and La Niña develop in a climate with a much higher energy potential. Thermal inertia of the oceans and marine currents may be involved

The North Atlantic Oscillation (NAO) index is based on the surface sea-level pressure difference between the Subtropical (Azores) High and the Subpolar - Low. The positive phase of the NAO reflects below-normal heights and pressure across the high latitudes of the North Atlantic and above-normal heights and pressure over the central North Atlantic, the eastern United States and Western Europe. The negative phase reflects an opposite pattern of height and pressure anomalies over these regions. Both phases of the NAO are associated with basin-wide changes in the intensity and location of the North Atlantic jet stream and storm track, and in large-scale modulations of the normal patterns of zonal and meridional heat and moisture transport, which in turn results in changes in temperature and precipitation patterns often extending from eastern North America to western and central Europe.

Strong positive phases of the NAO tend to be associated with above-normal temperatures in the eastern United States and across northern Europe and below-normal temperatures in Greenland and oftentimes across southern Europe and the Middle East [29,30]. They are also associated with above-normal precipitation over northern Europe and Scandinavia and below-normal precipitation over southern and central Europe. Opposite patterns of temperature and precipitation anomalies are typically observed during strong negative phases of the NAO. During particularly prolonged periods dominated by one particular phase of the NAO, abnormal height and temperature patterns are also often seen extending well into central Russia and north-central Siberia. The NAO exhibits considerable interseasonal and interannual variability, and prolonged periods (several months) of both positive and negative phases of the pattern are common.

The NAO index is obtained by projecting the NAO loading pattern to the daily anomaly 500 millibar height field over 0-90°N. The NAO loading pattern has been chosen as the first mode of a Rotated Empirical Orthogonal Function (EOF) analysis using monthly mean 500 millibar height anomaly data from 1950 to 2000 over 0-90°N latitude.

The NAO has been linked with a variety of meteorological and non-meteorological effects across a wide spatial and multiple temporal scales, and only a selection of these impacts can be mentioned here. For example, in [31] showed a strong relationship between the mass balance of Scandinavian glaciers and the NAO due to the controlling influence of the storm tracks by the NAO, which influenced precipitation amounts, and glacier mass balance as a result. Coincidentally, the NAO has been shown to explain a large amount of the variance in Norwegian streamflow (55%) and hydropower output (30%), influencing electricity consumption and prices [32,33]. Baltic sea-ice extent is also strongly related to NAO changes [33]. In work [34]) found an influence of the NAO as far south as 20°N in coastal upwelling-inducing winds along the northwest African coastline. The great-circle distance between northwest Africa and Scandinavia is ~5,700 km, indicating the great spatial extent of the NAO influence. Recent NAO–climate linkages literature includes a strong signal of the (non-summer) NAO on precipitation in Iraq [35], an influence on sea-ice

breakup date in south-central Ontario [36]) and even a Southern Hemisphere influence, via a decadal-scale mechanism, on subtropical eastern Australian rainfall [37].

Table 1. Five lowest and five highest NAO years for each calendar month and season, based on the Hurrell PC NAO index and the January 1899–February 2016 period, updated from [11,22].

Month	5 lowest	5 highest
Jan	1966, 1969, 1940, 1963, 1945	1993, 1989, 1983, 1928, 1990
Feb	1947, 2010, 1978, 1942, 1960	1990, 1989, 1997, 2000, 1959
Mar	2013, 1962, 1958, 1931, 1952	1986, 1990, 1913, 1920, 1994
Apr	1966, 1978, 1988, 1979, 2008	1947, 2011, 1943, 1990, 1904
May	1993, 2008, 1954, 1952, 1909	1956, 1963, 2009, 1914, 2015
Jun	1902, 1903, 2009, 1982, 2011/2012	1994, 1961, 1967, 1922, 1919
Jul	2015, 1907, 1962, 2009, 1918,	1964, 1920, 1946, 1935, 1975
Aug	1943, 1964, 1958, 2011, 1966	1991, 1971, 1983, 1961, 2013
Sep	1998, 1930, 1968, 1939, 1915	1975, 1947, 2009, 1917, 1950
Oct	2006, 1960, 2012, 1966, 1968	1986, 1957, 1983, 1938, 1935
Nov	1910, 1947, 1955, 1915, 1965	1978, 1982, 1992, 1953, 1913
Dec	2010, 2009, 1961, 1995, 1978	2011, 2006, 1951/1982, 2004

Particular increase in the NAO between the 1960s and 1990s was widely noted in previous work and was thought to be related to human-induced greenhouse gas forcing. However, since then this trend has reversed, with a significant decrease in the summer NAO since the 1990s and a striking increase in variability of the winter especially December—NAO that has resulted in four of the six highest and two of the five lowest NAO Decembers occurring during 2004–2015 in the 116-year record, with accompanying more variable year-to-year winter weather conditions over the United Kingdom. These NAO changes are related to an increasing trend in the Greenland Blocking Index (GBI; equals high pressure over Greenland) in summer and a significantly more variable GBI in December. Such NAO and related jet stream and blocking changes are not generally present in the current generation of global climate models, although recent process studies offer insights into their possible causes. Several plausible climate forcing and feedbacks, including changes in the sun's energy output and the Arctic amplification of global warming with accompanying reductions in sea ice, may help explain the recent NAO changes. Recent research also suggests significant skill in being able to make seasonal NAO predictions and therefore long-range weather forecasts for up to several months ahead for northwest Europe [3,38]. However, global climate models remain unclear on longer-term NAO predictions for the remainder of the 21st century.

Climate phenomena subject to MJO influences include the monsoons and several climate modes such as ENSO, the North Atlantic Oscillation (NAO), the AO and Antarctic Oscillation (AAO), the Pacific North American (PNA) pattern, and the Indian Ocean Dipole (IOD). While these climate modes all feed back to the MJO, discussions in this section focus on MJO effects on them.

During winter, the positive (negative) phase of the AO, also known as the Northern Annular Mode (NAM), is twice as likely to occur as the opposite phase when MJO convection is enhanced (suppressed) over the Indian Ocean. When MJO convection is enhanced (suppressed) in the Eastern Hemisphere, especially over the Maritime Continent, the number of days of positive (negative) AO phase becomes large. In November–March, 18–21% of the variance in extratropical 1000-hPa geopotential height is related to the MJO. The MJO influence on the AO is also through Rossby wave trains excited by MJO convection and propagating from the tropical Pacific into the extratropics.

The southern hemispheric counterparts of the NAM and AO are the Southern Annular Mode (SAM) and AAO. They are also influenced by the MJO. Negative (positive) phases of the AAO in austral winter tend to occur when MJO convection is enhanced (suppressed) over the central Pacific. The SAM reaches its maximum positive phase immediately after MJO convection peaks over the equatorial Indian Ocean. The Antarctic circumpolar transport can be accelerated by MJO-enhanced surface westerly wind associated with the SAM that covers almost the entire latitude circle at 60° S.

The NAO/NAM pattern is a result of the eddy-driven extratropical atmospheric circulation: specifically, the transport of heat and momentum by stationary eddies (longwaves or planetary waves in the northern polar jet stream) and transient eddies (cyclones and anticyclones forming within or along the jet stream) ([22,39]. The polar jet stream is directly related to NAO changes and has mean latitude somewhere between 50°N and 60°N over the eastern North Atlantic. The strongest westerly winds (of up to about 200 km/hr in the core of the jet near the tropopause) are typically experienced at these latitudes, and there is a clear clustering of extratropical storm tracks along the polar jet stream. The prevailing direction is westerly due to the Coriolis Effect of earth's rotation, which deflects air masses to the right of their direction of motion in the Northern Hemisphere. Longwaves develop in the jet stream because of orographic obstacles (e.g., the Rocky Mountains over North America) or east–west heating contrasts between land and sea, or variations in latent heating due to condensation and rainfall. Low- and high-pressure systems form due to strong horizontal contrasts in temperature, typically where cold polar air meets relatively warm tropical air masses. These transient eddies are very important in providing energy for maintaining the polar jet stream flow and mid-latitude westerlies, otherwise friction with the surface would slow and eventually halt the winds. However, a significant contribution to maintaining the westerlies-greater than in the Southern Hemisphere—comes from the stationary eddies: this is due to the much stronger land–ocean contrast effects in northern mid-latitudes [40,41].

Being linked with the jet stream, there is a deep and pronounced vertical structure to the AO and NAO, which extends up into the stratosphere; this is most notable for the AO, which lies further north and is more directly linked with the polar vortex. What happens in the stratosphere in polar winter can also have a big bearing on conditions in the troposphere: for example, stratospheric sudden warming are associated with a weakening and sometimes reversal of the polar vortex and development of negative NAO/ AO that sometimes occurs in mid- to late winter [38,42]. Stratosphere–troposphere interaction and coupling is not very well understood, yet is important for NAO dynamics [43]. It appears from theory and observations that planetary-scale Rossby waves can propagate upwards from the troposphere into the stratosphere under conditions of moderate westerly flow during boreal winter; the stratosphere is effectively decoupled from the troposphere in other seasons. If the wintertime polar vortex is weak (strong), the upward-propagating waves can (cannot readily) interact with and slow the upper-level westerly flow. There is also a kind of reverse effect where airflow anomalies in the stratosphere can propagate down to affect the near-surface circulation [44] Baldwin & Dunkerton, 2001). The time of operation of these changes is typically 2–3 weeks, although dynamical couplings range over timescales from daily to multidecadal [43].

Between the 1960s and 1990s the NAO was becoming more positive, but since then this trend has tended to reverse. Recently updated observational records and reanalyses showed increasing variability of winter NAO and AO, which is a feature not just of the 2000ts and early 2010ts but has been ongoing during the 20th century.

Conclusion

The forecasting systems were predicting the development of a potentially major El Niño – a warming of the equatorial Pacific Ocean which has impacts on weather patterns around the world. The 2015/16 El Niño turned out to be in the same class as the biggest such events recorded in the 20th century. Its evolution was well predicted by ECMWF forecasts as well as by EUROSIP multi-model forecasts. The latest forecasts for 2017 at the time of going to press are indicating the possibility of another El Niño developing later this year. El Niño is the warm phase of the El Niño Southern Oscillation (ENSO). The cool phase is known as La Niña. The two strongest El Niños of the 20th century were those of 1982/83 and 1997/98, each of which was considered at the time a 'once-in-a-century' event. The El Niño of 2015/16 is in the same class as those of 1982/83 and 1997/98, and it set new records in the NINO4 and NINO3.4 regions in the western and central Pacific.

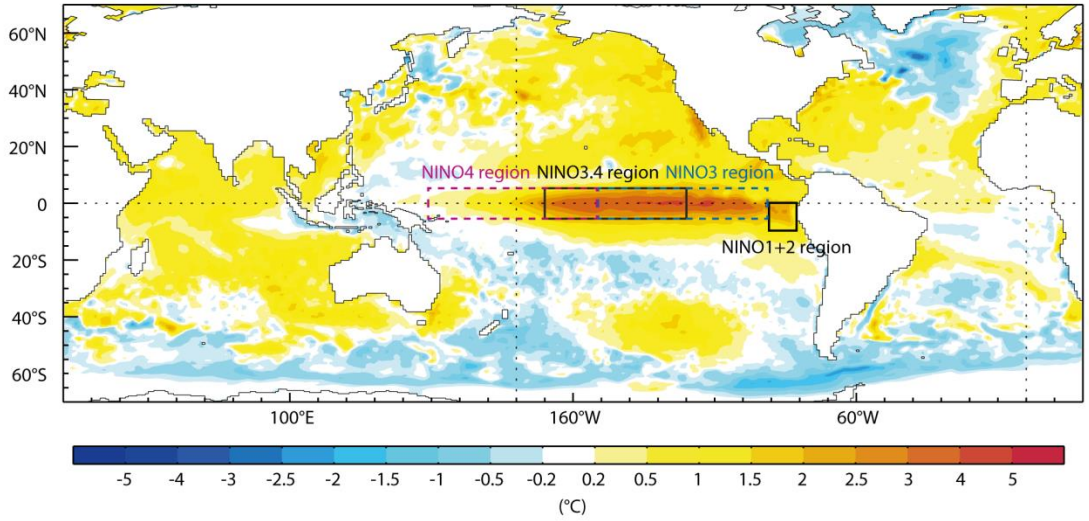

Fig. 1. Average sea-surface temperature anomalies in November 2015, when the El Niño event peaked in the NINO3.4 region. The chart shows SST anomalies compared to the 1981–2009 average.

Fig. 1 shows the spatial structure of the El Niño at its peak in November 2015. The vast extent of the event – more than 10,000 km in zonal (east–west) extent – and its ability to influence the deep tropical convection that drives the general circulation of the atmosphere is what gives El Niño its global impact. El Niño variability is generally monitored by the use of indices, calculated from average sea-surface temperatures (SST) over the regions marked on the map. NINO3.4, covering the central region of the equatorial Pacific, is most commonly used as a measure of the overall strength of an ENSO event.

The 2015/16 El Niño can best be understood by looking at the evolution of NINO3.4 SST (Fig. 2). In a normal year, there is a pronounced seasonal cycle in SST, as indicated by the red line. El Niño conditions are normally monitored as anomalies with respect to this mean seasonal cycle. At the beginning of 2015, the equatorial Pacific was already warm, as a leftover from borderline El Niño conditions which developed during 2014. The SST warmed at the usual rate during March, but continued warming through April and into May, with temperatures approaching 29°C. Normally, the ocean surface cools from June to September, as zonal winds strengthen and upwell cooler water at the equator, but in 2015/16 equatorial waters stayed warm for a whole year, with peak temperatures reached in November. Thus the usual seasonal cycle was completely upended. Due to the nature of the coupling between ocean and atmosphere in the equatorial Pacific, this dramatic change in SST was both a symptom and a cause of corresponding major changes in atmospheric winds and precipitation patterns.

The 2015/16 El Niño broke warming records in the central Pacific, represented by the NINO3.4 and NINO4 indices. At its peak in November 2015, the NINO3.4 SST anomaly reached 3.0°C, breaking the previous record of 2.8°C set in January 1983. In the NINO4 region, large positive anomalies are hard to achieve because average conditions are already warm. In 2015, the anomaly reached 1.7°C, a substantial increase of 0.4°C on the previous record, set in 2009. SST analyses become less precise going back in time, but the size of the anomalies in NINO4 and NINO3.4 means we are fairly confident that these are record

values for the whole of the observational period back to 1860. By contrast, in the eastern Pacific (monitored by indices for the NINO3 and NINO1+2 regions) the El Niño remained below the level of the 1982/83 and 1997/98 events. It must be borne in mind that the anomaly records depend on the reference climate, which in this case is a 30-year climate (1981–2010).

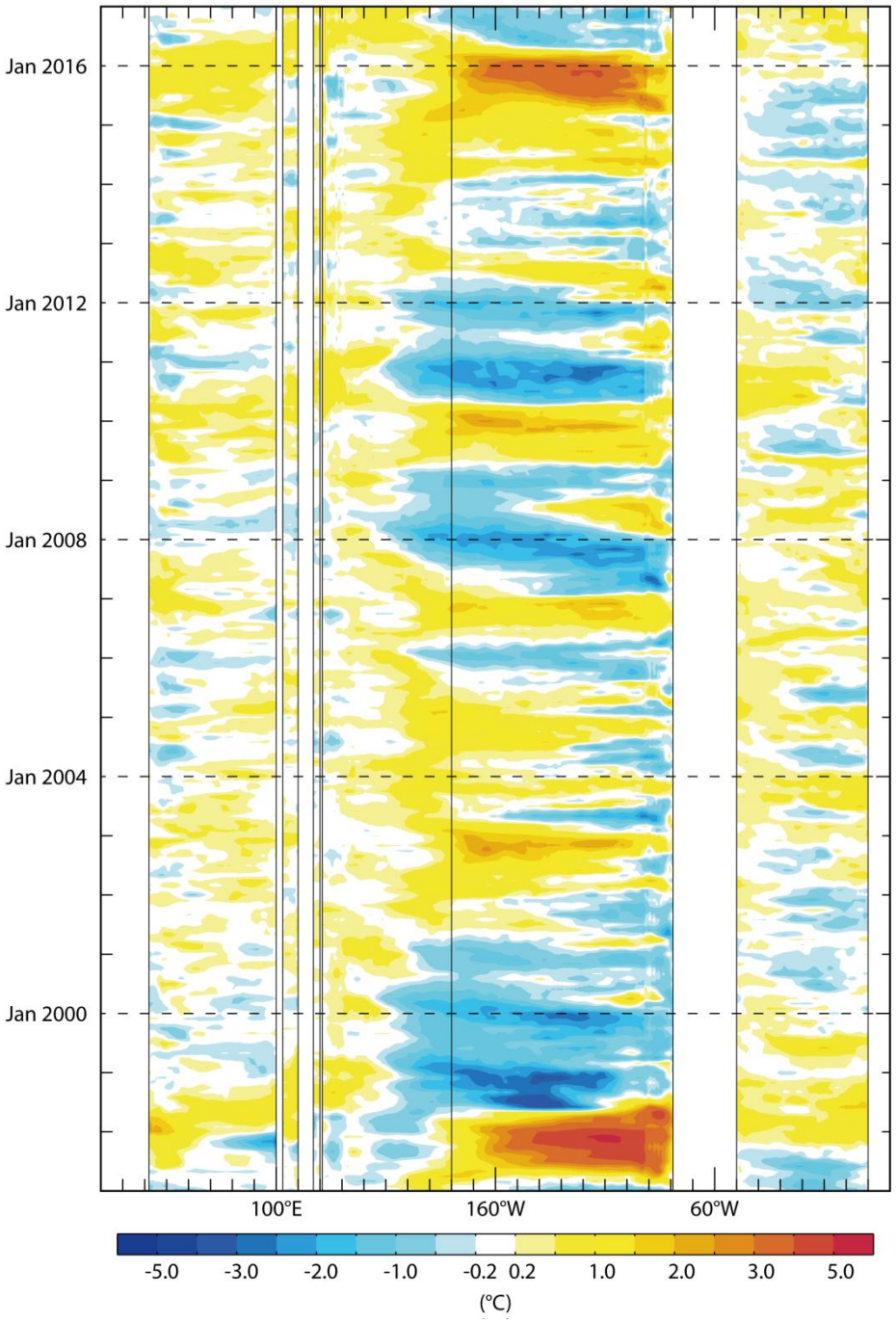

Fig. 2. Observed sea-surface temperature anomalies at the equator from January 1997 up to December 2016, compared to the 1981–2009 average.

Fig. 2 puts the current event in the context of the last 20 years. It shows the evolution of SST anomalies at the equator from January 1997 (bottom) to December 2016 (top), with conspicuous spikes in 1997/98 and at the end of 2015. It shows that at the equator the 2015/16 event was exceptionally strong, but not quite as strong as 1997/98. The peak warm anomalies were not so long-lived either, decaying quickly after November 2015. The aftermaths of the events are also remarkably different: 1997/98 was followed by an intense and long-lived cold La Niña episode, while the 2016 La Niña has been weak and short-lived. In between, the chart shows fluctuations between warm El Niño conditions and colder La Niña episodes in the central and eastern Pacific.

Although ENSO is a coupled ocean–atmosphere phenomenon centered over the tropical Pacific, its fluctuations affect the climate in other parts of the globe. During an ENSO event, the enhanced convection over the warm waters in the central and eastern tropical Pacific triggers changes in the strength of the Hadley circulation, leading to modifications in circulation patterns worldwide including, for example, the position of the jet stream that flows from west to east over the North Pacific in winter months. By strengthening the Hadley circulation, ENSO can trigger a cascade of deviations from normal rainfall and temperature patterns around the globe. These remote impacts are called ENSO teleconnections. ENSO teleconnection patterns are reflected in historical observations and are the basis of any empirical model.

The predictive skill of any dynamical model is strongly associated with the ability to accurately reproduce ENSO teleconnections. It follows that in years when ENSO is active, seasonal predictions are expected to be more accurate than in years when ENSO is in neutral conditions [45].

The year 2015 was hotter than any previous year in global datasets going back more than 130 years. Global near-surface temperature was well over 0.4°C warmer than the 1981–2010 average and almost 0.1°C warmer than the previous warmest year. The year 2016 was in turn nearly 0.2°C warmer than 2015 and about 1.3°C warmer than pre-industrial levels, according to data released by the EU-funded Copernicus Climate Change Service run by ECMWF. El Niño 2015/16 undoubtedly contributed to the record-breaking global temperatures. The size of that contribution will not be addressed here. It is, however, important to note that because of the warmer climate some of the ENSO impacts detected in historical data might not necessarily materialise. Indeed, the challenge of seasonal prediction is to forecast ENSO impacts in a changing mean climate. Dynamical models such as the one used by ECMWF have the potential to simulate the effects of ENSO in a warming climate.

The ECMWF seasonal forecast system has been operational for more than five years and will soon be replaced by an upgraded system, SEAS5. SEAS5 will benefit from the latest IFS cycle upgrades, bringing increased resolution in the ocean and atmospheric components. In a development of special interest for Europe, it will for the first time include a dynamic sea-ice model.

In a separate development, the Copernicus Climate Change Service (C3S) is trialling a prototype seasonal forecast service which offers multi-model El Niño forecasts and is expected to replace the EUROSIP multi-model system in due course. The core providers for this service are ECMWF, the UK Met Office and Météo-France. In addition, Italy's Euro-Mediterranean Center on Climate Change (CMCC) and Germany's National Meteorological Service (DWD) will start submitting data for inclusion in the service's product suite in the course of 2017. They are now set to be joined by NCEP and JMA

SST anomalies in the tropical Pacific are already above zero, and all forecasts included in the C3S seasonal multi-system predict that they will most likely continue to rise over the next few months. There is, however, still considerable uncertainty about how strong the event will be.

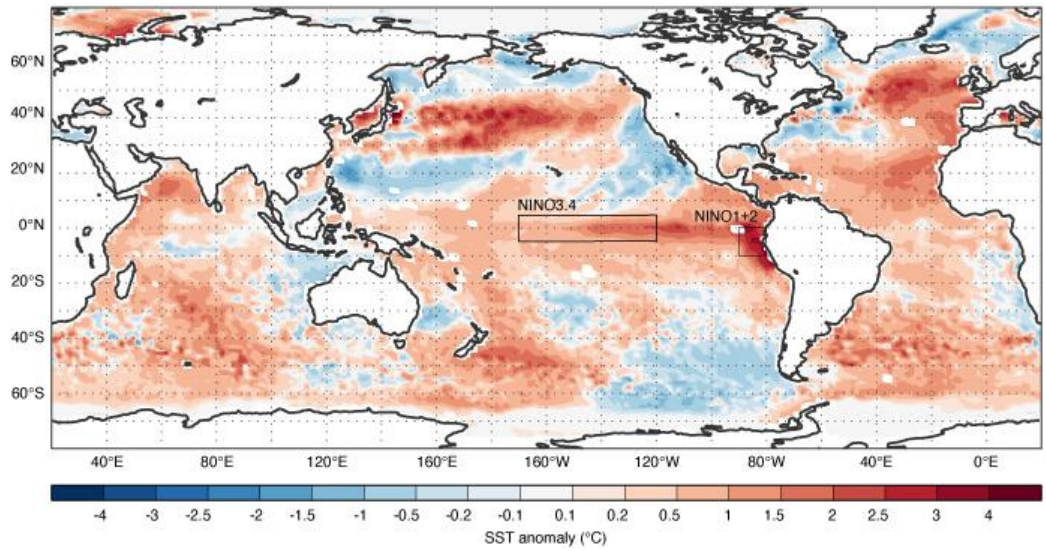

Fig. 3. The average sea-surface temperature anomalies from 1 to 8 June 2023, according to ECMWF's Ocean Reanalysis System 5 (ORAS5).

The plot shows average sea-surface temperature anomalies from 1 to 8 June 2023, according to ECMWF's Ocean Reanalysis System 5 (ORAS5). The SST anomalies are calculated based on the 1993–

2016 average. The boxes show commonly used areas for which anomalies are forecast. Areas around islands are left blank (Fig. 3).

An El Niño event temporarily increases global average 2-metre temperatures in the year after the peak of the event. That is why the WMO is saying that global temperatures will probably ”surge to record levels” over the next few years.

Substantial El Niño events are also associated with significant changes in weather patterns, especially in areas close to the tropical Pacific. The eastward movement of the warming of surface waters in the tropical Pacific brings higher than average pressure and less rain to the western Pacific, and lower pressure and more rain to the eastern Pacific.

El Niño events also contribute to other climate anomalies around the world. The specifics of the anomalies can differ from event to event, and the effects over Europe are particularly uncertain.

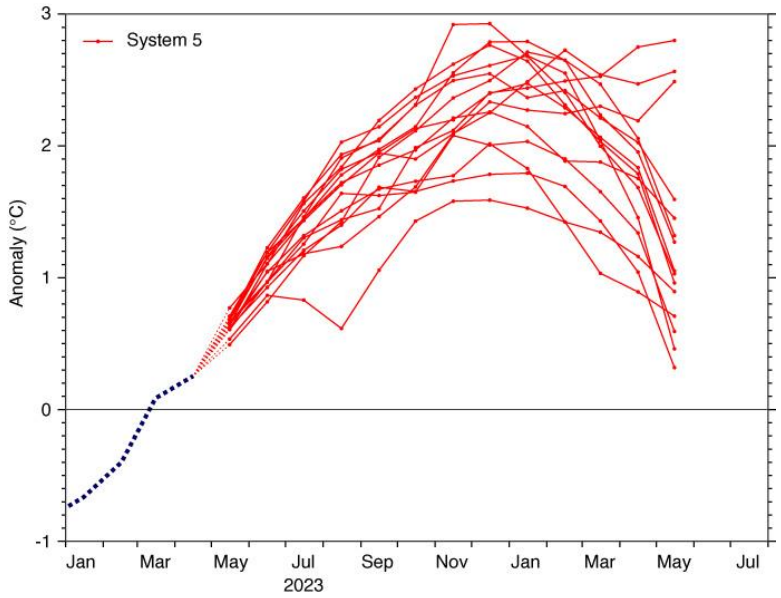

Fig. 4. 13-month NINO3.4 SST anomaly plume in an ECMWF forecast from 1 May 2023. The monthly mean anomalies are calculated relative to the 19812010 climatology.

ECMWF also issues 13-month NINO3.4 anomaly forecasts on 1 February, May, August and November as part of its open access forecasts. The May forecast suggests that high values are likely to dissipate in the first part of next year, although it predicts a small chance that high anomalies will continue well into 2024 (Fig. 4).

References

[1] Hurrell J. W., Kushnir Y., Ottersen, G. An overview of the North Atlantic oscillation. In J. W. Hurrell, Y. Kushnir, G. Ottersen, M. Visbeck, & M. H. Visbeck (Eds.), The North Atlantic Oscillation: Climatic Significance and Environmental Impact, 2003, pp. 1-35. Washington: American Geophysical Union. doi:10.1029/134GM01

[2] Hurrel J.W. Decadal Trends in the North Atlantic Oscillation. Science, 269 (5224), 676-9, 1995, DOI:10.1126/science.269.5224.676

[3] Cropper T., Hanna E., Valente M. A., Jónsson T. A daily Azores–Iceland North Atlantic Oscillation index back to 1850. Geoscience Data Journal, 2, 2015, pp. 12–24.

[4] Jones P.D., Jónsson T. Wheeler D. Extension to the North Atlantic Oscillation Using Early Instrumental Pressure Observations from Gibraltar and South-West Iceland. International Journal of Climatology, 17, 1997, pp. 1433-1450. https://doi.org/10.1002/(SICI)1097-0088(19971115)17:13

[5] Vanloon H., Rogers J. C. The seesaw in winter temperatures between Greenland and Northern Europe. Part I: General description. Monthly Weather Review, 106, 1978, pp. 296-310. doi:10.1175/1520-0493(1978)106<0296:TSIWTB>2.0.CO;2

[6] Stephenson, D.B., Wanner H., Brönnimann S., Luterbacher J. The history of scientific research on the North Atlantic Oscillation. The North Atlantic Oscillation: Climatic Significance and Environmental Impact. (2003), Geophys. Monogr. Ser., vol. 134, edited by J. W. Hurrell et al., 2003, pp. 37-50, AGU, Washington, D. C., DOI: 10.1029/134GM02
[7] Ottersen et al. Ecological Effects of the North Atlantic Oscillation. Oecologia 128(1), 2001, 1-14, DOI:10.1007/s004420100655
[8] Westgarth-Smith A.R., Roy D.B., Scholze M., Tucker A., Sumpter J.P. The role of the North Atlantic Oscillation in controlling U.K. butterfly population size and phenology. Ecol Entomol. 2012 Jun;37(3), 2012, pp. 221-232. doi: 10.1111/j.1365-2311.2012.01359.x. PMID: 22879687; PMCID: PMC3412218.
[9] Hurrell J. W. Climate Variability: North Atlantic and Arctic Oscillation. Encyclopedia of Atmospheric Sciences, 2nd edition, 2015.
[10] Thompson D.W.J., Wallace J.M. The Arctic Oscillation Signature in the Wintertime Geopotential Height and Temperature Fields. Geophysical Research Letters, 25, 1998, pp. 1297-1300. https://doi.org/10.1029/98GL00950
[11] Hanna E., Cropper T. E., Jones P. D., et al. Recent seasonal asymmetric changes in the NAO (a marked summer decline and increased winter variability) and associated changes in the AO and Greenland Blocking Index. International Journal of Climatology, 35 (9), 2015, pp. 2540-2554, https://doi.org/10.1002/joc.4157
[12] Hastenrath S. Circulation Mechanisms of Climate Anomalies in East Africa and the Equatorial Indian Ocean. Dynamics of Atmospheres and Oceans, 43, 2007, pp. 25-35. https://doi.org/10.1016/j.dynatmoce.2006.06.002
[13] Schove D. J. The Biennial Oscillation, Tree Rings and Sunspots. Weather, vol. 24, iss. 10, 1969, pp. 390-397, https://doi.org/10.1002/j.1477-8696.1969.tb03106.x
[14] Hamilton K. Observations of tropical stratospheric winds before World War II. Bulletin of the American Meteorological Society 79, no. 7, 1998, pp. 1367-1372.
[15] Tatishvili M. Developing Weather Forecasting System in Georgia. Ecology & Environmental Sciences, 2 (7), 2017, DOI:10.15406/mojes. 2017.02.00046.
[16] Tatishvili M.R., Palavandishvili A.M., Tsitsagi M.B., Suknidze, N.E. The Use of Structured Data for Drought Evaluation in Georgia. Journals of Georgian Geophysical Society, 25(1), 2022. https://doi.org/10.48614/ggs2520224806
[17] Tatishvili M., Khvedelidze Z., Demetrashvili D. On Some Weather Forecasting Models in Georgia. Journals of Georgian Geophysical Society, 23(2), 2020. https://doi.org/10.48614/ggs2320202727
[18] Tatishvili M.R., Megrelidze L.D., Palavandishvili A.M. Study of the Mean and Extreme Values, Intensity and Recurrence Variability of Meteorological Elements Based on the 1956-2015 Observation Data. Journals of Georgian Geophysical Society, 24(2), 2021, https://doi.org/10.48614/ggs2420213325
[19] Tatishvili M.R., Palavandishvili A.M.. Impact of Short-Term Geomagnetic Activity on Weather and Climate Formation in Georgian Region. Journal of the Georgian Geophysical Society, Physics of Solid Earth, Atmosphere, Ocean and Space Plasma, v. 23(2), 2020. https://doi.org/10.48614/ggs2320202730
[20] Tatishvili M., Bolashvili N., Palavandishvili A. Impact of short-term geomagnetic activity on the variability of meteorological parameters. Georgian Geographical Journal, Vol. 2 https://doi.org/10.52340/ggj.2022.756
[21] Kartvelishvili L., Tatishvili M., Amiranashvili A.,Megrelidze L., Kutaladze N. Weather, Climate and their Change Regularities for the Conditions of Georgia. Monograph, Publishing House "UNIVERSAL", Tbilisi 2023, 406 p., https://doi.org/10.52340/mng.9789941334658
[22] Tatishvili M., Khvedelidze, Z., Samkharadze I., Palavandishvili A. Influence of atmospheric circulation anomalies on weather end climate in Georgia. Proceedings of the IHM, GTU, vol. 131, 2021, pp.56-58 (in Georgian), https://dspace.nplg.gov.ge/handle/1234/335798
[23] Tatishvili M. On some considerations of cloud particles and photons interaction. Journal of the Georgian Geophysical Society, Physics of Solid Earth, Atmosphere, Ocean and Space Plasma, vol. 23(2), 2020, e-ISSN: 2667-9973, p-ISSN: 1512-1127 DOI: https://doi.org/10.48614/ggs2420213324
[24] Tatishvili M. Energy transformation in clouds according quantum principles. International Scientific Journal. Journal of Environmental Science, vol. 3, 2014, pp. 7-9.

[25] Holton J.R., Tan H. C. The Influence of the Equatorial Quasi-Biennial Oscillation on the Global Circulation at 50 mb. Journal of the Atmospheric Sciences, vol. 37, iss. 10, 1980, pp. 2200–2208, DOI: https://doi.org/10.1175/1520-0469(1980)037<2200:TIOTEQ>2.0.CO;2
[26] Holton J. R., Tan H. C. The quasi-biennial oscillation in the Northern Hemisphere lower stratosphere. Journal of the Meteorological Society of Japan. Ser. II, 60(1), 1982, pp. 140-148.
[27] Wanner H., Brönnimann S., Casty C. et al. North Atlantic Oscillation – Concepts And Studies. Surveys in Geophysics 22, 2001, pp. 321–381, https://doi.org/10.1023/A:1014217317898
[28] Bell G.D., Goldenberg, S., Landsea C., Blake E., Pasch,R., Chelliah M., Mo K. Tropical storms. Bull. Amer. Meteorol. Soc, 86, 2005, pp.S26-S29.
[29] Casanueva A., Rodríguez-Puebla C., Frías M. D., González Reviriego N. Variability of extreme precipitation over Europe and its relationships with teleconnection patterns. Hydrology and Earth System Sciences, 18, 2014, pp. 709–725.
[30] Edward H., Thomas E. Cropper Oxford Research Encyclopedia, Climate Science (climatescience.oxfordre.com). (c) Oxford University Press USA, 2016. DOI: 10.1093/acrefore/9780190228620.013.22
[31] Nesje A., Lie Ø, Dahl S.O. Is the North Atlantic Oscillation reflected in Scandinavian glacier mass balance records?. Journal of Quaternary Science: Published for the Quaternary Research Association, 15(6), 2000, pp.587-601.
[32] Cherry J., Cullen H., Visbeck M. et al. Impacts of the North Atlantic Oscillation on Scandinavian Hydropower Production and Energy Markets. Water Resour Manage 19, 2005, pp. 673–691, https://doi.org/10.1007/s11269-005-3279-z
[33] Karpechko A.Y, Peterson K.A, Scaife A.A, Gregow H. Skillful seasonal predictions of Baltic Sea ice cover. Environmental Research Letters, 10: 044007,2015, doi: 10.1088/1748-9326/10/4/044007.
[34] Cropper T. E., Hanna E., Bigg G.R. Spatial and temporal seasonal trends in coastal upwelling off Northwest Africa, 1981-2012. Deep-Sea Research Part I: Oceanographic Research Papers, 86, 2014, pp. 94-111, https://doi.org/10.1016/j.dsr.2014.01.007
[35] Khidher S. A., Pilesjö P. The effect of the North Atlantic Oscillation on the Iraqi climate 1982-2000. Theoretical and Applied Climatology, 122(3-4), 2015, pp. 771-782, https://doi.org/10.1007/s00704-014-1327-4
[36] Fu C., Yao H. Trends of ice breakup date in south-central Ontario. Journal of Geophysical Research: Atmospheres, vol.120, iss,18, 2015, pp. 9220-9236, https://doi.org/10.1002/2015JD023370
[37] Sun Ch., Li J., Feng J., Xie F. A Decadal-Scale Teleconnection between the North Atlantic Oscillation and Subtropical Eastern Australian Rain fall. Journal of Climate, vol. 28, iss. 3, 2015, pp.1074–1092, DOI: https://doi.org/10.1175/JCLI-D-14-00372.1
[38] Cohen J., Screen J. A., Furtado J. C., Barlow M., Whittleston D., Coumou D., et al. Recent Arctic amplification and extreme mid-latitude weather. Nature Geoscience, 7, 2014, pp. 627–637.
[39] Kaspi Y., Schneider T. The role of stationary eddies in shaping midlatitude storm tracks. Journal of the Atmospheric Sciences, 70, 2013, pp. 2596-2613.
[40] Diao Y., Xie S.-P., Luo D. Asymmetry of winter European surface air temperature extremes and the North Atlantic Oscillation. Journal of Climate, 28, 2015, pp. 517–530.
[41] Overland J. E., Wang M. Increased variability in the early winter subarctic North American atmospheric circulation. Journal of Climate, 28, 2015, pp. 7297–7305.
[42] Marshall A.G., Scaife A.A. Improved predictability of stratospheric sudden warming events in an atmospheric general circulation model with enhanced stratospheric resolution. Journal of Geophysical Research: Atmospheres, 115(D16), 2010.
[43] Kidston J., Scaife A.A., Hardiman S.C., Mitchell D.M., Butchart N., Baldwin M.P., Gray L.J. Stratospheric influence on tropospheric jet streams, storm tracks and surface weather. Nature Geoscience, 8(6), 2015, pp.433-440.
[44] Baldwin M.P., Dunkerton T.J. Stratospheric Harbingers of Anomalous Weather Regimes. Science, vol. 294, iss. 5542, 2001, pp. 581-584, DOI: 10.1126/science.106331
[45] https://www.cpc.ncep.noaa.gov/products/precip/CWlink/pna/nao.shtml

ატმოსფეროს პერიოდული ოსცილაციები

მ. ტატიშვილი, ა. ფალავანდიშვილი

რეზიუმე

ჩრდილო ატლანტიკური ოსცილაცია, კვაზი ბინალური ოსცილაცია, მათი უარყოფითი და დადებითი ფაზები განხილულია წარმოდგენილ სტატიაში. El Niño მოვლენა არის ზღვის ზედაპირის არანორმალურად მაღალი ტემპერატურის (SST) ხანგრძლივი პერიოდი ტროპიკულ წყნარ ოკეანეში. იგი ხდება ატმოსფერული პირობების ცვლილებებთან ერთად და შეიძლება ჰქონდეს ძლიერი გავლენა გლობალურ ამინდზე. ელ ნინიოს ასევე შეუძლია მნიშვნელოვნად იმოქმედოს გლობალურ საშუალო ტემპერატურაზე. ECMWF სეზონური პროგნოზის სისტემა ფუნქციონირებს ხუთ წელზე მეტი ხნის განმავლობაში და მალე ჩაანაცვლებს განახლებული სისტემით, SEAS5.UDC 551.576

საკვანძო სიტყვები: ჩრდილო ატლანტიკური რხევა (NAO), ზღვის დონის წნევა, კვაზი ორწლიანი რხევა (QBO), ზღვის ზედაპირის ტემპერატურა, ელ-ნინიო.

Атмосферные периодические колебания

М.Р. Татишвили, А.М. Палавандишвили

Резюме

В представленной статье рассмотрены Североатлантическое колебание, квазидвухлетнее колебание, их отрицательная и положительная фазы. Явление Эль-Ниньо – это длительный период аномально высоких температур поверхности моря (ТПМ) в тропической части Тихого океана. Он идет рука об руку с изменениями атмосферных условий и может иметь серьезные последствия для глобальных погодных условий. Эль-Ниньо также может существенно повлиять на глобальную среднюю температуру Система сезонных прогнозов ЕЦСПП работает уже более пяти лет и вскоре будет заменена модернизированной системой SEAS5.

Ключевые слова: Североатлантическое колебание (NAO), давление на уровне моря, квази двухлетнее колебание (QBO), температура поверхности моря, Эль-Ниньо.

Journal of the Georgian Geophysical Society, e-ISSN: 2667-9973, p-ISSN: 1512-1127
Physics of Solid Earth, Atmosphere, Ocean and Space Plasma, v. 26(1), 2023, pp. 63-66

Effect of Bordeaux Mixture on the Origin of Hail

[1]Shota A. Mestvirishvili, [1]Manon A. Kodua, [2]Mamuka O. Benashvili

[1]Georgian Technical University, Tbilisi, Georgia
manon.kodua@gmail.com; m.kodua@gtu.ge
[2]Agricultural University of Georgia, Tbilisi, Georgia

ABSTRACT

The paper discusses the territorial unit most vulnerable to hail in Georgia, Kakheti, and its istorical and current hail-related situation. With the help of the views of famous scientists as well as surveys, the authors of the paper concluded that nature isn't the only reason for hailstorms. The cause can also be the chemical substances used in the grapevine care process.
Key words: *hail, Bordeaux mixture, Kakheti, coagulation, poisoning.*

Introduction

The problem of hail damage is one of the most important problems in Georgia, in particular in the Kakheti region. Vakhushti Bagrationi (1696-1737) wrote about the devastating actions of the hail in the Vere Gorge but did not mention the Kakheti region. Well-known scientists M. Kordzakhia and academician F. Davitaya were of the opinion that during the time of Vakhushti Bagrationi there was no hail in Kakheti because, in the presence of abundant forest cover, there was no upward flow of air, which is one of the prerequisites for hail [1]. However, it is difficult for us to agree with this opinion because, in those days, Kakheti was a densely populated region with a well-developed agriculture. Probably, the vegetation cover of the region did not differ much from the present one, and the conditions for the occurrence of hail damage should have been approximately the same; and the vegetation cover, according to the scientists mentioned, prevents the upward flow of air. The authors involved the study of V. Gigineishvili, who believes that hail in Eastern Georgia, in particular in Kakheti, is mainly associated with the influx of cold air masses in the warm seasons. However, these inflows cause intense hail damage only when local atmospheric conditions are favorable during this particular period [1].

Main part

And if the formation of hailstones depends on local natural conditions, then the question of what changes in the natural conditions of Kakheti could have taken place in the period from the 18th to the 20th centuries that caused intense hailstorms in the region is appropriate. The answer to this question is partially given in the scientific work [2], which considers the effect of Bordeaux mixture drops, as well as aerosols on an increase in the crystallization temperature from -40 degrees to -5 degrees Celsius. The answer to the question posed by us can be attracted by the fact that at the end of the XX century the 100th anniversary of the use of Bordeaux mixture was celebrated worldwide, i.e. during the time of Vakhushti, Batonishvili did not resort to spraying Bordeaux liquid. The hailstone is formed not only under the influence of Cu and SO_4 ions contained in the Bordeaux mixture drops. The table of Zenger and Prupahar also lists other aerosols containing Cu - ions [3], which act similarly to Bordeaux drops and increase the freezing point of drops to -5 degrees Celsius. Among them is also a silver-iodine reagent. It is this reagent that is used today in an anti-hail rocket. The reagent at a height of 2.5 - 4.5 km dissipates in the clouds within 30-35 seconds. Research in the 1980s showed that during the spraying of vineyards in the settlements of Kakheti, the air contained Cu and SO_4 ions

in large quantities. And this means that in the conditions of an ascending air flow, they fall into the zone of city formation. This is confirmed by the fact that hail falls mainly in the interval from 2 to 5 hours. It is during this period of time that the number of droplets accumulated during spraying reaches its maximum in the atmosphere [1]. It is known that drops in clouds have different sizes and are often so supercooled that their temperature can be equal to -40 degrees Celsius [4]. At this moment, the drop is in a metastable state, and if a crystallization center enters it [5], the drop instantly turns into an ice crystal (hailstone). Therefore, the ingress of crystallization centers both naturally and artificially into such clouds, where drops of various sizes have already been formed, is especially dangerous, since this can lead to hail. It should also be noted that the drop expands in the process of turning into a hailstone, and, accordingly, its density decreases by about 9% compared to the density of water; in parallel, coagulation occurs and supercooled small water drops are attached to the hailstones, which quickly freeze and as a result turn not into smooth streamlined balls, but into rough hailstones of various shapes. Between the hail and the air, the coefficient of friction increases, and therefore the upward flow of air easily lifts the hailstone high into the colder layers. It increases significantly there, which is clearly seen from the Stokes formula [6]:

$$F = C\rho U^2 L^2 \quad (1)$$

where:

F - force of air resistance;

C is the drag coefficient;

ρ - air density;

U - hail speed;

L^2 - hailstone cross-sectional area;

The drag coefficient - C from the formula for streamlined bodies varies from 0.03 to 0.05, and for non-streamlined bodies - C = 1.0 to 1.5.

With an upward flow, the air expands adiabatically and, accordingly, cools, which leads to the formation of a hailstone crystal. In the process of crystal formation, heat is released, and a temperature difference is formed between the hailstone crystal and the surrounding air, which in turn forms a micro updraft around the hailstone. The ascending air flow carries the hail to higher layers of the atmosphere, which contributes to the growth of the hailstone crystal. It is also important that the longer the hail is in the clouds, the more the hail crystals, when colliding with each other, emit fragments, which, in turn, turn into crystallization centers. Crystal hailstones drift, begin to move randomly in different directions, since some of these crystals contain both positive and negative ions and they are affected by the electronic forces formed in the clouds, the Earth's magnetic field, the force of attraction and the Coriolis force. Clouds move together with hail, and the area of hail damage significantly increases [2]. The degree of coagulation also increases.

According to our research, spraying vineyards against hail damage is not a painless process. Apparently, therefore, economically developed European countries have abandoned the method of introducing crystallization centers into clouds using rockets to protect vineyards from hail, despite the fact that at one time they were the pioneers of its application.

Hailstorms did not take place in the Pankisi Gorge, since vineyards were not planted there; and after the 1980s, when vineyards appeared in the gorge like other regions, hailstorming became an intense phenomenon. But in contrast to the Pankisi Gorge, in regions where instead of vines they began to breed another agricultural crop that does not require spraying, hailstorming has ceased. For example, on the territory of Enamta, on the agricultural land of the Dedoplistskharo municipality, vineyards were planted on an area of 300 hectares. In Soviet times, they were sprayed with chemicals (Bordeaux liquid), while using heavy equipment. Over the past 20 years, the area of vineyards has decreased to 2 hectares, sprayed by hand, which minimizes the level of bardo liquid in the atmosphere. After the decrease in the area of vineyards in Enamta, no hail was recorded.

During spraying, it is necessary to take into account the ecological state of both air and water, since the sprayed substance eventually enters the water, and then the human body. Copper is a heavy metal and poison, as is S4, which, when exposed to water, forms sulfuric acid - H_2SO_4 .

On Fig. 1 we see the spraying process and a large amount of Bordeaux liquid that has entered the air with a large dispersion, the main part of which is carried by the ascending flow to the clouds. There, the liquid trapped in the clouds begins to act as a center of condensation as well as crystallization [1]. Therefore, the fight against hailstorms primarily involves the search for spraying methods that reduce the aimless spraying of $CuSO_4$ Bordeaux mixture in the air.

Fig.1. Spraying the vineyard with Bordeaux mixture

We consider it necessary to note that hail damage occurs not only during the spraying of vineyards, but also during the grape harvest. This is explained by the fact that when picking grapes, people come into intensive contact with the vines, and the $CuSO_4$ dust remaining on the branches of the vine after the evaporation of the Bordeaux mixture enters the high layers of the atmosphere, which can cause hail.

This assumption is confirmed by the fact that, as it turned out, aerosol pollution of the atmosphere, including radioactive, has a significant impact on thunderstorm, hail processes and precipitation [7-12]. Bordeaux mixture, as part of the general aerosol pollution of the atmosphere, especially in Kakheti, can contribute to this influence.

References

[1] Kordzakhiya M.O. Klimat Gruzii. Tb., 1961.

[2] Mestvirishvili Sh.A. O prichine uvelicheniya chastoty gradobitiy v vinogradarskikh rayonakh. Soob. Akad. Nauk Gruzii, 140, N 2, 1990, (in Russian).

[3] Mestvirishvili Sh., Benashvili M., Kodua M. Some Things about Hail. International Conference of Young Scientists "Modern Problems of Earth Sciences", Proceedings, ISBN 978-9941-36-044-2, Publish House of Iv. Javakhishvili Tbilisi State University, Tbilisi, November 21-22, 2022, pp. 169-172, (in Georgian).

[4] Sulakvelidze G.K. Livnevyye osadki i grad. L., "Gidrometeoizdat", 1967, 412 s.

[5] Mazin I.P., Khrgian A.KH. Oblaka i oblachnaya atmosfera. L. Gidrometizdat, 1989, 647 s., Spravochnik.

[6] Kitaygorodskiy A.I. Vvedeniye v fiziku. M., Nauka, 1973, 688 s.

[7] Amiranashvili A.G., Gzirishvili T.G., Chumburidze Z.A. On the Role of Artificial Ice Forming Reagents and Radioactive Intermixtures in the Variation of Convective Clouds Thunderstorm and Hail Activity. Proc. 12th Int. Conf. on Clouds and Pricipitation, Zurich, Switzerland, August 19-23, vol. 1, 1996, pp. 267-270

[8] Amiranashvili A.G., Amiranashvili V.A., Bachiashvili L.L., Bibilashvili T.N., Supatashvili G.D. Influence of the Anthropogenic Pollution of the Atmosphere and Thunderstorms on the Precipitations Regime and their Chemical Composition in Alazani Valley Conditions. Proc. 14thInternational Conference on Clouds and Precipitation, Bologna, Italy ,18-23 July 2004, 2_3_216.1-2_3_216.2.

[9] Amiranashvili A. G. Issledovaniye grozo-gradovykh protsessov v Gruzii i ikh svyazi s aerozol'nym zagryazneniyem atmosfery. Avtoreferat dissertatsiy na soiskaniye uchenoy stepeni doktora fiziko-matematicheskikh nauk, Tbilisi, 2006, 53 s., http://www.openlibrary.ge/bitstream/123456789/4920/1/Amiranashvili_Avtoreferat_2006.pdf.

[10] Amiranashvili A. Influence of the Anthropogenic Pollution of Atmosphere on the Changeability of Hail Processes Intensity. Trans. of Mikheil Nodia Institute of Geophysics, ISSN 1512-1135, vol. 64, Tbiisi, 2013, pp. 160-177. http://dspace.gela.org.ge/bitstream/123456789/697/1/Tom-64_Amiranashvili.pdf
[11] Adzhiyev A.KH., Amiranashvili A.G., Chargazia Kh.Z. Vliyaniye aerozol'nogo zagryazneniya atmosfery na effektivnost' protivogradovykh rabot v Kakhetii i na Severnom Kavkaze. Doklady Vserossiyskoy otkrytoy konferentsii po fizike oblakov i aktivnym vozdeystviyam na gidrometeorologicheskiye protsessy, posvyashchennoy 80-letiyu El'brusskoy vysokogornoy kompleksnoy ekspeditsii AN SSSR, 7-9 oktyabrya 2014 g., chast' 2, FGBU «Vysokogornyy geofizicheskiy institut», Nal'chik, 2015, s. 387-395. http://www.dspace.gela.org.ge/bitstream/123456789/5264/1/Аджиев,Амиранашвили,Чаргазиа_Докл_Нальчик_2014%20(2015).pdf
[12] Kartvelishvili L., Tatishvili M., Amiranashvili A., Megrelidze L., Kutaladze N. Weather, Climate and their Change Regularities for the Conditions of Georgia. Monograph, Publishing House “UNIVERSAL”, Tbilisi 2023, 406 p., https://doi.org/10.52340/mng.9789941334658

ბორდოს ხსნარის გავლენა სეტყვის წარმოშობაზე

შ. მესტვირიშვილი, მ. კოდუა, მ. ბენაშვილი

რეზიუმე

განხილულია საქართველოს სეტყვისგან ყველაზე მოწყვლადი ტერიტორიული ერთეული კახეთი და ამ რეგიონში სეტყვასთან დაკავშირებული როგორც ისტორიული, ასევე დღევანდელი მდგომარეობა. მოყვანილია ცნობილი მეცნიერების ნაშრომებში დადასტურებული შეხედულებები, ასევე მოსახლეობის გამოკითხვებიც, რომელთა შედეგადაც ნაშრომის ავტორები მივიდნენ იმ დასკვნამდე, რომ სეტყვის მოსვლის ინიცირებას მარტო ბუნება კი არა, ადამიანებიც ახდენენ ვაზის მოვლის პროცედურით და იმ ქიმიური ნივთიერებებით,რომელიც გამოყენებულია ვაზის მოვლის პროცესში.

საკვანძო სიტყვები: სეტყვა, ბორდოს ხსნარი, კახეთი, კოაგულაცია, შეწამვლა

Влияние бордосской жидкости на происхождение града

Ш.А. Мествиришвили, М.А. Кодуа, М.О. Бенашвили

Резюме

Рассмотрен вопрос градобития и нанесенный им ущерб на территориальной единице Грузии – Кахети, а также состояние в регионе с точки зрения градобития и в прошлом и в настоящем времени. Привлечены мнения известных ученых, опрос местного населения по проблеме, все это и позволило авторам заключит, что градобитие инициировано не только природой, но и процедурой ухода за виноградниками и использованными в процессе ухода человеком химическими веществами.

Ключевые слова: – град, бордоская жидкость, Кахети, коагуляция, опрыскивание.

Journal of the Georgian Geophysical Society, e-ISSN: 2667-9973, p-ISSN: 1512-1127
Physics of Solid Earth, Atmosphere, Ocean and Space Plasma, v. 26(1), 2023, pp. 67-82

Statistical Characteristics of Monthly Mean and Annual Concentrations of Particulate Matter PM2.5 and PM10 in Three Points of Tbilisi in 2017-2022

Darejan D. Kirkitadze

M. Nodia Institute of Geophysics of I. Javakhishvili Tbilisi State University, Tbilisi, Georgia
darejan.kirkitadze@gmail.com

ABSTRACT

Results of the detailed statistical analysis of the average monthly and annual concentrations of particulate matter PM2.5 and PM10 at three locations in Tbilisi (Kazbegi av., Tsereteli av. and Varketili) in 2017-2022 are presented. An analysis of the correlations between the indicated characteristics of air pollution has been carried out. The variability of the average annual values of PM2.5 and PM10 in the study period of observations was studied. In particular, it was found that in 2020-2021 there was a significant decrease in the average annual concentration of aerosols due to restrictions on the movement of vehicles associated with the covid-19 pandemic. It is noted that for the entire observation period, the average annual concentration of PM2.5 and PM10 was above the permissible norm.

Key words: *Atmospheric aerosols, particulate matter, PM2.5, PM10.*

Introduction

Over the past four decades at the M. Nodia Institute of Geophysics, TSU, as well as with his participation, carried out theoretical and experimental studies of the physical characteristics and variations of mineral and secondary aerosols (size distribution, weight and number concentrations, coagulation, condensation and ice-forming properties, optical characteristics, the effect of ionizing radiation on the formation secondary aerosols, influence on solar radiation, connection with thunderstorm and hail processes, as well as atmospheric precipitation, environmental aspects of air pollution, numerical modeling of the distribution of particulate matter in various regions of Georgia, etc.) [1-4].

Thus, a theoretical study of the influence of the periodicity of the source of particles on the process of their coagulation was carried out; modeling of processes that control the change in dispersion and the state of various coagulating systems [5].

The spatial and temporal changes in the concentration of solid impurities in the area with a large source of emissions in the city of Zestaponi and the conditions for the formation of aerosols and their accumulation in cities were studied [6].

The analysis of data on the distribution of aerosols with a radius of more than 0.35 μm over the territory of Georgia was carried out. In particular, it was found that within the lower five-kilometer layer of the atmosphere, the size distribution of aerosols is quite stable and changes little with height and under the influence of cloudiness. However, on days with cumulus clouds, compared to cloudless days, the mass of aerosols in a five-kilometer atmospheric layer increases by about 1.4 times, and on days with clouds of various types, including cumulus, by 2.5 times [7–11].

The results of studies of the long-term dynamics of surface air pollution in Tbilisi (weight concentration of aerosols, nitrogen oxides, sulfur dioxide, ozone) are presented in [12,13].

Works have been carried out on the numerical calculation of the spectral density of the aerosol optical depth of the atmosphere according to the total intensity of direct solar radiation, modeling the transfer of solar radiation in the atmosphere with allowance for aerosol scattering, and determining the aerosol optical depth of the atmosphere for various wavelengths [14, 15].

The results of studies of long-term variations in the aerosol optical depth of the atmosphere for individual points in Georgia and for the territory of Georgia as a whole were presented in [15-21]. In particular, it was found that the increase in the total aerosol pollution of the atmosphere in Georgia from 1928 to 1990 is exponential.

Anthropogenic, random and background values of the aerosol optical depth of the atmosphere (AOD) have been established for various regions of Georgia in the period from 1928 to 1990. Between the stations (Tbilisi, Telavi, Tsalka, Anaseuli, Senaki, Sukhumi) there is a high linear correlation both in the observed AOD values and in the values of their random components.

It was found that the level of atmospheric pollution by aerosols of the optically active size range over Kakheti differs little from this level over Tbilisi. In Western Georgia (Anaseuli, Senaki, Sukhumi), the level of air pollution is much lower than in Kakheti and in the areas adjacent to Tbilisi.

A model of the spatial and temporal distribution of AOD in Georgia has been created and maps have been constructed that show the dynamics of changes in AOD over the specified territory for five-year periods from 1956 to 1990. The contribution of local sources of aerosol pollution of the atmosphere to the AOD value is estimated, which, in particular, in the period from 1981 to 1990 in Tbilisi and Telavi is 33% each, Anaseuli, Senaki, Sukhumi - 10%. It is shown that on weekdays AOD values in Tbilisi and Kakheti are higher than on weekends.

Results of aircraft studies of aerosol pollution of the lower five-kilometer layer of the troposphere and Kakheti in 1973-1977 in particular showed the following. More than 70% of the mass of aerosols 0.2–4.0 μm in size is concentrated in the lower three-kilometer layer of the atmosphere. On cloudless days over Kakheti, the mass of aerosols in a vertical air column 5 km high is 66 mg/m², on days with cumulus clouds it is 90 mg/m², and on days with varying cloudiness it is 165 mg/m². In Tbilisi, the proportion of AOD for mineral aerosols of its total value is about 23%, for sulfates - 26%, and for industrial dust, nitrates, etc. - 50%. It is shown that the aerosol is more hygroscopic in urban areas than in rural areas. In Kakheti, a significant excess of aerosol content on weekdays compared to weekends is observed at an altitude of 1.0 km for particles with sizes $d>0.7$ μm, $2.0\leq d<4.0$ and $d\geq4.0$ μm. Variations in AOD in Kakheti are approximately 49% due to the content of radon in the lower three-kilometer layer of the atmosphere and only 10% due to solid aerosols larger than 0.7 μm.

In clouds, as well as in the free atmosphere, there is a direct relationship between the level of air ionization (radon and cosmic radiation) and the content of condensation nuclei. Changing the ionization intensity from 5.75 ion pairs $cm^{-3}sec^{-1}$ to 8.0 ion pairs $cm^{-3}sec^{-1}$ increases the content of condensation nuclei by a factor of 1.56. In this case, the proportion of ionization intensity due to radon and short-lived products of its decay is small and does not exceed 10%.

A direct correlation was found between AOD and ozone content in the troposphere over Tbilisi, indicating the important role of ozone in the formation of secondary aerosols. It has been shown that AOD is a fairly representative characteristic of surface air pollution with small aerosols (at least up to a diameter of 0.8 μm) [15–20].

Studies [22-24] showed that the dynamics of total aerosol pollution in Georgia and the North Caucasus (Kislovodsk) is similar.

The work [25] presents some results of modeling the distribution of the aerosol optical depth of the atmosphere (AOD) over the territory of Georgia in accordance with the previously proposed methodology for the combined analysis of satellite and ground-based AOD measurements in Tbilisi [26,

27]. In particular, it was found that elevated AOD values are observed in places with high cloudiness. Despite the fact that in Tbilisi there is a strong aerosol pollution of the atmosphere, the value of the AOD on days with clouds here differs slightly from the AOD over other cities (Kutaisi, Batumi) and even less than in places with high cloudiness. On cloudless days, AOD values decrease with increasing distance from the main source of air pollution in the city of Tbilisi [25]. This quite satisfactorily agrees with the previously obtained results on the distribution of AOD over the territory of Georgia in cloudless weather [16, 19–21].

The issue of monitoring aerosol pollution of the atmosphere in Georgia was discussed as part of the global air pollution monitoring network [28,29]. The issues of prospects for active impacts on atmospheric aerosols in order to clean the air from them were discussed [30, 31].

A theoretical model of heterogeneous nucleation on modified aerosol particles has been developed. In this case, a generalized heterogeneous nucleation equation was used, which takes into account the dependence of the interfacial specific surface energy on water vapor supersaturation. The issues of the formation of secondary ice crystals and the influence of particle sizes on the ice-forming activity of aerosol are considered [32, 33].

A refined concept of the interaction of aerosols with convective clouds has been developed, taking into account electrical, ionization, and other processes occurring in the atmosphere and clouds. Based on the concept, it is concluded that this interaction should be characterized by regional features due to both the physical conditions of cloud formation processes and the physicochemical properties of aerosol-gas air pollution. It has been shown that powerful convective and thunderclouds can make a significant contribution to direct and indirect radiation effects [9, 19, 21, 34].

Particular attention was paid to studying the effect of ionizing radiation (radon, gamma radiation, cosmic rays) on the formation of secondary aerosols in the atmosphere according to the gas → particle scheme. It has been found that all of these types of ionizing radiation are catalysts for the formation of submicron aerosols from gases [19, 21, 35–38].

The analysis of monitoring data in 2009-2012 was carried out. smog-forming and accompanying atmospheric parameters in Tbilisi, both in the mode of continuous measurements at two stationary observation bases (territories of the atmospheric physics department and the cosmic ray laboratory of the Institute of Geophysics), and in the mode of episodic route measurements at 20 points in various parts of the city (the content of ozone in the air, submicron aerosols, radon, light ions; intensity of solar radiation, visibility range, cloud cover, temperature, humidity, wind, pressure; soil gamma radiation; intensity of galactic cosmic rays). A physical-statistical model of the relationship between the processes of formation of photochemical smog and ozone with various atmospheric parameters is presented, on the basis of which the conditions for the formation of smog ozone in different seasons of the year are established. Maps of the spatial distribution of ozone, aerosols, light ions, radon and soil gamma radiation are presented. It is shown that according to the data of a stationary measurement point (territory of the atmospheric physics department), it is possible to estimate the level of air pollution in the city Tbilisi as a whole.

The features of the effect of radionuclide radiation in the formation of secondary aerosols in the conditions of the city of Tbilisi (Tbilisi type of smog) are revealed. The intensification by ionization of aerosol pollution of the atmosphere in Tbilisi is so strong that it also leads to a deterioration in air quality in terms of its ionic composition. In general, the Tbilisi type of smog is characterized by an impossible in natural conditions feedback of the content of radon, gamma radiation and cosmic radiation with the concentration of light ions in the air, caused by the formation of secondary aerosols in an amount that, together with primary particles, is able to attach more ions to itself than their formed during ionization. It is assumed that the Tbilisi type of smog can also occur in other cities with a heavily polluted atmosphere [38-42].

In [43], the results of a study of variations in the concentration of submicron aerosols with a diameter of ≥0.1 μm and their relationship with the content of radon (Rn) in the surface air layer of the city of Tbilisi are presented.

Particular attention was paid to the study of the influence of various components of photochemical smog on human health [38]. Thus, in particular, it was found that at an average daily concentration of submicron aerosols of more than 1000 cm^{-3} in Tbilisi, an increase in the number of emergency medical calls by 11% was noted [44].

Considerable attention was paid to studies of the relationship between aerosol pollution of the atmosphere, including radioactive pollution, and thunderstorm and hail processes, as well as the precipitation regime [21, 45–53].

In recent years, work has been actively carried out on numerical modeling of dust distribution in various regions of Georgia, taking into account external conditions (wind, etc.) [54-61]. A comparative analysis of aerosol air pollution in Tbilisi and Kutaisi was carried out [62]. The possibility of using the METEOR 735CDP10 meteorological radar for monitoring the movement of dust formations in the atmosphere was considered [63].

Several studies have examined the effects of traffic restrictions in Tbilisi due to the COVID-19 pandemic on airborne air pollution levels [64-66] compared to the pre-pandemic period [67]. In general, it was found that the level of aerosol air pollution in the absence of vehicular traffic decreased significantly. In particular, in [64], ground-based measurements of solid aerosol particles PM2.5 and PM10 were compared with satellite measurements of the aerosol optical depth of the atmosphere. It was found that there is a direct relationship between these parameters. We note that qualitatively similar results were obtained by us earlier [68] when comparing data on the AOD of the atmosphere, measured using actinometric observations, with the countable concentration of aerosols in the surface layer of the Tbilisi atmosphere.

This work is a continuation of previous studies [34-67]. Below are the results of the statistical analysis of the average monthly and annual concentrations of particulate matter PM2.5 and PM10 at three locations in Tbilisi (Kazbegi av., Tsereteli av. and Varketili) in 2017-2022.

Study Area, Materials and Methods

Study area – three locations of Tbilisi (A. Kazbegi av. - KZBG, A. Tsereteli av. - TSRT, Varketili - VRKT). Coordinates of these locations of air pollution measurements points in [67] is presented.

The data of Georgian National Environmental Agency about the daily mean values of dust concentration (atmospheric particulate matter - PM2.5 and PM10) [http://air.gov.ge/reports_page] that averaged on three indicated stations are used. Period of observation: January 2017 - December 2022.

In the proposed work the analysis of data is carried out with the use of the standard statistical analysis methods [69]. Missed data of time-series of observations were restored in the correspondence with the standard methods [70].

The following designations will be used below: Min – minimal values; Max - maximal values; St Dev - standard deviation; Cv = 100·St Dev/Average, coefficient of variation (%); R coefficient of linear correlation. KZBG(PM2.5), KZBG(PM10) …etc. - concentrations of particulate matter PM2.5 and PM10 on the Kazbegi av. measurement point, etc.; Av_Tb or Av(PM2.5) and Av(PM10) - averaged over all three stations PM2.5 and PM10; Δ(2018-2017) … etc. - difference between mean annual values of PM2.5 and PM10 for different year. The difference between the mean values of PM with the use of Student's criterion was determined (level of significance α is not worse than 0.15).

In the correspondence with the standards of the World Health Organization maximum permissible concentration (MPC) composes: annual mean for PM2.5 - 10 μg/m³ and for PM10 - 20 μg/m³ [71]. In the text below, the dimension of aerosol concentration (μg/m³) is mostly omitted.

Results and Discussions

Results in Fig. 1-4 and Tables 1-4 are presented.

In Fig. 1 and 2 for clarity for clarity time-series of mean monthly and annual values of PM2.5 and PM10 at three points in Tbilisi and their averaged values for all measurement points in 2017-2022 are presented.

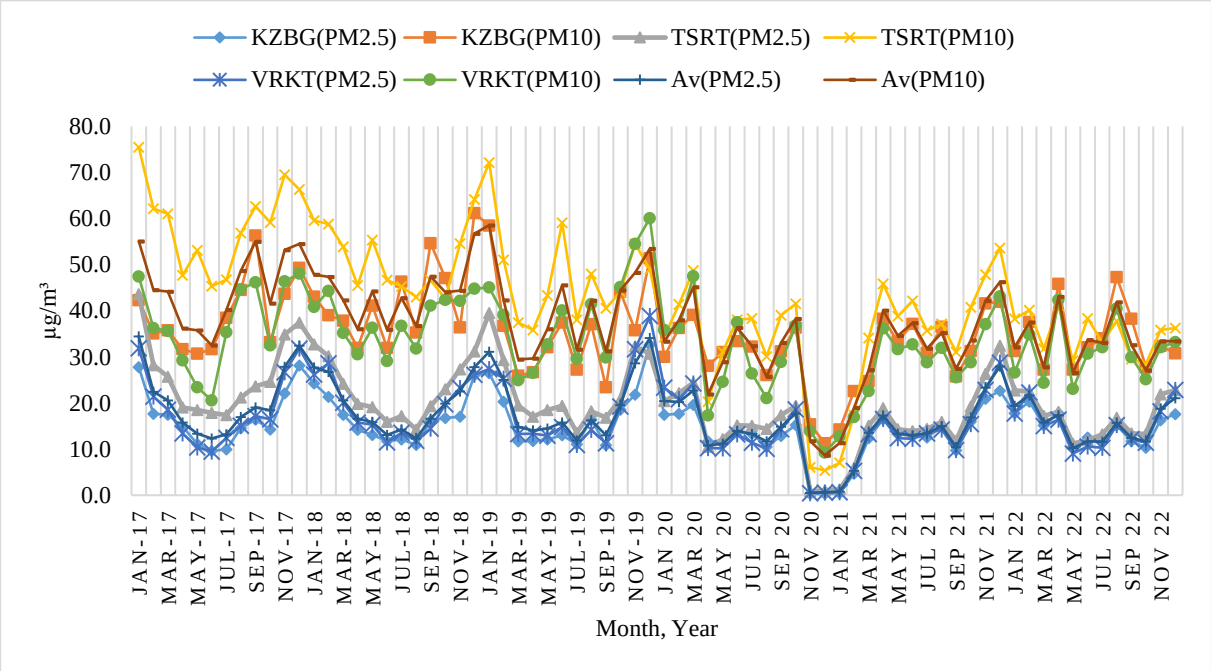

Fig. 1. Time-series of mean monthly values of PM2.5 and PM10 at three points in Tbilisi and their averaged values for all measurement points in 2017-2022.

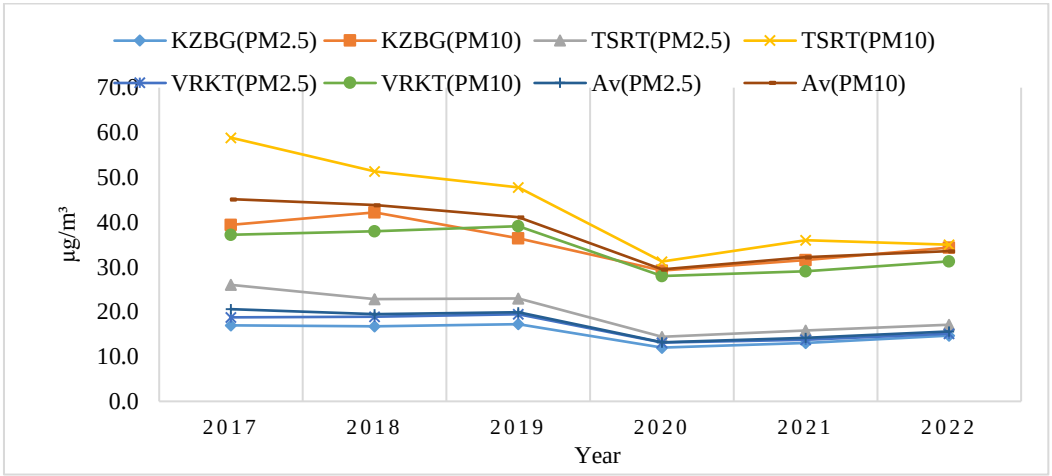

Fig. 2. Time series of mean annual values of PM2.5 and PM10 at three points in Tbilisi and their averaged values for all measurement points in 2017-2022.

In Table 1 statistical characteristics of mean monthly values of PM2.5 and PM10 at three points in Tbilisi and their averaged values for all measurement points in 2017-2022 are presented. In Table 2 the ratio between PM10 and PM2.5 at three points in Tbilisi and their averaged values for all measurement points are presented.

Analysis of the data presented in Fig. 1-2 and in Table 1-2 shows the following.

Table 1. Statistical characteristics of mean monthly values of PM2.5 and PM10 at three points in Tbilisi and their averaged values for all measurement points in 2017-2022 (μg/m³).

Variable	KZBG (PM2.5)	KZBG (PM10)	TSRT (PM2.5)	TSRT (PM10)	VRKT (PM2.5)	VRKT (PM10)	Av (PM2.5)	Av (PM10)
Year	2017							
Max	28.2	56.3	43.6	75.5	31.9	48.0	34.4	55.1
Min	9.6	30.7	17.3	45.3	9.5	20.6	12.3	32.5
Average	17.0	39.4	26.0	58.8	18.7	37.2	20.6	45.1
St Dev	6.2	8.0	8.5	9.4	7.7	9.5	7.4	8.1
Cv, %	36.7	20.3	32.9	15.9	41.3	25.7	36.2	18.0
Year	2018							
Max	26.1	61.2	32.7	64.2	28.7	44.8	27.8	56.7
Min	11.0	32.0	14.3	42.6	11.5	29.1	12.3	35.9
Average	16.8	42.2	22.9	51.3	18.9	37.9	19.5	43.8
St Dev	4.9	8.9	6.3	7.3	6.0	5.4	5.6	5.9
Cv, %	29.2	21.2	27.4	14.2	31.9	14.3	28.9	13.5
Year	2019							
Max	32.7	58.5	39.5	72.1	38.9	60.1	34.1	58.6
Min	10.8	23.4	13.6	35.8	10.9	24.9	11.9	29.4
Average	17.2	36.4	23.0	47.8	19.4	39.1	19.9	41.1
St Dev	7.0	10.7	7.9	10.5	9.2	11.0	7.8	9.6
Cv, %	40.7	29.3	34.6	21.9	47.4	28.1	39.0	23.5
Year	2020							
Max	19.6	39.1	24.4	48.8	24.3	47.5	22.7	45.1
Min	0.3	11.3	0.8	5.4	0.5	9.3	0.5	8.6
Average	12.0	29.2	14.4	31.2	13.1	28.0	13.2	29.4
St Dev	6.1	8.3	7.5	13.8	7.8	11.3	7.1	10.9
Cv, %	51.0	28.5	51.8	44.3	59.3	40.4	53.6	36.9
Year	2021							
Max	22.6	41.9	32.4	53.6	28.8	43.2	27.9	46.2
Min	0.4	14.3	1.3	7.0	0.7	12.7	0.8	11.3
Average	13.1	31.5	15.8	35.9	13.7	29.0	14.2	32.2
St Dev	6.2	8.4	8.2	12.9	7.3	8.6	7.2	9.8
Cv, %	47.2	26.6	52.0	35.9	52.9	29.6	50.5	30.5
Year	2022							
Max	20.3	47.3	22.8	41.1	22.9	42.4	21.7	43.1
Min	10.3	27.2	11.2	28.4	9.1	23.1	10.2	26.5
Average	14.7	34.3	17.1	35.0	15.1	31.3	15.6	33.5
St Dev	3.3	6.8	4.5	4.4	4.6	6.1	4.1	5.2
Cv, %	22.8	19.7	26.2	12.7	30.4	19.4	26.0	15.6
Year	2017-2022							
Max	32.7	61.2	43.6	75.5	38.9	60.1	34.4	58.6
Min	0.3	11.3	0.8	5.4	0.5	9.3	0.5	8.6
Average	15.1	35.5	19.8	43.3	16.5	33.7	17.2	37.5
St Dev	5.9	9.4	8.2	14.1	7.5	9.7	7.1	10.2
Cv, %	39.1	26.5	41.5	32.5	45.2	28.8	41.1	27.3

Year 2017:

Monthly average PM2.5 concentrations range from 9.5 (VRKT) to 43.6 (TSRT) and PM10 from 20.6 (VRKT) to 75.5 (TSRT). The range of change in the average annual concentration of PM2.5 is 17.0 (KZBG) ÷ 26.0 (TSRT), and PM10 - 37.2 (VRKT) ÷ 58.8 (TSRT). The ratio between average annual concentration of PM10 and PM2.5 change from 1.98 (VRKT) to 2.32 (KZBG).

A significant difference between the average annual concentrations of PM2.5 is noted for the following pairs of points and the city average concentrations (Av_Tb): KZBG-TSRT, TSRT-VRKT, Av_Tb-TSRT, and for PM10: KZBG-TSRT, TSRT-VRKT, Av_Tb-KZBG, Av_Tb-TSRT, Av_Tb-VRKT.

Year 2018:

Monthly average PM2.5 concentrations range from 11.0 (KZBG) to 32.7 (TSRT) and PM10 from 29.1 (VRKT) to 64.2 (TSRT). The range of change in the average annual concentration of PM2.5 is 16.8 (KZBG) ÷ 22.9 (TSRT), and PM10 - 37.9 (VRKT) ÷ 51.3 (TSRT). The ratio between average annual concentration of PM10 and PM2.5 change from 2.01 (VRKT) to 2.52 (KZBG).

A significant difference between the average annual concentrations of PM2.5 is noted for the following pairs of points and the city average concentrations (Av_Tb): KZBG-TSRT and TSRT-VRKT, and for PM10: KZBG-TSRT, TSRT-VRKT, Av_Tb-TSRT, Av_Tb- VRKT.

Year 2019:

Monthly average PM2.5 concentrations range from 10.8 (KZBG) to 39.5 (TSRT) and PM10 from 23.4 (KZBG) to 72.1 (TSRT). The range of change in the average annual concentration of PM2.5 is 17.2 (KZBG) ÷ 23.0 (TSRT), and PM10 - 36.4 (KZBG) ÷ 47.8 (TSRT). The ratio between average annual concentration of PM10 and PM2.5 change from 2.01 (VRKT) to 2.11 (KZBG).

A significant difference between the average annual concentrations of PM2.5 is noted for the following pairs of points and the city average concentrations (Av_Tb): KZBG-TSRT, and for PM10: KZBG-TSRT, TSRT-VRKT, Av_Tb-TSRT.

Table 2. The ratio between PM10 and PM2.5 at three points in Tbilisi and their averaged values for all measurement points.

Year	KZBG (PM10/PM2.5)	TSRT (PM10/PM2.5)	VRKT (PM10/PM2.5)	Av (PM10/PM2.5)
2017	2.32	2.27	1.98	2.19
2018	2.52	2.25	2.01	2.25
2019	2.11	2.08	2.01	2.07
2020	2.43	2.17	2.13	2.24
2021	2.41	2.28	2.11	2.26
2022	2.33	2.05	2.07	2.14
2017-2022	2.35	2.18	2.04	2.19

Year 2020: Period with COVID-19 restrictions on the movement of vehicles.

Monthly average PM2.5 concentrations range from 0.30 (KZBG) to 24.4 (TSRT) and PM10 from 5.4 (TSRT) to 48.8 (TSRT). The range of change in the average annual concentration of PM2.5 is 12.0 (KZBG) ÷ 14.4 (TSRT), and PM10 - 28.0 (VRKT) ÷ 31.2 (TSRT). The ratio between average annual concentration of PM10 and PM2.5 change from 2.13 (VRKT) to 2.43 (KZBG).

A significant difference between the average annual concentrations of PM2.5 is noted for the following pairs of points and the city average concentrations (Av_Tb): no significant difference, and for PM10: no significant difference.

Year 2021: Period with COVID-19 restrictions on the movement of vehicles.

Monthly average PM2.5 concentrations range from 0.40 (KZBG) to 32.4 (TSRT) and PM10 from 7.0 (TSRT) to 53.6 (TSRT). The range of change in the average annual concentration of PM2.5 is 13.1 (KZBG) ÷ 15.8 (TSRT), and PM10 - 29.0 (VRKT) ÷ 35.9 (TSRT). The ratio between average annual concentration of PM10 and PM2.5 change from 2.11 (VRKT) to 2.41 (KZBG).

A significant difference between the average annual concentrations of PM2.5 is noted for the following pairs of points and the city average concentrations (Av_Tb): no significant difference, and for PM10: TSRT-VRKT.

Year 2022: Post-COVID-19 period.

Monthly average PM2.5 concentrations range from 9.1 (VRKT) to 22.9 (VRKT) and PM10 from 23.1 (VRKT) to 47.3 (KZBG). The range of change in the average annual concentration of PM2.5 is 14.7 (KZBG) ÷ 17.1 (TSRT), and PM10 - 31.3 (VRKT) ÷ 35.0 (TSRT). The ratio between average annual concentration of PM10 and PM2.5 change from 2.07 (VRKT) to 2.33 (KZBG).

A significant difference between the average annual concentrations of PM2.5 is noted for the following pairs of points and the city average concentrations (Av_Tb no significant difference, and for PM10: TSRT-VRKT.

In Table 3 data on the Min, Max and Average values of linear correlation coefficient between concentrations of particulate matter for all point and Av(PM) are presented.

Table 3. Min, Max and Average values of linear correlation coefficient between concentrations of particulate matter for all point and Av(PM).

Year	Parameter	Min	Max	Average
2017	R	0.44	1.0	0.81
	Pair of point	TSRT(PM2.5)-KZBG(PM10)	Av(PM2.5)-VRKT(PM2.5)	
2018	R	0.28	1.0	0.74
	Pair of point	VRKT(PM2.5)-KZBG(PM10)	Av(PM2.5)-TSRT(PM2.5)	
2019	R	0.54	0.98	0.82
	Pair of point	VRKT(PM2.5)-TSRT(PM10)	Av(PM2.5)-VRKT(PM2.5)	
2020	R	0.87	0.99	0.94
	Pair of point	VRKT(PM2.5)-KZBG(PM10)	Av(PM2.5)-KZBG(PM2.5), TSRT(PM2.5),VRKT(PM2.5)	
2021	R	0.86	1.0	0.95
	Pair of point	TSRT(PM2.5)-KZBG(PM10)	Av(PM2.5)-TSRT(PM2.5), VRKT(PM2.5)	
2022	R	0.13	0.98	0.63
	Pair of point	TSRT(PM2.5)-KZBG(PM10)	Av(PM2.5)-TSRT(PM2.5), VRKT(PM2.5)	
2017-2022	R	0.66	0.98	0.84
	Pair of point	VRKT(PM2.5)-KZBG(PM10)	Av(PM2.5)-KZBG(PM2.5), TSRT(PM2.5), VRKT(PM2.5)	

As follows from Table 3 values of R between study parameters change from 0.13 (pair TSRT(PM2.5)-KZBG(PM10), 2022, “negligible correlation”) to 1.0 (pairs Av(PM2.5)-VRKT(PM2.5), 2017; Av(PM2.5)-TSRT(PM2.5), 2018; Av(PM2.5)-TSRT(PM2.5), Av(PM2.5)-VRKT(PM2.5), 2021 “very high correlation”). Average value of R change from 0.63 (2022, “moderate correlation” to 0.95 (2021, “very high correlation”). It should be noted that the highest average values of R between the studied parameters of air pollution in Tbilisi were observed in 2020 and 2021 with restrictions on the movement of vehicles due to the covid-19 pandemic (“very high correlation”). The lowest average R value was observed in 2022 in the post-COVID-19 period.

In Table 4 data on the Min, Max and Mean values of linear correlation coefficient between PM2.5 and PM10 for separated point and Av(PM) are presented.

Table 4. Min, Max and Mean values of linear correlation coefficient between PM2.5 and PM10 for separated point and Av(PM).

Year	Parameter	Min	Max	Average
2017	R	0.52	0.93	0.76
	Point	KZBG	TSRT	
2018	R	0.54	0.83	0.73
	Point	KZBG	TSRT	
2019	R	0.79	0.89	0.85
	Point	TSRT	VRKT	
2020	R	0.92	0.96	0.94
	Point	VRKT	TSRT	
2021	R	0.92	0.94	0.93
	Point	TSRT,VRKT	Av(PM)	
2022	R	0.35	0.60	0.45
	Point	KZBG	TSRT	
2017-2022	R	0.76	0.88	0.84
	Point	KZBG	TSRT	

Values of R between indicated parameters change from 0.35 (KZBG, 2022, “low correlation”) to 0.96 (TSRT 2020, “very high correlation”). Average value of R change from 0.45 (2022, “low correlation” to 0.94 (2020, “very high correlation”). As in the previous case (Table 3) the highest average values of R between the studied parameters were observed in 2020 and 2021 during the COVID-19 pandemic (“very high correlation”), and lowest – in post-COVID-19 period (“low correlation”).

In Fig. 3 data on difference between mean annual values of PM2.5 and PM10 at three points in Tbilisi and their averaged values for all measurement points in 2018-2017, 2019-2018, 2020-2019, 2021-2020 and 2022-2021 are presented.

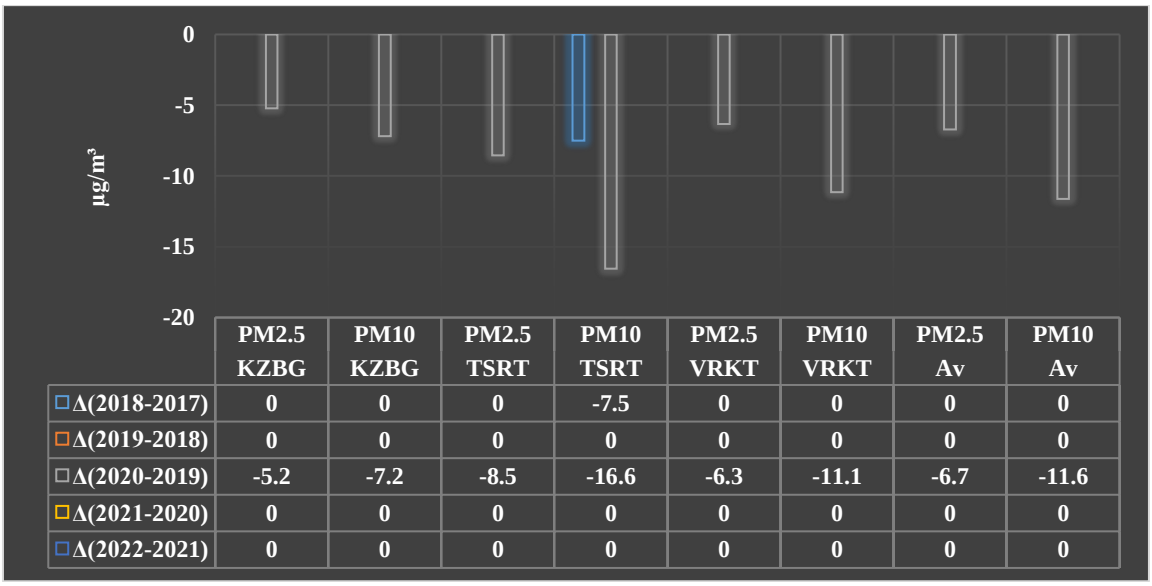

	PM2.5 KZBG	PM10 KZBG	PM2.5 TSRT	PM10 TSRT	PM2.5 VRKT	PM10 VRKT	PM2.5 Av	PM10 Av
Δ(2018-2017)	0	0	0	-7.5	0	0	0	0
Δ(2019-2018)	0	0	0	0	0	0	0	0
Δ(2020-2019)	-5.2	-7.2	-8.5	-16.6	-6.3	-11.1	-6.7	-11.6
Δ(2021-2020)	0	0	0	0	0	0	0	0
Δ(2022-2021)	0	0	0	0	0	0	0	0

Fig. 3. Difference between mean annual values of PM2.5 and PM10 at three points in Tbilisi and their averaged values for all measurement points in 2018-2017, 2019-2018, 2020-2019, 2021-2020 and 2022-2021 (0 - not significant difference, $\alpha>0.15$).

As follows from Fig. 3 a significant difference between the average annual concentrations of aerosol air pollution in Tbilisi in neighboring years is noted for PM10 for the TSRT measurement point (a decrease of 7.5 in 2018 compared to 2017), as well as for all points in 2020 (the period with the COVID-19 pandemic) compared to 2019. Δ(2020-2019) values change from –16.6 (TSRT point for PM10) to –5.2 (KZBG point for PM2.5).

In Fig. 4 data on difference between mean annual values of PM2.5 and PM10 at three points in Tbilisi and their averaged values for all measurement points in 2019-2017, 2020-2017, 2021-2017 and 2022-2017 are presented.

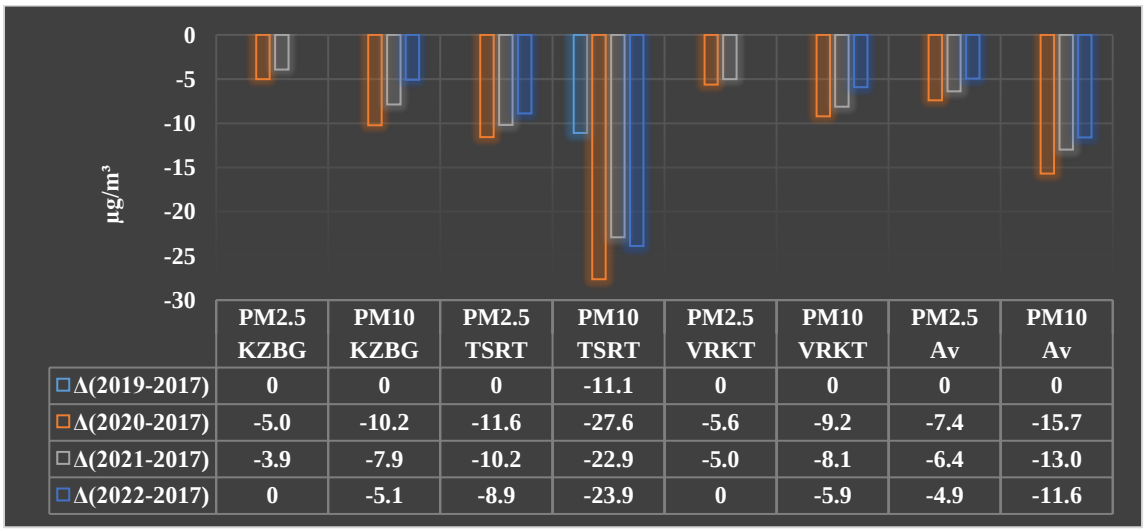

	PM2.5 KZBG	PM10 KZBG	PM2.5 TSRT	PM10 TSRT	PM2.5 VRKT	PM10 VRKT	PM2.5 Av	PM10 Av
Δ(2019-2017)	0	0	0	-11.1	0	0	0	0
Δ(2020-2017)	-5.0	-10.2	-11.6	-27.6	-5.6	-9.2	-7.4	-15.7
Δ(2021-2017)	-3.9	-7.9	-10.2	-22.9	-5.0	-8.1	-6.4	-13.0
Δ(2022-2017)	0	-5.1	-8.9	-23.9	0	-5.9	-4.9	-11.6

Fig. 4. Difference between mean annual values of PM2.5 and PM10 at three points in Tbilisi and their averaged values for all measurement points in 2019-2017, 2020-2017, 2021-2017 and 2022-2017 (0 - not significant difference, α>0.15).

As follows from Fig. 4 a significant value of Δ(2019-2017) only on point TSRT for PM10 is observed. A significant values of Δ(2020-2017) and Δ(2021-2017) for all measurement points are fixed. A significant values of Δ(2022-2017) for all measurement points except KZBG and VRKT for PM2.5 are observed.

Δ(2020-2017) values change from –27.6 (TSRT point for PM10) to –5.0 (KZBG point for PM2.5), Δ(2021-2017) values change from –22.9 (TSRT point for PM10) to –3.9 (KZBG point for PM2.5). Greatest value Δ(2022-2017) is -23.9 (TSRT point for PM10).

Note that in 2020-2021, the largest decrease in the average annual concentration of aerosols was observed due to restrictions on the movement of transport associated with the COVID-19 pandemic. In 2022, there was a slight increase in aerosol pollution of the atmosphere compared to the years with the COVID-19 pandemic.

However, for the entire period of observation, the average annual concentration of both PM2.5 and PM10 was higher than the permissible norm. On average in the city of Tbilisi, this increase was correspondingly. For PM2.5: 2017 (106%), 2018 (95%), 2019 (99%), 2020 (32%), 2021 (42%), 2022 (56%). For PM10: 2017 (126%), 2018 (119%), 2019 (105%), 2020 (47%), 2021 (61%), 2022 (68%).

On average, in 2017-2022, the least polluted air in terms of PM2.5 was recorded at the KZBG point (exceeding the concentration of PM2.5 compared to the permissible norm - 51%), the most polluted - at the TSRT point (exceeding - 98%). The least polluted air according to PM10 was recorded at the VRKT point (exceeding the concentration of PM10 compared to the permissible norm - 69%), the most polluted - at the TSRT point (exceeding - 117%).

Conclusion

In the near future, it is planned to continue similar studies of the variability of daily, average monthly and average annual values of PM2.5 and PM10 in both Tbilisi and other regions of Georgia.

References

[1] Kirkitadze D., Nikiforov G., Chankvetadze A., Chkhaidze G. Some Results of Studies of Atmospheric Aerosols in M. Nodia Institute of Geophysics in the Recent Three Decades. Trans. of Mikheil Nodia Institute of Geophysics, ISSN 1512-1135, vol. 66, Tbilisi, 2016, pp. 178-185, (in Russian).

[2] Gigauri N.G., Gverdtsiteli L.V., Surmava A.A., Intskirveli L.N. Numerical Simulation of Industrial Dust Distribution in the Territory of Zestafoni, Georgia. WIT Transaction on Ecology and Environment, 230, 2018, pp. 119-128. Doi:10.2495/AIR1180111.

[3] Gigauri N., Pipia M., Beglarashvili N., Mdivani S. Evaluation of the Content of Microparticles in the Atmosphere of Rustavi by Experimental Measurements. International Conference of Young Scientists "Modern Problems of Earth Sciences", Proceedings, ISBN 978-9941-36-044-2, Publish House of Iv. Javakhishvili Tbilisi State University, Tbilisi, November 21-22, 2022, pp. 97-101, (in Georgian).

[4] Kukhalashvili V., Pipia M., Gigauri N., Surmava A., Intskirveli L. Study of Tbilisi City Atmosphere Pollution with PM2.5 and PM10-Microparticles During COVID-19 Pandemic Period. Journal of the Georgian Geophysical Society, e-ISSN: 2667-9973, p-ISSN: 1512-1127, Physics of Solid Earth, Atmosphere, Ocean and Space Plasma, v. 25(2), 2022, pp. 29–37. DOI: https://doi.org/10.48614/ggs2520225958

[5] Gorchakov G.I., Emilenko A.S., Kartsivadze A.I., Metreveli D.M., Sidorov V.N. Variation of Submicron Aerosol Structure. Proc. 9th Int. Conf. on Atmospheric Aerosols, Condensation and Ice Nuclei, Budapest, Hungary, 3-8 September, vol.1, 1984, p. 159-163.

[6] Kharchilava D.F., Lomaia O.V., Bukia G.N. The Conditions of Aerosols Formation and Accumulation in Cities. Proc. 3th Int. Aerosol Conf., Kyoto, Japan, Pergamon, vol. 2, 24-27 September, 1990, p. 986-989.

[7] Styra B., Amiranashvili A. Aerosol Distribution above Georgia Investigations. Institute of Physics of the Academy of Sciences of the Lithunian SSR, Atmospheric Physics, ISSN 0135-1419, vol. 8, Vilnius, Mokslas, 1983, pp. 18-24, (in Russian).

[8] Amiranashvili A.G., Gzirishvili T.G., Kartsivadze A.I., Nodia A.G. Aircraft investigations of the distribution of aerosols in the lower troposphere. Proc. 9th Int. Conf. on Atmospheric Aerosols, Condensation and Ice Nuclei, Budapest, Hungary, 3-8 September, vol.1, 1984, p. 148-153.

[9] Amiranashvili A.G., Gzirishvili T.G. Aerosols and Ice Crystals in the Atmosphere. Tbilisi, Metsniereba, 1991, 113 p. (in Russian).

[10] Amiranashvili A., Amiranashvili V., Chochishvili K., Kirkitadze D. The Distribution of Aerosols over the Georgian Territory in the Lower Troposphere, Journal of Georgian Geophysical Society, ISSN 1512-1127, Jssue B. Physics of Atmosphere, Ocean and Space Plasma, Vol. 8 B, 2003, Tbilisi, 2004, pp. 70-76.

[11] Amiranashvili A. G. Boleslovas Styra. 105 Years from the Birthday. His Role in the Formation, Development and Modern Evolution of Nuclear Meteorology in Georgia. Journal of Georgian Geophysical Society, ISSN 1512-1127, Jssue B. Physics of Atmosphere, Ocean and Space Plasma, Vol. 20 B, 2017, Tbilisi, 2017, pp. 73-87.

[12] Amiranashvili A., Amiranashvili V., Gzirishvili T., Gunia G., Intskirveli L., Kharchilava J. Variations of the Weight Concentrations of Dust, Nitrogen Oxides, Sulphur Dioxide and Ozone in the Surface Air in Tbilisi. Proc.15th Int. Conf. on Nucleation and Atmospheric Aerosols, Rolla, Missouri, USA, 2000, August, 6-11, AIP, Conference Proc., vol.535, Melville, New York, 2000, p. 793-795.

[13] Amiranashvili A.G., Chikhladze V.A., Kharchilava J.F., Buachidze N.S., Intskirveli L.N. Variations of the Weight Concentrations of Dust, Nitrogen Oxides, Sulphur Dioxide and Ozone in the Surface Air in Tbilisi in 1981-2003, Proc. 16th International Conference on Nucleation&Atmospheric Aerosols, Kyoto, Japan, 26-30 July 2004, pp. 678-681.

[14] Amiranashvili V. Numerical Calculation of the Spectral Aerosol Optical Depth Using Data on Integral Irradiance of the Direct Solar Radiation. Abstr. IUGG 99, 19-30 July 1999, Birmingham UK, p. A.236.

[15] Amiranashvili V. Modelling of Solar Radiation Transfer in the Atmosphere with Allowance to Aerosol Diffusion. J. Aerosol Sci., Vol. 30, Suppl 1, Pergamon Press, 1999, p. S625-S626.
[16] Amiranashvili A., Amiranashvili V., Tavartkiladze K. Dynamics of the Aerosol Pollution of the Atmosphere in Georgia in 1956-1990, J. Aerosol Sci, Pergamon, vol.30, Suppl.1, 1999, S667-S668.
[17] Amiranashvili A., Amiranashvili V., Khurodze T.,Tavartkiladze K.,Tsitskishvili M. Some Characteristics of the Aerosol Pollution of the Atmosphere Over the Territory of Kakheti in the Warm Season, Proc. Int. Conf. Dedicated to Memory of Prof. A. Sutugin, Moscow, Russia, June 26-30, 2000, 128-129.
[18] Amiranashvili A.G., Amiranashvili V.A., Kirkitadze D.D., Tavartkiladze K.A. Some Results of Investigation of Variations of the Atmospheric Aerosol Optical Depth in Tbilisi , Proc. 16th Int. Conf. on Nucleation&Atmospheric Aerosols, Kyoto, Japan, 26-30 July 2004, 416-419.
[19] Amiranashvili A.G., Amiranashvili V.A., Gzirishvili T.G., Kharchilava J.F., Tavartkiladze K.A. Modern Climate Change in Georgia. Radiatively Active Small Atmospheric Admixtures, Institute of Geophysics, Monograph, Trans. of M. Nodia Institute of Geophysics of Georgian Acad. of Sci., ISSN 1512-1135, vol. LIX, 2005, 128 p.
[20] Tavartkiladze K., Begalishvili N., Kharchilava J., Mumladze D., Amiranashvili A., Vachnadze J., Shengelia I., Amiranashvili V. Contemporary Climate Change in Georgia. Regime of Some Climate Parameters and their Variability. Monograph, Tbilisi, ISBN 99928-885-4.7, 2006, 177 p., (in Georgian), http://openlibrary.ge/handle/123456789/535
[21] Amiranashvili A. G. Issledovaniye grozo-gradovykh protsessov v Gruzii i ikh svyazi s aerozol'nym zagryazneniyem atmosfery. Avtoreferat dissertatsiy na soiskaniye uchenoy stepeni doktora fiziko-matematicheskikh nauk, Tbilisi, 2006, 53 s., http://www.openlibrary.ge/bitstream/123456789/4920/1/Amiranashvili_Avtoreferat_2006.pdf.
[22] Amiranashvili A., Kirilenko A., Kortunova Z., Povolotskaia N., Senik I., Tavartkiladze K. Changeability of the Aerosol Pollution of Atmosphere in Tsalka and Kislovodsk in 1941-1990. Proc. of Int. Conf. "Modern Problems of Geography", Dedicated to the 80th Anniversary Since the Fondation of Vakhushti Bagrationi Institute of Geography, Collected Papers New Series, N 5(84), ISSN 2233-3347, Tbilisi, 2013, pp. 178-181, (in Russian). http://109.205.44.60/bitstream/123456789/662/1/Geography_2013_Amiranashvili_2....pdf
[23] Amiranashvili A.G., Tavartkiladze K.A, Kirilenko A.A., Kortunova Z.V., Povolotskaya N.P., Senik I.A. Dynamics of the Aerosol Pollution of Atmosphere in Tbilisi and Koslovodsk. Trans. of the Institute of Hydrometeorology, Georgian Technical University, ISSN 1512-0902, 2013, vol. 119, pp. 212-215, (in Russian).
[24] Amiranashvili A.G., Tavartkiladze K.A., Kirilenko A.A., Kortunova Z.V., Povolotskaya N.P., Senik I.A. Dinamika obshchego aerozol'nogo zagryazneniya atmosfery v Kislovodske i nekotorykh rayonakh Gruzii v 1941-1990 gg. Mezhdunarodnaya konferentsiya «Aerozol' i optika atmosfery» (k stoletiyu G.V. Rozenberga), Tezisy dokladov, 21-24 oktyabrya, Moskva, 2014, s. 10.
[25] Stankevich S., Titarenko O., Amiranashvili A., Chargazia Kh. Determination of Atmospheric Aerosol Optical Depth over Territory of Georgia during Different Regimes of Cloudiness Using the Satellite and Ground-Based Measurements Data. Bulletin of the Georgian National Academy of sciences, v. 9, No. 3, 2015, pp. 91-95.
[26] Stankevich A.S., Titarenko O.V., Amiranashvili A.G., Chargazia Kh. Z. Determination of Distribution of Ozone Content in Lower Troposphere and Atmospheric Aerosol Optical Thickness over Territory of Georgia Using Satellite Data and Ground Truth Measurements. Journal of the Georgian Geophysical Society, Issue (B). Physics of Atmosphere, Ocean, and Space Plasma, ISSN: 1512-1127, v.17b, 2014, pp. 26-37.
[27] Stankevich S. A., Titarenko O., V., Amiranashvili A., G., Chargazia Kh., Z. Analysis of the Atmosphere Aerosol and Ozone Condition Over Tbilisi Using Satellite Data and Ground Truth Measurements. 14th Ukrainian Conference on Space Research, Uzhgorod, September, 8-12, 2014, Abstracts, Kyiv, 2014, p. 161.

[28] Amiranashvili A., Amiranashvili V., Tavartkiladze K., Laulaineni N. Atmosperos aerozoluri dachuchqianebis monitoringi Sakartveloshi. Hidrometeorologiis institutis shromebi, ISSN 1512–0902, tomi 108, Tbilisi, 2002, gv. 19–23.
[29] Tsitskishvili M.S., Amiranashvili A.G. Global'nyy monitoring dinamiki aerozol'noy komponenty atmosfery srednikh shirot na sinkhronno-sopryazhennykh fonovykh statsionarakh severnogo i yuzhnogo Kavkaza (predlozheniye po sovmestnomu proyektu). Mezhdunarodnaya konferentsiya «Aerozol' i optika atmosfery» (k stoletiyu G.V. Rozenberga), Tezisy dokladov, 21-24 oktyabrya, Moskva, 2014, s. 86.
[30] Tsitskishvili M., Lushnikov A., Zagaynov V., Pkhaladze M., Amiranashvili A., Tskhakaya K., Chikhladze V., Kikvadze R., Goginava I.B. Nekotoryye rezul'taty issledovaniy i perspektivy aktivnykh vozdeystviy na atmosfernyye aerozoli. International Scientific Conference «Modern Problems of Ecology», Collection of reports, ISSN 1512 -1976, Kutaisi, 2014, s. 180-191.
[31] Amiranashvili A.G., Tsitskishvili M.S. Aerozol'naya ekspress ochistka atmosfery. Mezhdunarodnaya konferentsiya «Aerozol' i optika atmosfery» (k stoletiyu G.V. Rozenberga), Tezisy dokladov, 21-24 oktyabrya, Moskva, 2014, s. 98.
[32] Gzirishvili T.G., Kartsivadze A.I., Okudzhava A.M. Heterogennaya nucleatsia of l'da. Tb.:, "Metsniereba", 1984, 140 p.
[33] Gzirishvili T.G., Khorguani V.G. About Secondary Ice Crystal Production. Proc. 10-th Int. Conf. Cloud Phys. Bad-Homburg, FRG, 1988, p. 254-256.
[34] Amiranashvili A. Scheme of the interaction of atmospheric aerosols and convective clouds. IUGG 2003 Abstract, Sapporo, Japan, June 30-July 11, 2003, MI02b/D-041.
[35] Amiranashvili A.G. , Amiranashvili V.A., Kirkitadze D.D., Chiabrishvili N.G., Chochishvili K.M. To a Question About the Formation of Secondary Aerosols in the Atmosphere. Trans. of M. Nodia Institute of Geophysics of Georgian Acad. of Sci., ISSN 1512-1135, vol. 58, Tb., 2004, pp.119-126 , (in Russian).
[36] Amiranashvili A.G. On the Role of Cosmic and Radioactive Radiation on the Formation of the Secondary Aerosols in Atmosphere, Int. Conference "Near-Earth Astronomy 2007" Abstract, Terskol, Russia, 3-7 September 2007.
[37] Amiranashvili, A.G., Amiranashvili, V.A., Bakradze, T.S., Chikhladze, V.A., Glonti, N.Ya., Kharchilava, J.F.,Tuskia, I.I On the Influence of Cosmic Rays on the Secondary Aerosols Formation in the Atmosphere. 7th Int. Conference "Problems of Geocosmos", Abstract, 26 - 30 May, 2008, St. Petersburg, Russia.
[38] Amiranashvili A., Bliadze T., Chikhladze V. Photochemical smog in Tbilisi. Monograph, Trans. of Mikheil Nodia institute of Geophysics, ISSN 1512-1135, vol. 63, Tbilisi, 2012, 160 p., (in Georgian).
[39] Amiranashvili A., Bliadze T., Kirkitadze D., Nikiforov G., Nodia A., Kharchilava j., Chankvetadze A., Chikhladze V., Chochishvili K., Chkhaidze G.P. Some Preliminary Results of the Complex Monitoring of Surface Ozone Concentration (SOC), Intensity of Summary Solar Radiation and Sub-Micron Aerosols Content in Air in Tbilisi in 2009-2010. Trans. of Mikheil Nodia Institute of Geophysics, ISSN 1512-1135, vol. 62, Tbilisi, 2010, pp. 189-196, (in Russian).
[40] Amiranashvili A. Negative Correlation Between of Light Ions Content and Radon Concentration: Particularity of Tbilisi City Air Pollution, or Norm for the Urbanized Locality? Proc. of the 14th Int. Conf. on Atmospheric Electricity, Rio de Janeiro, Brazil, August 07-12, 2011, http://www.icae2011.net.br/.
[41] Amiranashvili A. The feedback effect of intensity of ionizing radiation with the light ions content in atmosphere. Paradox (the Tbilisi type of a smog), or usual phenomenon for the strongly pollution cities? Proc. of Int. Conf. "Environment and Global Warming", Dedicated to the 100th Birthday Anniversary of Academician F. Davitaya, Collected Papers New Series, N 3(82), ISSN 2333-3347, Tbilisi, 2011, pp. 95-100.
[42] Amiranashvili A. Tbilisi Type of Smog as Attribute of Feedback Effect Between the Air Ionization Intensity and Small Ions Concentration. Proc. of 7th Asia-Pacific Int. Conf. on Lightning, Chengdu, China, November 1-4, 2011, http://www.apl2011.net/.
[43] Amiranashvili A., Chargazia Kh. Intra-Annual and Seasonal Variations of Sub-Micron Aerosols Concentration and their Connection with Radon Content in Surface Boundary Layer of Tbilisi City. Bulletin of the Georgian National Academy of Sciences, vol. 10, N 2, 2016, p. 72-78.

[44] Amiranashvili A.G., Bliadze T.G., Kirkitadze D.D., Chikhladze V.A., Chankvetadze A.SH. Submikronnyye aerozoli v atmosfere Tbilisi i ikh vliyaniye na zdorov'ye lyudey. Mezhdunarodnaya konferentsiya «Aerozol' i optika atmosfery» (k stoletiyu G.V. Rozenberga), Tezisy dokladov, 21-24 oktyabrya, Moskva, 2014, s. 68.
[45] Amiranashvili A.G., Gzirishvili T.G., Chumburidze Z.A. On the Role of Artificial Ice Forming Reagents and Radioactive Intermixtures in the Variation of Convective Clouds Thunderstorm and Hail Activity. Proc. 12th Int. Conf. on Clouds and Pricipitation, Zurich, Switzerland, August 19-23, vol. 1, 1996, pp. 267-270
[46] Amiranashvili A.G., Amiranashvili V.A., Bachiashvili L.L., Bibilashvili T.N., Supatashvili G.D. Influence of the Anthropogenic Pollution of the Atmosphere and Thunderstorms on the Precipitations Regime and their Chemical Composition in Alazani Valley Conditions. Proc. 14thInternational Conference on Clouds and Precipitation, Bologna, Italy ,18-23 July 2004, 2_3_216.1-2_3_216.2.
[47] Amiranashvili A., Amiranashvili V., Nodia A., Kirkitadze D. Connection of Thunderstorm Processes Intensity with Aerosol Pollution of the Atmosphere, Proc. 13th Int. Conf. on Atmospheric Electricity, Beijing, China, 13-18 August 2007.
[48] Amiranashvili A. Connection Between the Characteristics of Thunderstorm Activity and Air Pollution in Kakheti Region of Georgia, Proc. of IX Int. Symposium on Lightning Protection, Foz do Iguaçu, Brazil, 26-30 November 2007.
[49] Amiranashvili A. Effect of Air Pollution on the Precipitations in Eastern Georgia, IUGG 2007 Abstract, Perugia, Italy, 2 -13 July 2007
[50] Amiranashvili A. Statistical Models of Connection of Lightning Activity with Aerosol Pollution of Atmosphere, Proc. of X Int. Symposium on Lightning Protection, Curitiba, Brazil, 9-13 November 2009, pp.261-266.
[51] Amiranashvili A. Influence of the Anthropogenic Pollution of Atmosphere on the Changeability of Hail Processes Intensity. Trans. of Mikheil Nodia Institute of Geophysics, ISSN 1512-1135, vol. 64, Tbiisi, 2013, pp. 160-177. http://dspace.gela.org.ge/bitstream/123456789/697/1/Tom-64_Amiranashvili.pdf
[52] Adzhiyev A.KH., Amiranashvili A.G., Chargazia Kh.Z. Vliyaniye aerozol'nogo zagryazneniya atmosfery na effektivnost' protivogradovykh rabot v Kakhetii i na Severnom Kavkaze. Doklady Vserossiyskoy otkrytoy konferentsii po fizike oblakov i aktivnym vozdeystviyam na gidrometeorologicheskiye protsessy, posvyashchennoy 80-letiyu El'brusskoy vysokogornoy kompleksnoy ekspeditsii AN SSSR, 7-9 oktyabrya 2014 g., chast' 2, FGBU «Vysokogornyy geofizicheskiy institut», Nal'chik, 2015, s. 387-395. http://www.dspace.gela.org.ge/bitstream/123456789/5264/1/Аджиев,Амиранашвили,Чаргазиа_Докл_Нальчик_2014%20(2015).pdf
[53] Kartvelishvili L., Tatishvili M., Amiranashvili A., Megrelidze L., Kutaladze N. Weather, Climate and their Change Regularities for the Conditions of Georgia. Monograph, Publishing House "UNIVERSAL", Tbilisi 2023, 406 p., https://doi.org/10.52340/mng.9789941334658
[54] Surmava A., Gigauri N., Gverdtsiteli L., Intskirveli L. Numerical Modeling of Zestafoni City Dust Distribution in Case of Background Western, Light Air, Gentle and Fresh Breezes. Trans. of Mikheil Nodia Institute of Geophysics, ISSN 1512-1135, vol. 69, Tbilisi, 2018, pp. 182-191, (in Georgian).
[55] Surmava A. A. Numerical Modeling of Zestafoni City Dust Dispersion in case of Western Wind. Journal of the Georgian Geophysical Society, ISSN: 1512-1127, Physics of Solid Earth, Atmosphere, Ocean and Space Plasma, v. 21(2), Tbilisi, 2018, pp. 21-26.
[56] Surmava A., Gigauri N., Kukhalashvili V., Intskirveli L., Mdivani S. Numerical Modeling of the Anthropogenic Dust Transfer by Means of Quasistatic and Non-Quasistatic Models. International Scientific Conference "Natural Disasters in Georgia: Monitoring, Prevention, Mitigation". Proceedings, ISBN 978-9941-13-899-7, Publish Hous of Iv. Javakhishvili Tbilisi State University, December 12-14, Tbilisi, 2019, pp. 134-137.
[57] Surmava A., Intskirveli L., Kukhalashvili V., Gigauri N. Numerical Investigation of Meso- and Microscale Diffusion of Tbilisi Dust. Annals of Agrarian Science, 18, No. 3, 2020, pp. 295-302.
[58] Kukhalashvili V.G., Gigauri N.G., Surmava A.A., Demetrashvili D.I, Intskirveli L.N. Numerical Modelling of Dust Propagation in the Atmosphere of Tbilisi City: The Case of Background Eastern

Fresh Breeze. Journal of the Georgian Geophysical Society, ISSN: 1512-1127, Physics of Solid Earth, Atmosphere, Ocean and Space Plasma, v. 23(1), 2020, pp. 51-56.
[59] Kukhalashvili V.G., Kordzakhia G.I.,Gigauri N.G. , Surmava A.A., Intskirveli L.N. Numerical Modelling of Dust Propagation in the Atmosphere of Tbilisi City: The Case of Background Eastern Gentle Breeze. Journal of the Georgian Geophysical Society, ISSN: 1512-1127, Physics of Solid Earth, Atmosphere, Ocean and Space Plasma, v. 23(1), 2020, pp. 46-50.
[60] Gigauri N., Surmava A., Intskirveli L.,Demetrashvili D.,Gverdtsiteli L., Pipia M. Numerical Modeling of PM2.5 Propagation in Tbilisi Atmosphere in Winter. I. A Case of Background South Light Wind. International Scientific Conference „Natural Disasters in the 21st Century: Monitoring, Prevention, Mitigation“. Proceedings, ISBN 978-9941-491-52-8, Tbilisi, Georgia, December 20-22, 2021. Publish House of Iv. Javakhishvili Tbilisi State University, Tbilisi, 2021, pp. 74 - 78.
[61] Gigauri N., Surmava A. Evaluation of the Contamination of the Atmosphere of Rustavi with Microparticles by Numerical Modeling. International Conference of Young Scientists "Modern Problems of Earth Sciences", Proceedings, ISBN 978-9941-36-044-2, Publish House of Iv. Javakhishvili Tbilisi State University, Tbilisi, November 21-22, 2022, pp. 102-106, (in Georgian).
[62] Bliadze T.G., Kirkitadze D.D., Tchankvetadze A. Sh., Chikhladze V.A. Comparative Analysis of Air Pollution in Tbilisi and Kutaisi. International Scientific Conference „Modern Problems of Ecology“, Proceedings, ISSN 1512-1976, v. 6, Kutaisi, Georgia, 21-22 September, 2018, pp. 157-160.
[63] Amiranashvili A.G., Chikhladze V.A., Mitin M.N. Preliminary Results of the Analysis of Radar and Ground-Based Monitoring of Dust Formation in Atmosphere Above the Territory of Eastern Georgia on 27 July 2018. Journal of the Georgian Geophysical Society, ISSN: 1512-1127, Physics of Solid Earth, Atmosphere, Ocean and Space Plasma, v. 21(2), Tbilisi, 2018, pp. 61-69.
[64] Amiranashvili A.G., Kirkitadze D.D., Kekenadze E.N. Pandemic of Coronavirus COVID-19 and Air Pollution in Tbilisi in Spring 2020. Journal of the Georgian Geophysical Society, ISSN: 1512-1127, Physics of Solid Earth, Atmosphere, Ocean and Space Plasma, v. 23(1), 2020, pp. 57-72.
[65] Kirkitadze D. Changeability of Monthly Mean Values of PM2.5 and PM10 in Three Points of Tbilisi from January 2017 to October 2021. Pandemic of Coronavirus Covid-19 and PM2.5/10 in Tbilisi from March 2020 to August 2021. International Scientific Conference „Natural Disasters in the 21st Century: Monitoring, Prevention, Mitigation“. Proceedings, ISBN 978-9941-491-52-8, Tbilisi, Georgia, December 20-22, 2021. Publish House of Iv. Javakhishvili Tbilisi State University, Tbilisi, 2021, pp. 101 - 105.
[66] Kirkitadze D. Variability of Monthly Mean Values of PM2.5 and PM10 in Three Points of Tbilisi from January 2017 to May 2020. Pandemic of Coronavirus COVID-19 and PM2.5/10 in Spring 2020 in Tbilisi.Int. Sc. Conf. „Modern Problems of Ecology“, Proc., ISSN 1512-1976, v. 7, Tbilisi-Telavi, Georgia, 26-28 September, 2020, pp. 268-272.
[67] Kirkitadze D.D. Statistical Characteristics of Aerosol Pollution of Atmosphere in Three Points of Tbilisi in 2017-2018. Journal of the Georgian Geophysical Society, ISSN: 1512-1127, Physics of Solid Earth, Atmosphere, Ocean and Space Plasma, v. 22(2), 2019, pp. 55–62.
[68] Amiranashvili A.G., Amiranashvili V.A., Kirkitadze D.D., Tavartkiladze K.A. Connection Between Atmospheric Aerosol Optical Depth and Aerosol Particle Number Concentration in the Air in Tbilisi, Proc. 17th Int. Conf. on Nucleation&Atmospheric Aerosols, Galway, Ireland, 13-18 August 2007, 865-870.
[69] Hinkle D. E., Wiersma W., Jurs S. G. Applied Statistics for the Behavioral Sciences. Boston, MA, Houghton Mifflin Company, ISBN: 0618124055; 9780618124053, 2003, 756 p.
[70] Kobisheva N., Narovlianski G. Climatological processing of the meteorological information, Leningrad, Gidrometeoizdat, 1978, 294 p., (in Russian).
[71] WHO Air quality guidelines for particulate matter, ozone, nitrogen dioxide and sulfur dioxide. Global update 2005 Summary of risk assessment. World Health Organization, 2006, 22 p., http://apps.who.int/iris/bitstream/handle/10665/69477/WHO_SDE_PHE_OEH_06.02_eng.pdf;jsessionid=48F380E7090ADBB4A166AC7A8610624A?sequence=1

თბილისის სამ წერტილში 2017-2022 წლებში მყარი ნაწილაკების PM2.5 და PM10-ის საშუალო თვიური და წლიური კონცენტრაციების სტატისტიკური მახასიათებლები

დ. კირკიტაძე

რეზიუმე

წარმოდგენილია PM2.5 და PM10 ნაწილაკების საშუალო თვიური და წლიური კონცენტრაციების დეტალური სტატისტიკური ანალიზის შედეგები თბილისის სამ წერტილში (ყაზბეგის გამზ., წერეთლის გამზ. და ვარკეთილი) 2017-2022 წლებში. ჩატარდა ჰაერის დაბინძურების მითითებულ მახასიათებლებს შორის კორელაციის ანალიზი. შესწავლილი იყო PM2.5 და PM10 საშუალო წლიური მნიშვნელობების ცვალებადობა საკვლევი დაკვირვების პერიოდში. კერძოდ, დადგინდა, რომ 2020-2021 წლებში დაფიქსირდა აეროზოლების საშუალო წლიური კონცენტრაციის მნიშვნელოვანი შემცირება COVID-19-ის პანდემიასთან დაკავშირებული მანქანების გადაადგილების შეზღუდვის გამო. აღნიშნულია, რომ დაკვირვების მთელი პერიოდის განმავლობაში PM2.5 და PM10 საშუალო წლიური კონცენტრაცია დასაშვებ ნორმაზე მაღალი იყო.

საკვანძო სიტყვები: ატმოსფერული აეროზოლები, მყარი ნაწილაკები, PM2.5, PM10.

Статистические характеристики среднемесячных и годовых концентраций твердых частиц PM2.5 и PM10 в трех пунктах города Тбилиси в 2017-2022 гг.

Д.Д. Киркитадзе

Резюме

Представлены результаты детального статистического анализа среднемесячных и годовых концентраций твердых частиц PM2.5 и PM10 в трех точках Тбилиси (пр. Казбеги, пр. Церетели и Варкетели) в 2017-2022 гг. Проведен анализ корреляционных связей между указанными характеристиками загрязнения воздуха. Изучена изменчивость среднегодовых значений PM2.5 и PM10 в исследуемый период наблюдений. В частности получено, что в 2020-2021 наблюдалось значительное понижение среднегодовой концентрации аэрозолей из-за ограничений перемещений транспорта, связанного с ковид-19 пандемией. Отмечается, что за весь период наблюдений среднегодовая концентрация PM2.5 и PM10 была выше допустимой нормы.

Ключевые слова: Атмосферные аэрозоли, твердые частицы, PM2.5, PM10.

Information for contributors

Papers intended for the Journal should be submitted in two copies to the Editor-in-Chief. Papers from countries that have a member on the Editorial Board should normally be submitted through that member. The address will be found on the inside front cover.

1. Papers should be written in the concise form. Occasionally long papers, particularly those of a review nature (not exceeding 16 printed pages), will be accepted. Short reports should be written in the most concise form not exceeding 6 printed pages. It is desirable to submit a copy of paper on a diskette.
2. A brief, concise abstract in English is required at the beginning of all papers in Russian and in Georgian at the end of them.
3. Line drawings should include all relevant details. All lettering, graph lines and points on graphs should be sufficiently large and bold to permit reproduction when the diagram has been reduced to a size suitable for inclusion in the Journal.
4. Each figure must be provided with an adequate caption.
5. Figure Captions and table headings should be provided on a separate sheet.
6. Page should be 20 x 28 cm. Large or long tables should be typed on continuing sheets.
7. References should be given in the standard form to be found in this Journal.
8. All copy (including tables, references and figure captions) must be double spaced with wide margins, and all pages must be numbered consecutively.
9. Both System of units in GGS and SI are permitted in manuscript
10. Each manuscript should include the components, which should be presented in the order following as follows:
    Title, name, affiliation and complete postal address of each author and dateline.
    The text should be divided into sections, each with a separate heading or numbered consecutively.
    Acknowledgements. Appendix. Reference.
11. The editors will supply the date of receipt of the manuscript.

CONTENTS - სარჩევი

საქართველოს გეოფიზიკური საზოგადოების ჟურნალი

მყარი დედამიწის, ატმოსფეროს, ოკეანისა და კოსმოსური პლაზმის ფიზიკა

ტომი 26 , № 1

ჟურნალი იბეჭდება საქართველოს გეოფიზიკური საზოგადოების პრეზიდიუმის დადგენილების საფუძველზე

ტირაჟი 20 ცალი

JOURNAL OF THE GEORGIAN GEOPHYSICAL SOCIETY

Physics of Solid Earth, Atmosphere, Ocean and Space Plasma

Vol. 26, № 1

Printed by the decision of the Georgian Geophysical Society Board

Circulation 20 copies

ЖУРНАЛ ГРУЗИНСКОГО ГЕОФИЗИЧЕСКОГО ОБЩЕСТВА

Физика Твердой Земли, Атмосферы, Океана и Космической Плазмы

Том 26, № 1

Журнал печатается по постановлению президиума Грузинского геофизического общества

Тираж 20 экз

Tbilisi-თბილისი-Тбилиси
2023